THE UNIVERSITY OF CHICAGO

CHARACTERIZATION OF ADVANTAGEOUS TRAITS ACROSS HETEROGENEOUS ENVIRONMENTS AND THEIR IMPLICATIONS FOR MUSSEL PERSISTENCE IN A CHANGING OCEAN

A DISSERTATION SUBMITTED TO
THE FACULTY OF THE DIVISION OF THE BIOLOGICAL SCIENCES
AND THE PRITZKER SCHOOL OF MEDICINE
IN CANDIDACY FOR THE DEGREE OF
DOCTOR OF PHILOSOPHY

DEPARTMENT OF ECOLOGY AND EVOLUTION

BY

CASEY STEVEN RICHARDS

CHICAGO, ILLINOIS

AUGUST 2026

TABLE OF CONTENTS

LIST OF TABLES

LIST OF FIGURES

ACKNOWLEDGEMENTS

My dissertation research would not have been possible without the help of numerous people, organizations, and funding sources. First, I would like to thank my advisor Cathy Pfister for her unwavering support and professional guidance throughout my PhD. Cathy`s knowledge in population ecology and experience in field experimentation proved to be an invaluable source of information and my research would not have been successful without her encouragement and our impromptu meetings in the field and lab. Next, I would like to acknowledge my committee chair, Tim Wootton, as his comprehension of natural systems and how they function was an influential part of my thesis and will continue to motivate how I pursue ecological research. Thank you to my committee members John Novembre and Marcus Kronforst for their expertise and thoughtful contributions throughout this research.

I am extremely grateful to the Makah Tribe for allowing me to research on their land, and the Clallam Bay community, particularly Rick, Mary K., Gus, Mary Lee, Leroy, Fidel, and Felix for welcoming me with open arms during each of my field seasons. Thank you to my cohort and friends, Gwen Kettenburg, Sofia Sheikh, Katja Della Libera, Mahmoud Yousef, Shuanger Li, Taylor Hains, Will Koval, Paula Fernandez-Begne, Kiseok Lee, and Justin Kosiewsk for being inspirational scientists, making this a memorable experience, and listening to my frustrations along the way. Thank you to the Pfister and Wootton lab groups for helping me think through hypotheses throughout my PhD and being a collaborative network of scientists who embrace the unknowns of slippery systems. Thank you, Friday Harbor Laboratories and The Field Museum's Pritzker Laboratory for allowing me to perform lab work in your facilities. Thank you, Washington Department of Fisheries and Wildlife for approval of collecting and transferring scientific specimens in the state of Washington.

This research would not have been possible without the funding of the Pat Tillman Foundation, The National Science Foundation (OCE-9711802, OCE-0117801, OCE-0452687, DEB-0919420, OCE-0928232, DEB-1148867, DEB-1556874 and OCE-1851489), The U. S. Department of Education (GAANN Fellowship-P200A210054), The National Institute of General Medical Sciences-T32-GM139782, The Society for Integrative and Comparative Biology, American Malacological Society, The Malacological Society of London, Henry Hinds Fund, the Andrew W. Mellon Foundation, NSF GEO-VETS, and University of Chicago's Department of Ecology & Evolution.

I would like to thank my parents for all the love and support along the way and always being a voice of reason. Thank you to my grandparents for your unconditional love throughout my life and always being my biggest fan. Thank you to my wife for being my best friend in life and my biggest inspiration. Finally, I would like to acknowledge our late dog Vera, whose eagerness to explore the world continues to influence how I view the planet and reminds me to enjoy the little things.

ABSTRACT

Anthropogenic stressors have intensified the need to better understand linked cellular, evolutionary, and ecosystem processes to predict how systems will respond to climate induced changes. Although theoretical and empirical evidence demonstrates that ecological systems have the capacity to respond to climate change, the mechanisms and tempo of these responses are less understood, particularly in natural environments. Understanding how species respond to environmental stress is especially important in marine systems, where the combined effects of increasing sea surface temperatures and ocean acidification are altering organismal physiology, reshaping patterns of selection, and driving changes in community structure at an alarming rate. To address this, my thesis investigates adaptive responses across biological scales using the foundational intertidal bivalve *Mytilus californianus* as a study system. Coastal marine systems are characterized by pronounced and dynamic environmental variability, where strong diel cycles in photosynthesis and respiration drive fluctuations in seawater chemistry. For example, in coastal habitats pH can range almost a single unit (an order of magnitude), from 'normal' pH values of ~8.1 during the day to low values of 7.3 during darkness. Spatial gradients can further magnify these fluctuations as individuals positioned higher on the intertidal experience greater environmental stress due to longer emergence times during low tidal cycles. Beyond local-scale heterogeneity, environmental variation across broader geographic scales also plays a critical role in shaping the genetic backgrounds of individuals, directly influencing their capacity to respond to future environmental change. Despite growing recognition of these multiscale stressors, the extent to which plastic and evolutionary responses mitigate their effects remain unclear. Accordingly, this thesis addresses three primary questions: (i) how fine-scale environmental gradients shape phenotypic plasticity and local adaptation within populations; (ii) how spatial

environmental heterogeneity and gene flow interact to structure genetic variation and influence adaptive potential across species ranges; and (iii) how organismal and evolutionary processes scale up to influence community stability under long-term environmental change. Together, this work advances our understanding of how adaptive responses emerge across natural populations distributed throughout heterogeneous environments and provides a mechanistic framework for predicting the resilience of marine organisms and communities to ongoing climate changes.

INTRODUCTION

Human activity and the continuous release of carbon dioxide (CO_2) into the atmosphere over the last two centuries have had a profound effect on our planet and oceans. Much of this carbon remains in our atmosphere contributing to the increase in greenhouse gases associated with global warming. However, since the 1800's about 118 Pg C, or about 25% of human released carbon have been absorbed into our oceans leading to shifts in ocean chemistry that have resulted in decreased pH, increased sea surface temperatures (SST), decreased saturation rates in calcium carbonate, and a decrease in dissolved oxygen (DO) concentration (Hönisch et al., 2012; Sabine et al., 2004). We can thus expect global change in the ocean to impact linked cellular, ecosystem, and evolutionary processes and the functions we rely on in ocean ecosystems.

The variety of responses intertidal species exhibit from living in a dynamic environment has likely contributed to the intertidal being one of the most biodiverse places on the planet. To fully understand linked cellular, ecosystem, and evolutionary processes, it is important to consider how organisms will respond to environmental change. In the ocean, both decreasing pH and increasing sea surface temperatures (SST) are stressors that have already led to significant responses and may further limit species across different communities. For example, coccolithophores have shifted to areas that are cooler, with lower saturation-state for calcite (Gibbs et al., 2016), while other calcifying species experience decreased fitness under ocean acidification (OA) (Bitter et al., 2019; Kroeker et al., 2010). However, some species have phenotypic traits that allow them to persist in more extreme temperature and pH environments. For instance, dinoflagellates have benefited from global change, increasing in productivity with higher SST in the North Pacific Ocean (Trainer et al., 2020). Other species also show adaptations

to changing environments through the maintenance of genetic variation (Bitter et al., 2019; Teixidó et al., 2020). The capacity for species to persist in a changing ocean will be dependent on plastic or genetic changes especially in intertidal systems, where tides ebb and flow daily and strong gradients in temperature, DO, and pH result from changes in both seawater and atmospheric features. In this dissertation, I test species plasticity and resilience, through physiological response and genetic capacity in changing environments. My results provide insight into mussel responses to stressors, the potential for adaptation, and their ability to maintain their foundational status in future oceans.

Marine species interact with the water column, responding to seawater chemistry and in turn altering seawater chemistry. The stoichiometry of key elements such as carbon and nitrogen may respond locally to global change, both from abiotic changes and from alterations to the species that are present. For example, we have known for decades that elemental stoichiometry is maintained within plankton where a relatively constant ratio of carbon to nitrogen to phosphorus (106:16:1) has been observed (Redfield, 1934), though some latitudinal and basin level differences exist. Further, different species require different chemical investments that alter elemental stoichiometry within ecological systems (Elser et al., 1996). In the ocean, we can expect that there will be species differences in how they interact with carbon and nitrogen, with calcifying species and those that feed by filtering particles having potentially strong feedback with ocean chemistry.

As our understanding of how marine species respond to environmental change develops, it is increasingly demonstrated that decreasing pH alters ecosystem dynamics, with calcareous species showing the greatest vulnerability to OA (Wootton et al., 2008). The California mussel *Mytilus californianus* is a foundational calcifying bivalve species along rocky shores of the

northeast Pacific Ocean. Disruptions in populations of dominant species such as mussels, a species known for increasing richness within communities (Gutiérrez et al., 2003), and a prey for numerous animals, could have implications throughout the food web (Paine, 1974). Rocky intertidal shores on the outer coasts of the northeast Pacific ocean have mussel densities in the thousands per square meter; mussels modify nutrients that limit primary productivity and influence ecosystem processes (Atkinson et al., 2013). Thus, it is important to understand and mitigate the effects of OA and increasing SST on these organisms, as it has the potential to cause drastic changes to marine ecosystems if these taxa are compromised by future ocean changes.

I hypothesize that the environmental stress gradients in the marine intertidal over space and time would select on several functional traits key to survival in mussels including respiration, calcification, and morphology. In Chapter 1, I test how tidal mediated stress in the high intertidal effects trait adaptation within a *M. californianus* population, and the costs and trade-offs of these adaptations. To achieve this, I combined a classical reciprocal transplant experiment with next generation sequencing (NGS) to assess genetic and phenotypic differentiation between mussels indigenous to the low and high intertidal. Through this, I demonstrate differences in how functional traits respond to environmental stress: morphological traits exhibit phenotypic plasticity, whereas physiological traits are fixed, or locally adapted. These results imply there will be evolutionary differences in how functional traits respond to ocean change, as both adaptive phenotypic plasticity and the rapid adaptation of locally adapted alleles will mitigate extinction risks.

Along the geographic range of *M. californianus*, a pronounced environmental gradient occurs along the Strait of Juan de Fuca due to its complex coastline and bathymetry. In Chapter 2, I leverage this gradient to examine how environmental stress influences genetic variation and

metabolic rates across *M. californianus*. Analysis of the genome of *M. californianus* across 14 sites and 181 km, suggest that geographically separated *M. californianus* populations have genetic distinctions, despite high connectivity from larval dispersal that can last ~45 days (Trevelyan & Chang, 1983). Additionally, I experimentally test the range of metabolic responses of *M. californianus* individuals from different geographic locales under predicted future ocean conditions. By combining NGS with common garden experiments using experimentally manipulated seawater, I quantify phenotypic plasticity to increased temperature and decreased pH conditions across these genetically distinct populations. These results demonstrate that strong selection associated with spatial environmental heterogeneity favors local adaptation over phenotypic plasticity. However, the introduction of these "locally adapted alleles" into larger populations via larval dispersal driven by tidally mediated currents can increase genetic diversity and enhance adaptive phenotypic plasticity. As a result, centrally located populations exhibit greater variability in metabolic responses across a wider range of stressors, thereby increasing fitness in more heterogenous environments and suggesting two possible mechanisms for adaptive traits to evolve to future ocean conditions.

Foundation species are widely recognized for enhancing resilience to environmental stress within ecological communities (Dayton, 1972; Stachowicz, 2001). Chapter 3 examines the role of mussels within a community of species and the associated responses to environmental changes. Using data from a 31-year long term ecological experiment in the rocky intertidal, our results reiterated how foundation species increase community stability by ameliorating stress for non-dominant species. However, communities without foundation species demonstrated an adaptive community response to increasing environmental stress through the introduction of dominant species. Together, the chapters of this thesis elucidate how existing adaptations shape

the evolutionary mechanisms organisms will deploy to cope with future climate conditions and reveals how communities will respond based on the presence or absence of a foundation species in a system.

CHAPTER 1: SPATIALLY VARYING SELECTION AMPLIFIES INTRAPOPULATION DIFFERENTIATION AMONG PHENOTYPIC TRAITS IN THE ROCKY-SHORE MUSSEL, *MYTILUS CALIFORNIANUS*

CITATION: Richards, C. S., Vera Cruz, D., Shapiro, J. W., Wootton, J. T., & Pfister, C. A. (2025). Spatially Varying Selection Amplifies Intrapopulation Differentiation Among Phenotypic Traits in the Rocky-Shore Mussel, Mytilus californianus. *Ecology and Evolution*, *15*(7), e71641.

ABSTRACT

Strong ecological gradients along heterogeneous environments play an important role in shaping population differentiation across species ranges. Thus, the selective pressure of environmental variation on phenotypic variation strongly affects an organism's ability to persist across diverse or new environments. We investigated the spatial variability of biological responses in the intertidal bivalve *Mytilus californianus* to highlight the costs and trade-offs of local adaptation and phenotypic plasticity across various functional traits in a dynamic environment, the marine intertidal. To test this, we performed a reciprocal transplant experiment with *M. californianus* individuals originating from the upper and lower intertidal measuring relevant phenotypic traits, followed by Whole Genome Sequencing (WGS). We determined that morphological traits in individuals demonstrated phenotypic plasticity when moved to new environments, whereas physiological traits such as metabolism exhibited constraints in plasticity. Additionally, mussels from high intertidal zones, which experience greater heat and aerial exposure stress, maintained lower metabolic rates and showed increased frequencies of non-synonymous mutations in functionally relevant heat shock proteins when compared to low

intertidal mussels. These results suggest that morphological and physiological traits responded differently to spatially varying selection within the marine intertidal.

INTRODUCTION

Understanding how species adapt to their environments is a fundamental theme in biology. Strong ecological gradients along heterogenous environments reveal the patterns and processes that shape population genetic structure and phenotypic variation across species ranges (Endler, 1986). Across heterogenous environments the interplay between environmental and genetic differences on phenotypic variation can result in the local adaptation of populations (Levins, 1968), where local genotypes have higher fitness in their indigenous environment compared to immigrating genotypes from neighboring populations (Savolainen et al., 2013). For connected populations, gene flow prevents the evolution of local adaptation when the strength of selection cannot overcome the stabilizing effects of migration (Wright, 1969) and limits adaptive genetic differentiation over steep environmental gradients (Bachmann et al., 2020; Lenormand, 2002). Therefore, over microgeographic scales selection may favor 'phenotypically plastic phenotypes' opposed to 'fixed phenotypes' that have increased fitness in a particular environment (Hollander, 2008; Levins, 1968; Scheiner, 1998). For example, phenotypic flexibility are reversible phenotypic transformations that allow individuals to respond to environmental stochasticity over time, while developmental plasticity allows individuals to respond to heterogeneous environments across space (Piersma & Drent, 2003). However, there is growing evidence that local adaptation occurs over microgeographic scales both in terrestrial systems (e.g. Antonovics, 2006; Yadav et al., 2021) and especially in marine systems (e.g. Gurski, 2016; Hays et al., 2021; Sanford & Kelly, 2011; Thomas et al., 2022), suggesting strong

selection associated with spatial environmental heterogeneity could drive local adaptation even with population connectivity (Yeaman, 2022; Yeaman & Otto, 2011).

Coastal marine systems are dynamic, and the intertidal zone is especially so with many species residing in environments where tides ebb and flow daily, imparting strong changes in temperature, dissolved oxygen (DO), and pH. The variety of responses intertidal species exhibit from living in a dynamic environment has likely contributed to the intertidal being one of the most biodiverse places on the planet. Rocky shores along the marine intertidal are no exception as they exhibit high biodiversity and experience large variations in temperature, pH, DO, and nutrient supply on seasonal and daily time scales. As a result, rocky shores have attracted much attention over the years for experimental analysis of population and community structure in response to spatial elevation as temperature variation, sunlight, and aerial exposure increases with height (Connell, 1972; Dayton, 1971; Paine, 1974; Wootton, 2005). These extreme environmental stress gradients in the marine intertidal over space and time can select phenotypic traits important for survival. Testing species plasticity and resilience across steep environmental gradients on small spatial scales in the rocky intertidal provides insight into the phenotypic response to stressors, the possibility for adaptation, and the role of genetic variation in shaping the evolution of populations that persist throughout heterogeneous environments.

In marine systems, most organisms reproduce via broadcast spawning potentially connecting populations over large distances and possibly limiting adaptive differentiation. Yet many broadcast spawning species exhibit spatially structured genetic variation within populations (e.g. Luttikhuizen et al., 2003; Palumbi, 1994; Thomas et al., 2022). Foundational species that broadcast spawn are particularly interesting for studying local adaptation because they experience high population connectivity across rapidly fluctuating ocean environments, are

numerically abundant, and significantly affect ecosystem function (Dayton, 1972; Ellison, 2019). *Mytilus californianus*, a broadcast spawning bivalve that dominates rocky intertidal shores of the northeast Pacific Ocean, serves as a foundational species by forming habitats and providing food for a myriad of species (Gutiérrez et al., 2003; Paine & Levin, 1981). *M. californianus* experiences strong environmental gradients over relatively small spatial scales and may show high intrapopulation diversity as a result (Hays et al., 2021). Previous analysis of gene expression of in-situ *M. californianus* mussels originating from the high intertidal showed a reduction in expression patterns of genes involved in metabolic activity and perturbations to cellular homeostasis when compared to in-situ low intertidal mussels (Place et al., 2012). How the environment determines expression patterns in *M. californianus* mussels is unknown and could be the result of phenotypic plasticity or local adaptation. The induction of genes involved in stress response for intertidal mussels may come at a substantial energetic cost to other biological functions, specifically, a trade-off between increased fitness and growth rate (Lang et al., 2009). Untangling genetic versus phenotypic responses on spatially varying individuals provides insight into the scope of mussel response across diverse environments on microgeographic scales.

In this study, we assessed functional traits within a continuous mussel population on a steep sloping shelf to test the role of strong environmental differences on phenotypic plasticity versus genetic response. To achieve this, we used reciprocal transplant experiments combined with next generation sequencing to identify intrapopulation genetic and phenotypic variation between *M. californianus* individuals positioned in the low and high intertidal. This study addresses three questions:

(1) Are observed phenotypic differences between low and high *M. californianus* individuals a result of phenotypic plasticity or another mechanism such as local adaption or canalization?

(2) If there is evidence of local adaptation based on signatures of selection in candidate Single Nucleotide Variants (SNVs)?

(3) What are the costs and trade-offs between environment and indigenous locale on important phenotypic traits in *M. californianus* individuals on microgeographic scales?

Given that experimental mussels were in close proximity and a part of a continuous mussel bed, the stabilizing effects of high gene flow (Wright, 1969) combined with high panmixia observed in many broadcast spawning species (Lourenço et al., 2017; Ridgway et al., 2001; Tay et al., 2016) will limit adaptive genetic differentiation over steep environmental gradients (Bachmann et al., 2020; Lenormand, 2002). Therefore, we hypothesized that selection would favor phenotypic plasticity over local adaption (Hollander, 2008; Levins, 1968; Scheiner, 1998). Because in-situ *M. californianus* mussels originating from the high intertidal show a reduction in the expression of genes involved in metabolic activity (Place et al., 2012), we hypothesized reduced metabolic activity for mussels exposed to the more stressful high intertidal would trade-off with increased survival, resulting in a cost to growth (Lang et al., 2009). Testing species plasticity and resilience across steep environmental gradients on small spatial scales in the rocky intertidal provides insight into the phenotypic response to stressors, the possibility for adaptation, and the role of genetic variation in shaping the evolution of populations that persist throughout heterogeneous environments.

METHODS

Reciprocal transplant experiment

The experimental tractability of mussels allowed a test of how plastic or fixed mussel responses were to intertidal stressors. Individual mussels that were naturally growing in either the low and high intertidal, ranging from 39 to 51mm in length, were collected during a -0.41m low tide in 2022 across a steep sloping shelf along a continuous mussel bed on northern Tatoosh

Island, Makah Indian Reservation, WA (48°23.680'N, 124°44.174'W) (Figure 1.1A & 1.1B). Immediately following collection, individual mussels were transferred into fresh seawater. Initial measurements on all individuals included maximum shell length, shell width, shell height, total weight in air, and buoyant weight as a proxy and non-destructive method for obtaining approximate shell weight (Palmer, 1982) using calipers and an Ohaus precision balance. All individuals were marked on the umbo of the left or right shell valve to designate indigenous locale using bee tags adhered with J-B KWIK Weld^{TM} and "Fire Red" EZPoxy paint (PETTIT) (Figure A1) to characterize individual mussels throughout the reciprocal transplant experiment. Individually labeled mussels were then randomly selected and evenly distributed by treatment: either transplanted back to their original intertidal position (in-situ) or cross-transplanted to the experimental tidal position in the low or high intertidal where they had not originally been living (transplant) (Figure 1.2). Mussels were housed in two separate 19L buckets based on assigned treatment plot with fresh seawater maintained at 11°C overnight until individuals could be placed in their respective plot during the following morning low tide. This overnight period also allowed for in-situ and transplanted individuals going into the same treatment plot to attach to each other through byssus production, which formed a large cluster of mussels that increased the likelihood for survival when placed under their experimental enclosures in the field (personal observation). The experimental enclosures for both intertidal plots consisted of a steel cage wrapped with 1/4" plastic Vexar mesh held together with zip ties (Figure A1B). Experimental enclosures were zip tied to stainless steel screw eyes anchored to the rocks in the low and high intertidal plots (Figure A1C). In total, 44 mussels were placed in each plot in the intertidal (88 mussels total), where each treatment plot consisted of 22 in-situ and 22 transplanted individuals.

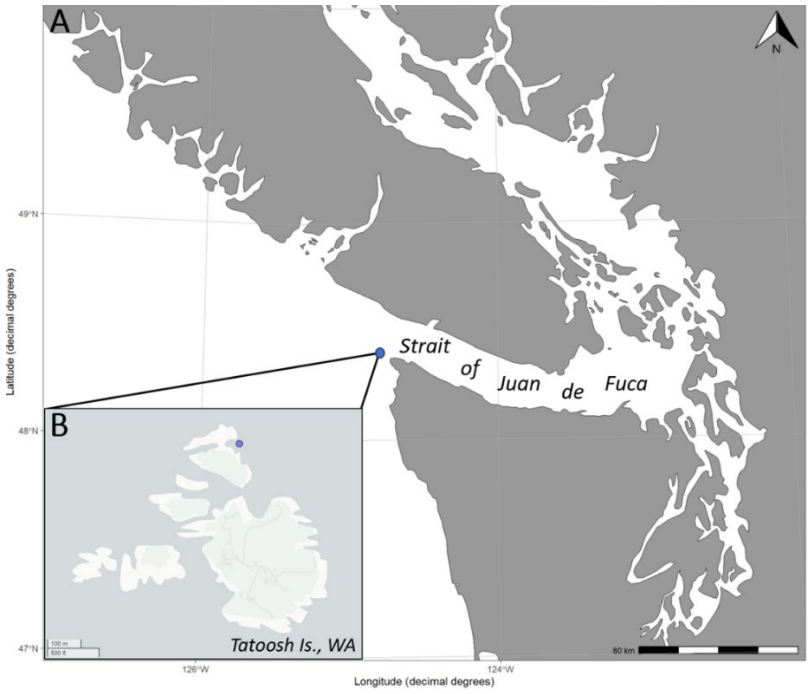

Figure 1.1: (A) Map of Strait of Juan de Fuca region. (B) Map of Tatoosh Island, Makah Indian Reservation, WA. Purple dots indicate location of Tatoosh Island (1.1A) and site of experimental population and reciprocal transplant experiment (1.1B).

The reciprocal-transplant experiment was initiated in June 2022 and lasted 44 days. The hottest air temperatures occur during the summer months of the year, but were intensified during the study by a record setting heat wave in July 2022 in the Pacific Northeast (NOAA National Centers for Environmental Information) resulting in the high intertidal plot experiencing significantly hotter than `normal` aerial exposure temperatures for prolonged periods when low tides occurred during daytime periods (see results and Figure A2). These intense stressors resulted in 100% mortality for all mussels positioned in the high intertidal plot between days 18-29. Therefore, on day 30 we repeated the methods above to replicate another high intertidal plot consisting of 10 in-situ and 10 transplanted mussels that were placed under the experimental enclosure on the morning of day 31. Six of these individuals did not survive (three in-situ, three transplants) over the course of the next 13 days, bringing the sample size to seven in-situ and

seven transplanted mussels for the high intertidal plot. In contrast, 43 out of 44 individuals survived in the low intertidal plot throughout the 44-day experiment. At the conclusion of the experiment the enclosures were removed, and mussels were collected and kept in fresh seawater maintained at 11°C until final measurements could be obtained. We recorded maximum shell length, shell width, shell height, total weight in air, buoyant weight, and respiration rates for each individual in each treatment. After these measurements were obtained, a tissue sample of the gill was collected for DNA comparison between experimental mussels who originated from the low and high intertidal. The shells of the individual mussels were dried for 72hrs at 50°C in a drying oven to obtain dried shell weight. After this the left shell valves were coated with J-B KWIK Weld™, sliced longitudinally (umbo – ventral margin) with a trim saw equipped with a diamond saw blade, and aged under a dissecting scope following the methods from McCoy et al. (2018).

To test whether mussel size was important to individual plasticity, a second transplant experiment was performed in May 2023 with smaller `juvenile` individuals that were half the length of mussels in the first experiment (12-28mm). Both the low and high intertidal plots contained 40 individuals (80 total across the entire experiment) at the beginning of the experiment. The methods and experimental site were the same as the reciprocal transplant but the experiment used only juvenile mussels living in the low intertidal and lasted 74 days to increase the chance of detecting plasticity. Juvenile mussels were not sourced from the high intertidal because they could not be differentiated from slow growing adults nor other *Mytilus spp.* who dominate the high intertidal (Suchanek, 1978). Throughout the experiment, only four of these 80 individuals perished, all of them individuals transplanted to the high intertidal plot. Unlike the reciprocal transplant experiment performed with adult mussels, tissue samples, dried shell weight, and age data were not collected on these juveniles as they were returned to their

respective treatment plots for an additional 333 days where morphometric and tissue weight data were recorded using the methods described below. Of the 76 individuals returned to the intertidal, 55 survived.

Temperature and elevation measurements

Vertical elevation of each plot was determined by calculating meters (m) above mean lower low water (MLLW) using preexisting markers on Tatoosh Island from Kandur (2014) and a DEWALT Laser Level with Tripod**.** In this study, mussels were sampled from sites at 1.10m (low intertidal) and 2.37m (high intertidal) above MLLW. Temperature measurements were recorded in 5-minute intervals throughout the entire experimental period for both intertidal plots using Onset HOBO data loggers that were attached to anchored screw eyes positioned next to the experimental enclosures (Figure A1B).

Morphological trait measurements

To test whether each treatment had an effect on the phenotypes of individual mussels, changes in shell length (mm), shell width (mm), shell height (mm), shell weight (g), tissue weight (g), and total weight in air (g) were recorded for all individuals used in the reciprocal transplant experiment. These changes in morphological traits for each individual were determined by calculating the differences between measurements at the beginning and the end of the experiment divided by the number of days in their experimental plot. Shell and tissue weight changes were estimated because precise shell weights could only be obtained at the conclusion of the experiment once mussels had been sacrificed. To achieve these estimates, we derived a least squares linear regression model using the dried shell weight (Y) and final buoyant weight (X) of each individual mussel, which explained >99% of the variation ($R^2 = 0.995$), then estimated the beginning shell weight for each individual using the beginning buoyant weight. Because tissue is

neutrally buoyant when submerged (Palmer, 1982), we subtracted total weight in air from shell weight to obtain estimated tissue weights at the beginning and end of the experiment.

Respiration rate

Mussel respiration rates were quantified at the conclusion of the transplant experiments after final morphological measurements had been collected. Mussels were randomly selected from each treatment and kept in fresh seawater maintained at 11°C for approximately 1hr prior to measuring respiration rates from oxygen consumption (mg O_2 g^{-1} h^{-1}). This was achieved by placing each mussel in their own individual closed 12-ounce glass container filled with fresh seawater and dissolved oxygen (DO) was measured every second over a 1hr period using a FireSting FSPRO-4 equipped with oxygen sensor spots and a temperature sensor (Pyroscience, Aachen, Germany). All containers were maintained at 11°C and kept in darkness. Seawater controls lacked mussels but had the same freshly collected seawater used with mussels. Metabolic rates from an additional 32 mussels from a neighboring population (l6 in-situ low individuals, l6 in-situ high individuals) that were not used in the reciprocal transplant experiment were assayed as an additional control to quantify if the transplantation itself had a significant effect on mussel function.

Net calcification rate and growth rate

The net calcification rates (g $CaCO_3$ d^{-1}) for all individuals used in the reciprocal transplant experiment were estimated from changes in their buoyant weight (g) throughout the experiment divided by the number of days in their experimental plot, following the methods of Duarte et al. (2015). For the transplant experiment with juvenile mussels, net calcification totals (g $CaCO_3$) were recorded by subtracting the final buoyant weight for each individual from the beginning average buoyant weight. Growth rates were determined by calculating the differences

in shell length (mm) at the beginning and the end of the experiment divided by the number of days in their experimental plot.

Intrapopulation genetic diversity

After all biological measurements were recorded, gill tissue from 10 individuals used in the experiment, five indigenous to the low intertidal and five indigenous to the high intertidal, was collected and immediately placed in RNAlater (Invitrogen™) and stored at -20°C until DNA extractions could be completed. DNA was extracted from gill tissue using the E.Z.N.A.® DNA/RNA Isolation Kit (Omega Bio-Tek) following manufacturers protocols. To obtain regional genomic data and identify candidate SNVs for the experimental population, an additional 44 *M. californianus* mussels were collected across 4 populations extending 148km eastward into the Strait of Juan de Fuca (Figure A3). All 54 extracted DNA samples were sent to the University of Chicago Functional Genomics Core Facility (RRID:SCR_019196) where whole genome DNA libraries were constructed and sequenced on 2 NovaX-10B-300 lanes with an average coverage of 8.3X per sample.

Germline variant calling and annotation

Germline variant calling and annotation were conducted using various bioinformatics tools for read preprocessing, alignment, variant calling, filtering, and annotation using the *M. californianus* assembly (NCBI RefSeq assembly: GCA_021869535.1) as a reference genome. Data were processed using the nextflow pipeline nf-core/sarek v3.1.2 (doi: 10.12688/f1000research.16665.2, 10.5281/zenodo.4063683). The sarek pipeline performed read preprocessing using FastP (0.23.2) and alignment using BWA-mem (0.7.17). BAM files were processed using the MarkDuplicates, BaseRecalibrator, and ApplyBQSR tools, followed by variant calling using HaplotypeCaller from the GATK suite version 4.2.6.1. The resulting

variants per sample were further filtered and consolidated with the GATK SelectVariants, GenomicsDBImport, GenotypeGVCFs tools, and Picards's MergeVCFs. The filter criteria aimed to keep germline variants with the PASS filter tag. Variant annotation was performed using snpEff toolbox (Cingolani et al., 2012).

Initial analysis yielded over one million variants per sample, which was a result of a large number of duplicated genes within the *M. californianus* reference genome. To overcome this issue, we used a reciprocal BLAST search to identify highly similar regions within the reference genome. These included regions that were over 95% identical or with an alignment length greater than 300 nucleotides. The remaining CDS regions in the genome were added to a BED file and used to filter the variant calling results to recover the most reliable SNVs. EggNOG-mapper 2.1.12 was used to provide additional functional annotations of candidate SNVs.

Variant filtering and analysis

Annotated, biallelic SNPs with the PASS filter tag and complete GT tag were used for the subsequent analysis using R. A total of 133,617 variants with coverage in all the samples, defined genotypes and present in at least 1 population at a frequency of 50% or higher, were used to create a genotypes matrix and a matrix variant frequency per population. To identify variants that distinguish populations, PCA was calculated using the genotypes matrix for individuals (Figure A4A), and variant frequency per population matrix (Figure A4B). The number of SNVs chosen for a given PC was proportional to the explained variation related to that PC. For each variant, the *Fst* coefficient was calculated using the genotypes of all the samples per population. For comparison between low and high individuals sourced from the experimental population, only the top variants that had significant loadings above 0.0075 or below -0.0075 for PC1 were used, since PC1 distinguished individuals by their population in an agnostic PCA, based on the

sample's genotypes (Figure A4C). This process identified 638 SNVs which were used as our candidate SNVs in our population analysis.

Statistical analyses

All analyses were conducted using the R statistical platform version 4.4.1 (R Core Team, 2024). A one-way ANOVA was used to test for differences in temperature between the two intertidal plots, morphological characteristics (beginning total weight, shell height, shell weight, shell width), physiological characteristics (net calcification rate, respiration rate), and tissue weights of juvenile mussels used in the long-term transplant experiment. All biological responses (shell height change, shell weight change, total weight change, shell width change, growth rate, respiration rate, net calcification rate, tissue weight) were analyzed using a two-way ANOVA, with indigenous locale and treatment (in-situ or transplant) as the main fixed factors. Differences between groups (a posteriori comparison) were evaluated using a Tukey HSD test. We used a Breusch-Pagan test to test for heteroscedasticity. When data were heteroscedastic, log transformation did not alter overall significance conclusions for any ANOVA. Principal Component Analyses (PCA) were used to capture phenotypic variation among treatments and intrapopulation genetic variation and SNVs discovery between individuals who were indigenous to the low or high intertidal (Horne & Camp, 2004). Phenotypic variation among treatments was also tested using permutational multivariate analysis of variance (PERMANOVA) with the *adonis2* function in *vegan* (999 permutations; Oksanen et al., 2018), based on Euclidean distances. Z-standardization was performed on phenotypic trait data prior to PCA and PERMANOVA. The Mann–Whitney *U* test was used to compare metabolic rates of experimental and non-experimental individuals of differing samples sizes. A F-test for

homogeneity of variance was used to compare age variability differences between mussels indigenous to the low and high intertidal.

RESULTS

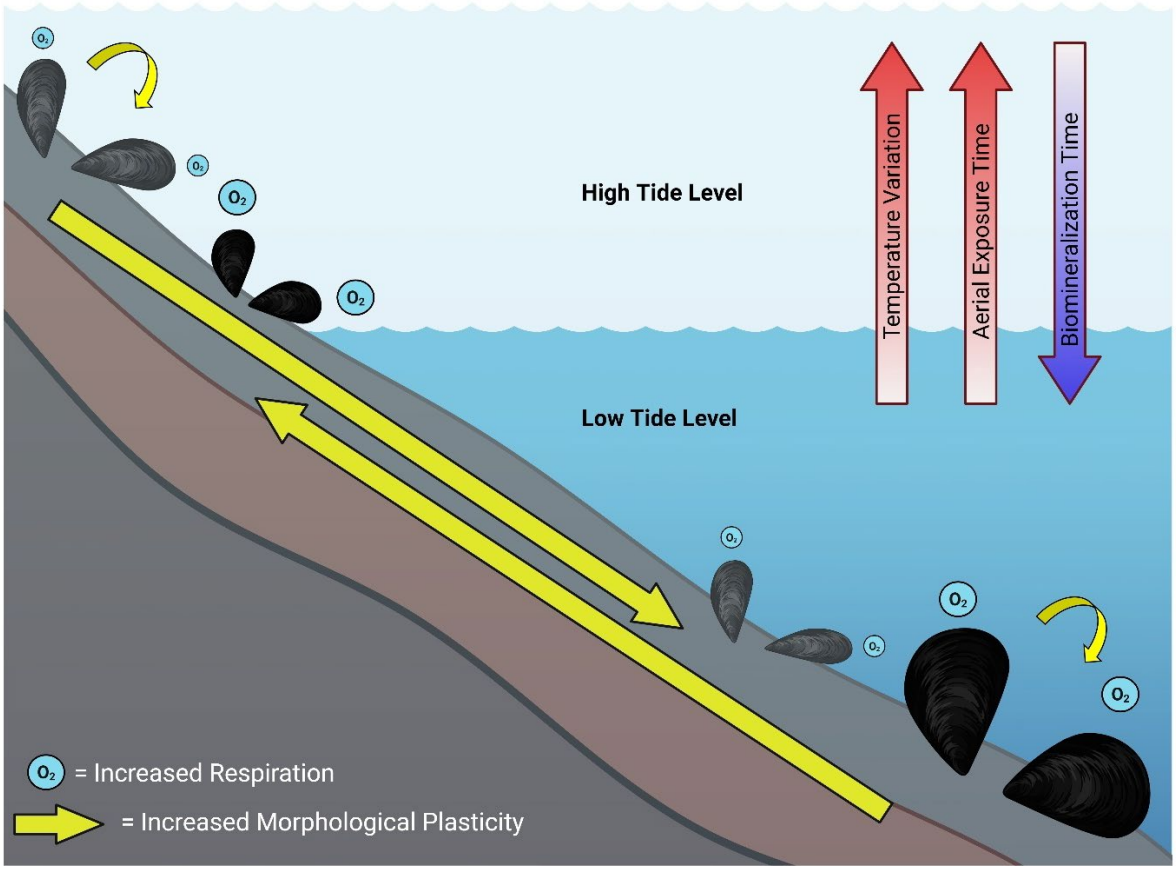

Figure 1.2: Graphical summary of the results from a reciprocal transplant experiment between *Mytilus californianus* individuals indigenous to the upper (grey mussels) and lower (black mussels) intertidal. Yellow arrows denote the reciprocal transplant experiment, with arrow thickness representing the degree of plasticity. Grey shells of mussels indigenous to the high intertidal represent loss of periostracum from increased incidence of endolithic phototrophs.

Contrasting temperatures between spatially varying intertidal positions

The low and high intertidal demonstrated contrasting environmental conditions, where the low intertidal had a mean temperature of 11.3°C and the high intertidal had a significantly greater mean temperature of 15.6°C (One-way ANOVA: $F_{(1,26471)} = 4{,}851$, $p < 0.0001$) indicating the longer aerial exposure times for high intertidal individuals. The average daily range of

temperature was two times greater in the high intertidal compared to the low (21.5°C versus 9.6°C). The low intertidal reached a maximum air temperature of 32.8°C; the high intertidal exceeded this temperature on 20 of the 44 days the temperature logger was deployed, reaching a maximum air temperature of 43.4°C (Figure A2).

Phenotypic traits differ with tide height

Although the individuals used in the experiment showed no significant differences in maximum shell length between low and high intertidal plots prior to the transplant experiment (One-way ANOVA: $F_{(1,55)} = 2.263$, $p = 0.138$), the morphometrics of *M. californianus* mussels differed depending on whether they were growing in the low or high intertidal. Individuals indigenous to the high intertidal had thicker shells (One-way ANOVA: $F_{(1,55)} = 66.28$, $p < 0.0001$, Figure 1.3A), heavier shells ($F_{(1,55)} = 64.17$, $p < 0.0001$, Figure 1.3B), and higher total weights ($F_{(1,55)} = 14.87$, $p = .0003$, Figure 1.3C) compared to individuals indigenous to the low intertidal. In contrast, individuals indigenous to the low intertidal had wider shells compared to their high intertidal counterparts ($F_{(1,55)} = 24.8$, $p < 0.0001$, Figure 1.3D). Similar increases in protective layering have been observed in other species in low intertidal environments (Figure 1.4).

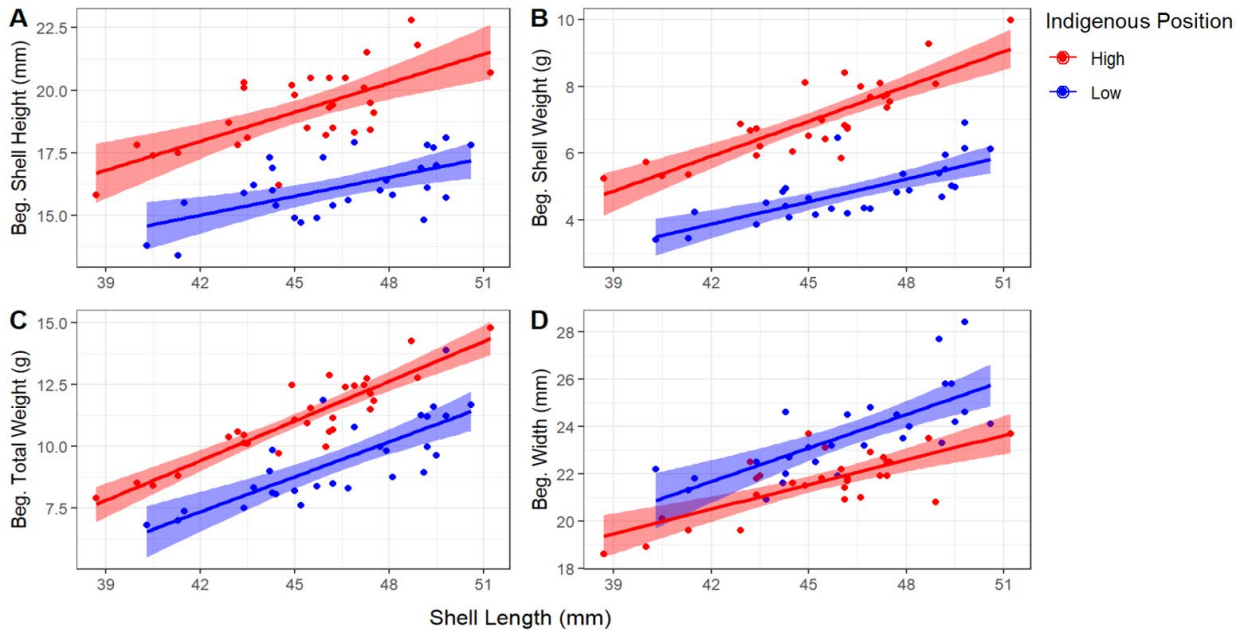

Figure 1.3: Relationship between maximum shell length (mm) and (A) shell height (mm), (B) shell weight estimated as the buoyant weight (g), (C) total weight measured as weight in air (g), and (D) shell width (mm) of low and high intertidal adult (38—51mm) mussels at the beginning of a reciprocal transplant experiment between the two locales. Shaded red and blue areas represent the 95% CI.

At the conclusion of the reciprocal transplant experiment, mussels from both plots showed a significant interaction between indigenous and experimental position in shell height (Figure 1.5A and Table 1.1a), shell weight (Figure 1.5B and Table 1.1b), total weight (Figure 1.5C and Table 1.1c), shell width (Figure 1.5D and Table 1.1d), and growth rate (Figure 1.5E and Table 1.1e). The shell height of in-situ individuals in the high intertidal plot (mean = 0.010 ± SE = 0.002 mm d^{-1}) had similar responses to transplanted mussels indigenous to the low intertidal (0.006 ± 0.002 mm d^{-1}; Tukey HSD test: p = 0.8206, Figure 1.5A). However, in-situ mussels in the low intertidal plot added more shell height (0.020 ± 0.002 mm d^{-1}) when compared to mussels transplanted to the low intertidal plot (0.011 ± 0.001 mm d^{-1}; Tukey HSD test: p = 0.0298, Figure 1.5A) and mussels transplanted to the high intertidal plot but indigenous to the low intertidal (0.006 ± 0.002 mm d^{-1}; Tukey HSD test: p = 0.0089, Figure 1.5A). The weight of individuals shells showed a similar response as in-situ mussels in the high intertidal

plot (0.011 ± 0.001 g d^{-1}) as changes in shell weight did not significantly differ from transplanted mussels indigenous to the low intertidal (0.008 ± 0.004 g d^{-1}; Tukey HSD test: p = 0.8926, Figure 1.5B). Additionally, in-situ mussels in the low intertidal plot significantly increased their shell weight (0.021 ± 0.002 g d^{-1}) when compared to those sourced from the high intertidal (0.013 ± 0.0009 g d^{-1}; Tukey HSD test: p = 0.0192, Figure 1.5B) and to mussels transplanted to the high intertidal plot but indigenous to the low intertidal (0.008 ± 0.004 g d^{-1}; Tukey HSD test: p = 0.003, Figure 1.5B).

In-situ mussels in the high intertidal plot significantly increased their total weight (0.096 ± 0.011 g d^{-1}) when compared to transplanted mussels indigenous to the low intertidal (0.052 ± 0.011 g d^{-1}; Tukey HSD test: p = 0.002, Figure 1.5C). However, mussels transplanted to the low intertidal experienced significantly decreased weights (0.039 ± 0.002 g d^{-1}) when compared to in-situ mussels positioned in the high intertidal (0.096 ± 0.011 g d^{-1}; Tukey HSD test: p = 9.0e-7, Figure 1.5C). Total weight changes did not significantly differ when comparing in-situ mussels indigenous to the low intertidal (0.042 ± 0.004 g d^{-1}) to transplanted mussels indigenous to the high intertidal (0.052 ± 0.011 g d^{-1}; Tukey HSD test: p = 0.9869, Figure 1.5C). Shell width changes were similar where in the high intertidal plot in-situ mussels had increased shell width changes (0.023 ± 0.006 mm d^{-1}) when compared to transplanted mussels indigenous to the low intertidal, although it was not significant (0.004 ± 0.003 mm d^{-1}; Tukey HSD test: p = 0.090, Figure 1.5D). However, in the low intertidal plot, in-situ mussels had significantly increased shell weight changes (0.024 ± 0.004 mm d^{-1}) when compared to transplanted mussels indigenous to the high intertidal (0.008 ± 0.001 mm d^{-1}; Tukey HSD test: p = 0.0044, Figure 1.5D), but did not significantly differ from in-situ mussels indigenous to the high intertidal (0.023 ± 0.006 mm d^{-1}; Tukey HSD test: p = 0.996, Figure 1.5D).

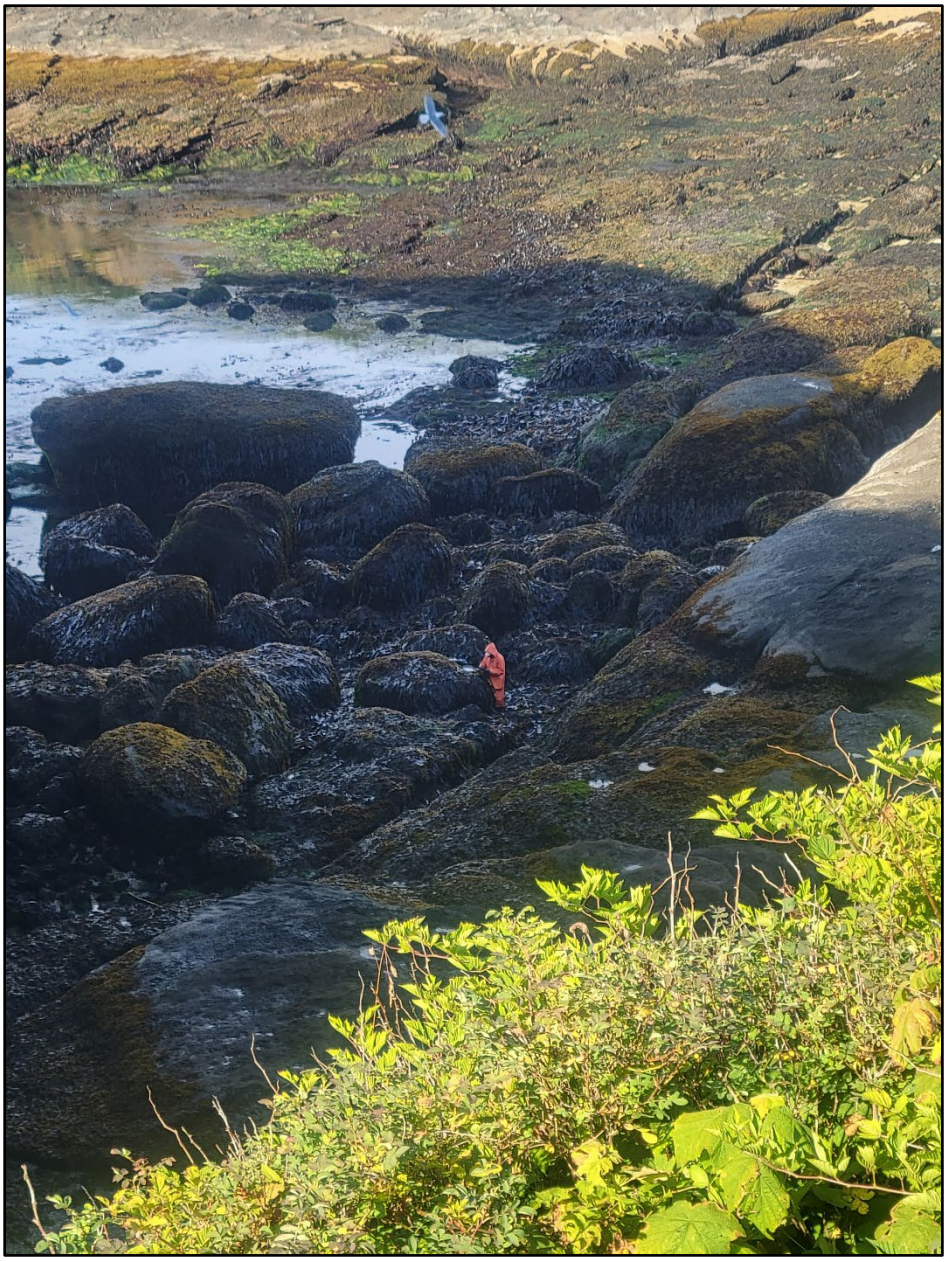

Figure 1.4: *Homo sapiens* exhibiting increased protective layering while venturing to low intertidal locales.

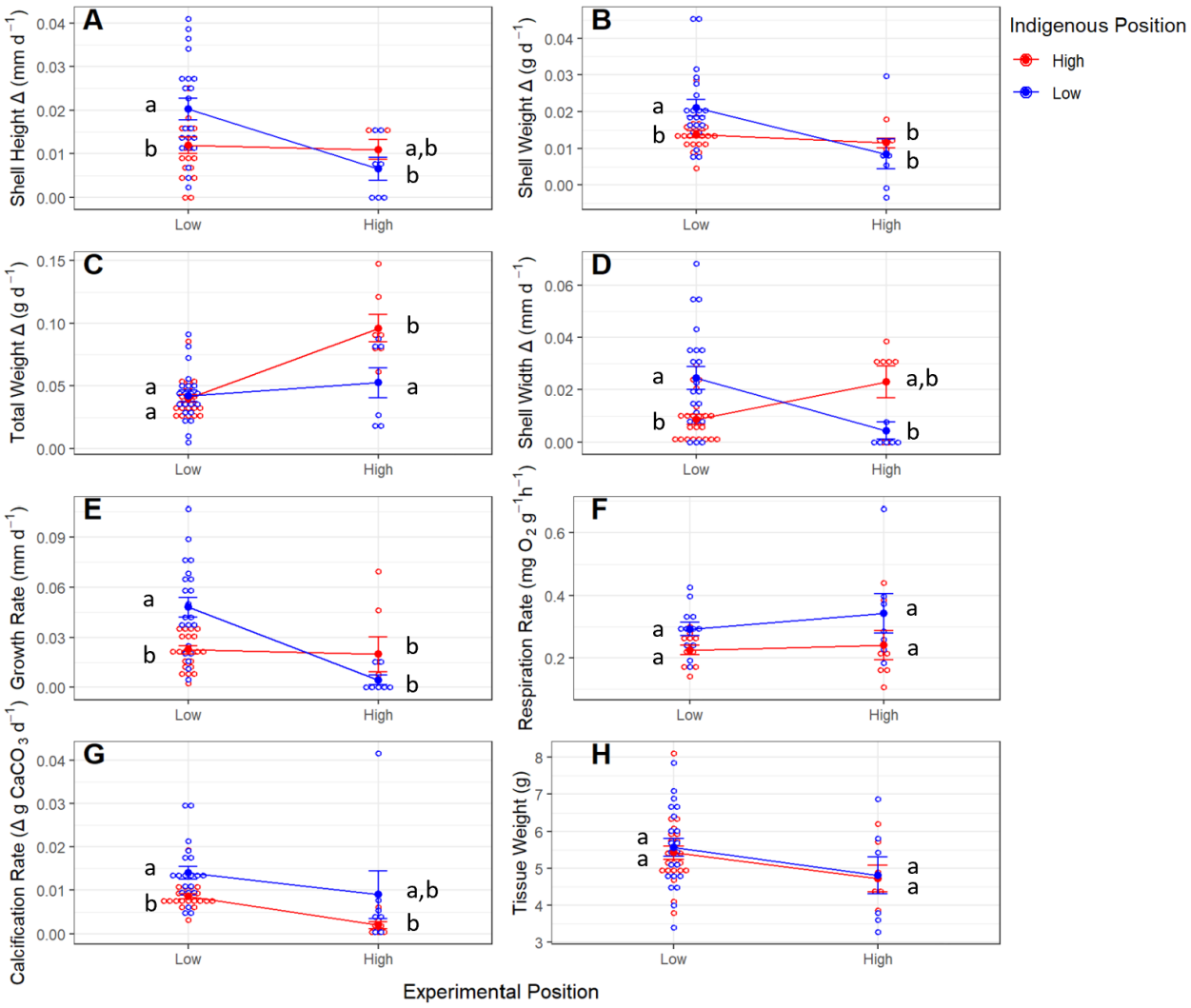

Figure 1.5: (A) Shell height change (mm d^{-1}), (B) shell weight change (g d^{-1}), (C) total weight change measured as weight in air (g d^{-1}), (D) shell width change (mm d^{-1}), (E) growth rate measured as change in shell length (mm d^{-1}), (F) respiration rate measured as oxygen consumption (mg O_2 g^{-1} h^{-1}), (G) net calcification rate measured as change in buoyancy (g $CaCO_3$ d^{-1}), and (H) tissue weight (g) of in-situ and transplanted *Mytilus californianus* individuals positioned in the low or high intertidal throughout the reciprocal transplant experiment. Individual data points and means ± SE are shown. Different letters beside each symbol indicate significant differences between experimental treatments evaluated using the Tukey HSD test as a post hoc comparison.

Table 1.1: ANOVA results for mussel responses to a reciprocal transplant. Effects on (a) shell height (mm d^{-1}), (b) shell weight estimated as the buoyant weight (g d^{-1}), (c) total weight measured as weight in air (g d^{-1}), (d) shell width (mm d^{-1}), (e) shell length (mm d^{-1}), (f) respiration rate measured as oxygen consumption (mg O_2 g^{-1} h^{-1}), (g) net calcification rate measured as change in buoyancy (g $CaCO_3$ d^{-1}), and (h) tissue weight (g) in in-situ and transplanted *Mytilus californianus* individuals positioned in the low or high intertidal throughout a reciprocal transplant experiment. Bold text shows significant p-values at $\alpha = 0.05$. Data plotted in Figure 1.5.

Biological responses	**Source**	**df**	**MS**	**F**	**p**
a. Shell height Δ (mm d^{-1})	Indigenous position (IP)	1	0.0003	4.113	**0.0476**
	Experimental position (EP)	1	0.0005	6.259	**0.0155**
	IP x EP	1	0.0004	4.72	**0.0343**
	Residuals	53	0.0001		
	Total	56			
b. Shell weight Δ (g d^{-1})	IP	1	0.0003	5.051	**0.0288**
	EP	1	0.0005	9.516	**0.0032**
	IP x EP	1	0.0002	4.485	**0.0389**
	Residuals	53	0.0001		
	Total	56			
c. Total weight Δ (g d^{-1})	IP	1	0.0011	2.385	0.1285
	EP	1	0.0118	25.676	**<0.0001**
	IP x EP	1	0.0055	12.034	**0.0011**
	Residuals	53	0.0005		
	Total	56			
d. Shell width Δ (mm d^{-1})	IP	1	0.0008	3.554	0.0649
	EP	1	0.0001	0.371	0.5453
	IP x EP	1	0.0031	14.722	**0.0003**
	Residuals	53	0.0002		
	Total	56			
e. Growth rate (mm d^{-1})	IP	1	0.0033	7.829	**0.0072**
	EP	1	0.0056	13.324	**0.0006**
	IP x EP	1	0.0044	10.46	**0.0021**
	Residuals	53	0.0004		
	Total	56			
f. Respiration rate	IP	1	0.061	5.953	**0.0201**
(mg O_2 g^{-1} h^{-1})	EP	1	0.0096	0.934	0.3406
	IP x EP	1	0.0028	0.273	0.6050
	Residuals	34	0.0103		
	Total	37			
g. Net calcification rate	IP	1	0.0005	10.545	**0.0020**
(g $CaCO_3$ d^{-1})	EP	1	0.0004	7.983	**0.0066**
	IP x EP	1	0.0001	0.145	0.7045
	Residuals	53	0.0001		
	Total	56			
h. Tissue weight (g)	IP	1	0.209	0.195	0.6609
	EP	1	5.574	5.192	**0.0268**
	IP x EP	1	0.008	0.007	0.9337
	Residuals	53	1.074		
	Total	56			

Growth rates, measured as change in shell length, of in-situ low mussels in their indigenous position (0.047 ± 0.005 mm d^{-1}) were significantly higher than mussels indigenous to the high intertidal for both treatments (in-situ: 0.019 ± 0.010 mm d^{-1}; Tukey HSD test: $p = 0.013$, transplant: 0.022 ± 0.002 mm d^{-1}; Tukey HSD test: $p = 0.0008$, Figure 1.5E). However, in the high intertidal plot in-situ mussels had higher growth rates than transplanted mussels indigenous to the low intertidal (0.019 ± 0.010 versus 0.004 ± 0.002 mm d^{-1}, Figure 1.5E) indicated by the significant interaction between indigenous and experimental position on the growth rates of individual mussels (Table 1.1e).

In their indigenous position, mussels from the low intertidal had significantly higher metabolic rates (0.292 ± 0.016 mg O_2 g^{-1} h^{-1}), measured as oxygen consumption, compared to high intertidal mussels (0.240 ± 0.046 mg O_2 g^{-1} h^{-1}; One-way ANOVA: $F_{(1,35)} = 6.087$, $p = 0.0185$, Figure 1.5F). Experimentally transplanting mussels had no significant effect on oxygen consumption rates for mussels (Table 1.1f); transplanted mussels from the low intertidal maintained higher metabolic rates than mussels from the high intertidal regardless of where they were transplanted (0.342 ± 0.062 versus 0.240 ± 0.046 mg O_2 g^{-1} h^{-1}, Figure 1.5F) and mussels indigenous to the high intertidal maintained lower metabolic rates regardless of their position (0.225 ± 0.01 versus 0.292 ± 0.016 mg O_2 g^{-1} h^{-1}, Figure 1.5F). Metabolic rate assays from in-situ neighboring individuals not used in the reciprocal transplant experiment confirmed these results as low individuals maintained higher metabolic rates (0.374 ± 0.026 mg O_2 g^{-1} h^{-1}) compared to high intertidal individuals in common garden experiments (0.234 ± 0.022 mg O_2 g^{-1} h^{-1}; One-way ANOVA: $F_{(1,30)} = 16.8$, $p = 0.0003$). Additionally, there was no significant difference in metabolic rates between experimental and non-experimental individuals suggesting

that the transplantation itself did not significantly impact mussel function (Mann–Whitney U test: W = 716, p = 0.205).

Net calcification rates in mussels, measured as change in buoyancy, responded similarly to metabolic rates, where mussels indigenous to the low intertidal maintained higher net calcification rates than both transplanted (0.014 ± 0.001 versus 0.008 ± 0.0006 g $CaCO_3$ d^{-1}, Figure 1.5G) and in-situ (0.009 ± 0.005 versus 0.001 ± 0.0008 g $CaCO_3$ d^{-1}, Figure 1.5G) mussels indigenous to the high intertidal. However, experimental position was shown to have a significant effect (Table 1.1g) where mussels positioned in the low intertidal had net calcification rates that were two times greater than mussels positioned in the high intertidal (0.011 ± 0.0008 versus 0.005 ± 0.0028 g $CaCO_3$ d^{-1}), likely due to the longer periods of time spent underwater to feed and biomineralize $CaCO_3$.

For juvenile mussels, oxygen consumption rates at these smaller life stages were similar to adult mussels where experimental position again did not significantly affect metabolic rate (Figure 1.6A and Table 1.2a), though juvenile mussels did have significantly higher metabolic rates (1.130 ± 0.112 mg O_2 g^{-1} h^{-1}) when compared to adult mussels (0.270 ± 0.017 mg O_2 g^{-1} h^{-1}; One-way ANOVA: $F_{(1,55)} = 103.8$, $p = < 0.0001$). Juvenile mussels also exhibited net calcification totals that were two times greater in the low intertidal than the high intertidal (0.286 ± 0.026 versus 0.100 ± 0.018 g $CaCO_3$, Figure 1.6B and Table 1.2b), however, adult mussels had significantly higher net calcification rates (0.009 ± 0.001 g $CaCO_3$ d^{-1}) when compared to juvenile mussels (0.003 ± 0.0003 $CaCO_3$ d^{-1}; One-way ANOVA: $F_{(1,55)} = 11.73$, $p = 0.0012$).

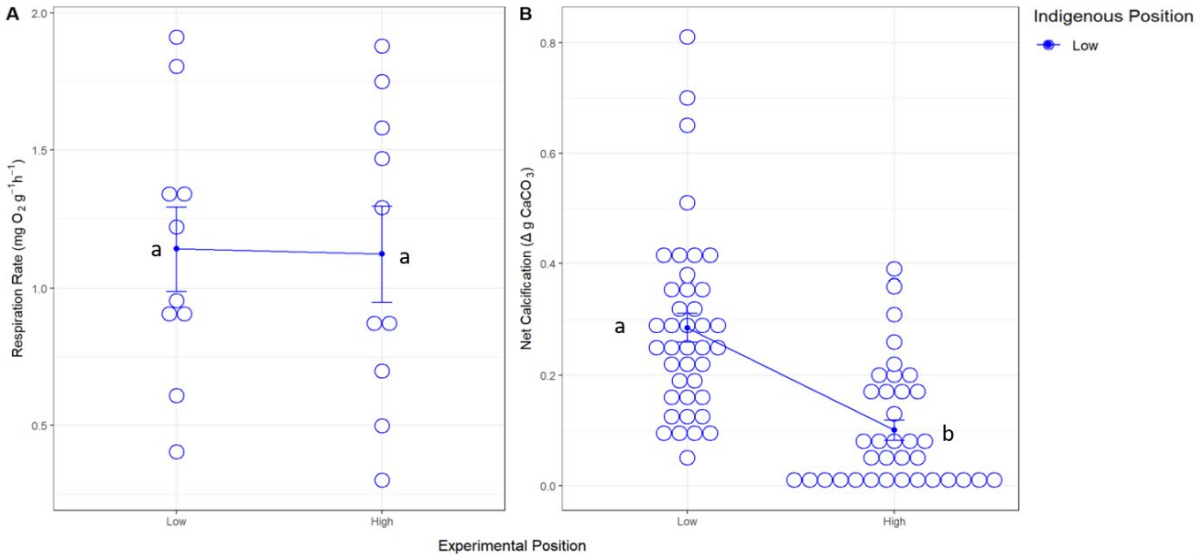

Figure 1.6: (A) Juvenile respiration rate measured as oxygen consumption (mg O_2 g^{-1} h^{-1}) and (B) net calcification measured as total change in buoyancy (g $CaCO_3$) of in-situ and transplanted juvenile *Mytilus californianus* individuals positioned in the low or high intertidal throughout the transplant experiment. Individual data points and means ± SE are shown. Different letters beside each symbol indicate significant differences between experimental treatments evaluated using the Tukey HSD test as a post hoc comparison.

Table 1.2: ANOVA results for juvenile mussel responses to a transplant. Effects on respiration rate measured as (a) oxygen consumption (mg O_2 g^{-1} h^{-1}) and (b) net calcification total measured as change in buoyancy (g $CaCO_3$) in in-situ and transplanted *Mytilus californianus* (juvenile) individuals positioned in the low or high intertidal throughout a transplant experiment. Bold text shows significant p-values at $\alpha = 0.05$. Data plotted in Figure 1.6.

Biological responses	**Source**	**df**	**MS**	**F**	**p**
a. Respiration rate	Experimental position (EP)	1	0.0018	0.007	0.936
(mg O_2 g^{-1} h^{-1})	Residuals	18	0.2665		
	Total	19			
b. Net calcification	EP	1	0.6516	31.95	**<0.0001**
(g $CaCO_3$)	Residuals	74	0.0204		
	Total	75			

Tissue weights in *M. californianus* individuals were lower for both transplanted and in-situ mussels positioned in the high intertidal (4.76 ± 0.30 g) when compared to transplanted and in-situ mussels positioned in the low intertidal (5.48 ± 0.151 g, Figure 1.5H and Table 1.1h), while indigenous position did not significantly affect tissue mass (Figure 1.5H and Table 1.1h). The long-term transplant experiment with juvenile mussels showed even greater differences in

tissue mass between mussels positioned in the low or high intertidal; low intertidal individuals maintained significantly higher tissue weights (4.14 ± 0.15 g) when compared to high intertidal individuals (1.84 ± 0.08 g; One-way ANOVA: $F_{(1,53)} = 99.25$, $p < 0.0001$).

Visualizing all trait parameters from the reciprocal transplant experiment with PCA further demonstrated the dual influence the environment and indigenous position had on trait and morphological variation in mussels as phenotypic variation significantly differed among treatments (PERMANOVA: $F_{(3,53)} = 6.289$, $R^2 = 0.26$, $p = 0.001$, Figure 1.7). PC1 described 44.4% of the variation and was positively correlated with calcification rate, growth rate, and change in shell width, height, and weight. PC2 described 20% of the variation and was positively correlated with respiration rate and negatively correlated with tissue weight. The PCA plot portrays that individuals indigenous to the low intertidal were strongly correlated to traits associated with PC1, while in-situ individuals indigenous to the high intertidal were strongly correlated to traits associated with PC2. Transplanted individuals indigenous to the low intertidal differentiated from low in-situ individuals by showing stronger correlations to PC2 corresponding to the decreases in tissue weight (Figure 1.5H) that were observed for those individuals throughout the experimental period. Alternatively, transplanted individuals indigenous to the high intertidal differentiated from high in-situ individuals by showing stronger correlations to PC1 corresponding to the increased net calcification rate that were observed for those individuals throughout the experimental period (Figure 1.5G).

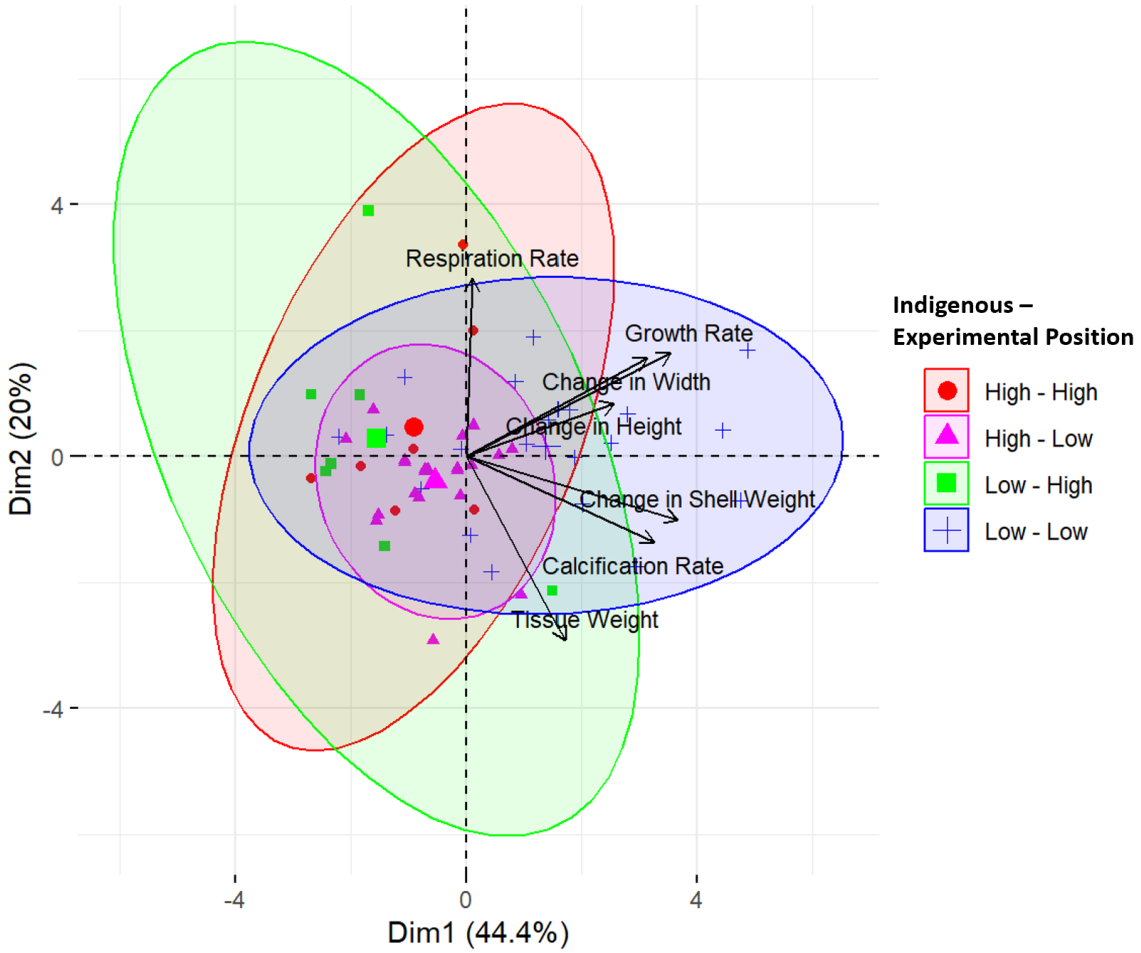

Figure 1.7: Biplot of Principal Component Analysis (PCA) showing changes in phenotypic traits based on treatment for adult *Mytilus californianus* individuals throughout a reciprocal transplant experiment.

Age variation within populations

The age composition of the low and high intertidal mussels 39-51mm in length ranged from 2 to 7 years of age. However, mussels from the high intertidal were significantly older, ranging from 4 to 7 with a mean of 5 years of age, compared to 3 years of age for low intertidal individuals (Students T-test: $t\ (44) = 12.2$, $p < 0.0001$). Additionally, mussels indigenous to the high intertidal showed higher age variability with a coefficient of variation of 0.158 compared to low intertidal mussels with a coefficient of variation of 0.151 (F test: $F_{(\text{low df: } 27, \text{ high df: } 28)} = 0.3145$, $p = 0.0035$).

Spatially varying selection on micro-geographic scales

Analysis of the 638 candidate SNVs revealed high genetic differentiation with an average F_{ST} of 0.20 among the five populations. The experimental population on Tatoosh Island had a lower mean observed heterozygosity (H_O = 0.26) across both low and high intertidal individuals compared to the four inland populations (H_O = 0.40) and the expected heterozygosity (H_E = 0.44), signifying a reduction in genetic variability within the Tatoosh Island population. Furthermore, the Tatoosh Island population had a higher proportion of candidate SNVs compared to the inland populations (P_O: 0.47 versus 0.44). Of the 638 candidate SNVs, 222 were non-synonymous mutations. Annotation of the 222 non-synonymous variants using eggNOG-mapper 2.1.12 uncovered multiple functional genes that have been characterized as affecting fitness across many bivalve species. These include genes involved in osmotic stress: VWDE (Abo-Al-Ela & Faggio, 2021); oxidative stress: TXR (Wang et al., 2013); immune response: ubiquitin-protein, BIRC2 (Nie, Jiang, et al., 2020; Place et al., 2012); antioxidant defense: GPX3 (Hlaing et al., 2020); DNA repair and recombination: RAD54 (Connor & Gracey, 2020); biomineralization: CA14 (Malachowicz & Wenne, 2019); and heat stress: HSP70 (Hofmann & Somero, 1995; Kourtidis et al., 2006; Liu et al., 2014; Nielsen et al., 2021; Place et al., 2012).

DISCUSSION

Evidence for phenotypic plasticity

Environmental and possible genetic influences on phenotypic variation in the intertidal mussel *M. californianus* were revealed by the reciprocal transplant and transplant experiments, demonstrating that environmental factors vary spatially, and result in spatially varying differentiation. The significant interaction between indigenous and experimental position on morphological traits such as shell length, shell height, shell weight, total weight, and shell width

(Table 1.1), suggest a genotype x environment interaction generates phenotypic variation among these traits in *M. californianus* mussels. Indigenous and experimental position also significantly affected net calcification rates for both adult and juvenile mussels; however, the lack of a significant interaction between indigenous and experimental position (Tables 1.1 and 1.2) suggests both genotype and environment affect calcification but not an interaction between the two. Alternatively, for tissue weights only the environment had a significant effect (Table 1.1h), while indigenous position and genotype were not significant. Thus, we can conclude that phenotypic differences in shell morphology, calcification, and tissue weight are a result of phenotypic plasticity with genotype or canalization having an additional effect on shell morphology and calcification but no effect on tissue weight. Given that heat stress and limited food availability has been shown to decrease tissue weight in *M. californianus* individuals (Fitzgerald-Dehoog et al., 2012), the decreases in tissue weights for animals that were positioned in the high intertidal are most likely a cost to being in an environment that experiences prolonged heat and aerial exposure events, whereas morphological plasticity is a tradeoff that allows these animals to maximize fitness in different environments. These results demonstrate that morphological traits for populations who range across heterogenous environments may exhibit phenotypic plasticity over fixed phenotypes or local adaptation.

Evidence for local adaptation

Local adaptation is advantageous when phenotypic plasticity, which allows an organism to adjust to varying environments, is costly and constrains the fitness of a single (plastic) genotype across diverse conditions, resulting in distinct genetic variants adapted to specific environments within a population (Tienderen, 1997; Yeaman, 2022). As selective pressures intensify, divergent selection enhances genetic differentiation by counteracting the neutral effects

of gene flow, thereby promoting local adaptation and reducing plasticity (Wadgymar et al., 2022; Wright, 1969). In the case of *M. californianus*, the metabolic rates of both adult and juvenile mussels were unrelated to where they were transplanted. Instead mussels retained the features of their indigenous position (Tables 1.1 and 1.2), indicating that oxygen consumption in mussels is locally canalized or adapted to the specific conditions of their native environment and is not a plastic response to environmental conditions. Notably, mussels from high intertidal zones, which experience greater heat and aerial exposure stress, maintained lower metabolic rates compared to those from low intertidal, even when they were transplanted to the more favorable low intertidal (Figure 1.5F).

Analyses of the DNA sequences of low and high intertidal mussels revealed further evidence of local adaptation; individuals indigenous to the high intertidal had increased frequencies of non-synonymous mutations in HSP70, a protein known to be differentially expressed between high and low *M. californianus* mussels (Place et al., 2012) and shown to significantly affect fitness across all 6 *Mytilus spp*. (e.g. Hofmann & Somero, 1995; Kourtidis et al., 2006; Liu et al., 2014; Nielsen et al., 2021; Osores et al., 2017; Roberts et al., 1997). Individuals indigenous to the low intertidal also had increased frequencies of non-synonymous mutations in CA14, a protein involved in calcification (Malachowicz & Wenne, 2019). Non-synonymous mutations can be an indicator of adaptive evolution (McDonald & Kreitman, 1991), and increased allele frequencies are typically linked to adaptive genetic differentiation (Jump et al., 2006; Liggins et al., 2020) that leads to a reduction in genetic variability (Bulmer, 1971). Here, WGS suggest that high intertidal individuals experience increased selection in HSP70, whereas low intertidal individuals experience increased selection in CA14. Our demonstration that in-situ individuals indigenous to the high intertidal had increased growth rates compared to

transplanted individuals (Figure 1.5E), while individuals indigenous to the low intertidal had increased calcification rates compared to individuals indigenous to the high intertidal (Figure 1.5G), indicates that particular proteins may enable organisms to thrive in their specific environmental niches.

Genetic consequences of adaptive traits

Quantifying phenotypic change across a population that spans a strong ecological gradient reveals the patterns and processes driving adaptive trait evolution. For example, if environmental and genetic influences on phenotypic variation act in concert (selection and plasticity covary positively), phenotypic differences will be distinct among native environments, and the phenotype of transplanted individuals would converge toward the indigenous phenotype, a phenomenon termed cogradient variation (CoGV) (Trussell, 2000). In contrast, if environmental and genetic influences on phenotypic variation act in opposition (selection and plasticity covary negatively), there is little phenotypic variation among native individuals, and transplanted individuals would be distinct in their phenotype from the native phenotype in the same environment, known as countergradient variation (CnGV) (Levins, 1968). The effects of CoGV and CnGV on functional trait evolution has revealed that CoGV traits more often involve morphology, whereas CnGV traits primarily involve physiological characteristics (Conover et al., 2009; Marcil et al., 2006). Our results support these findings as morphological traits in *M. californianus* mussels demonstrated greater phenotypic plasticity than physiological traits such as metabolic rate. Here, as in other studies within species (Conover et al., 2009; Marcil et al., 2006), we can expect functional differences in how traits evolve in response to environmental change.

Evolutionary changes in species traits are dependent on the rate and direction of environmental change and existing genetic variation within plastic or local adapted phenotypes. In changing environments, adaptive phenotypic plasticity can often ameliorate extinction by allowing time for populations to respond to new conditions (Kelly, 2019). Additionally, genetic variation within plastic traits can lead to selection for plasticity resulting in increased plasticity toward new fitness optimums, known as genetic accommodation (Baldwin, 1896; Lande, 2009; Scheiner et al., 2017). However, if the magnitude of change across a species range exceeds the thresholds of plasticity or plasticity decreases organismal fitness in their new environment (i.e. maladaptive plasticity) (Stamp & Hadfield, 2020), an adaptive phenotypic response can be delayed and the chance of extinction increased (Scheiner et al., 2017). In cases such as this where environmental change is large, locally adapted traits that are tightly linked and characterized by coadapted gene complexes are selected as they can be inherited in a single generation (Yeaman, 2022). This results in the rapid adaptation of populations as coadapted gene complexes selectively sweep through a population (i.e. soft sweep) which decreases the likelihood of extinction (Messer & Petrov, 2013) and increases organismal fitness in the new environment. However, in the long term soft sweeps could be disadvantageous for organisms who persist across rapidly fluctuating environments, such as the marine intertidal, as it reduces genetic variability and phenotypic plasticity thereby reducing organismal response to diverse conditions (Lalejini et al., 2021). The interplay between genetic variation and environmental change on adaptive traits is crucial for the survival of populations in changing ecosystems. While adaptive phenotypic plasticity and the rapid adaptation of locally adapted traits can mitigate extinction risks, the potential drawbacks, such as maladaptive plasticity and reduced genetic diversity, underscore the complexities of evolutionary responses in dynamic environments.

Understanding the genetic consequences increasing selective pressures have on different functional traits across ecological gradients is essential for predicting how species will cope with ongoing environmental challenges and will assist resource managers to proactively plan for these changes.

Drivers of microgeographic differentiation

The selective pressures associated with emersion stress within the marine intertidal is repeatedly associated with intraspecific differentiation on microgeographic scales (<10m) and is likely a significant driver of genetic and phenotypic divergence in intertidal marine species (Hays et al., 2021). This phenomenon arises partly from the combined effects of daily tidal fluctuations and coastal elevational gradients, which create daily temperature ranges comparable to those observed across extensive latitudinal gradients that exceed 1000 km, yet occur on scales of less than 10 m (Denny et al., 2011; Helmuth et al., 2006). Abiotic forces in the marine intertidal lead to divergence in *M. californianus* mussel beds along elevational gradients, as demonstrated by thicker shells (Figure 1.3A) and increased periostracum loss from increased incidence by endolithic phototroph infestation (Figure 1.2) (Gehman & Harley, 2019). While endolithic phototroph infestation is often lethal in *Mytilus spp.* because it accelerates shell degradation rates (Marquet et al., 2013), it can be beneficial for high intertidal individuals as the loss of periostracum whitens the individual's shell significantly increasing reflectivity and decreasing body temperatures during extreme heat stress thereby reducing mortality (Gehman & Harley, 2019; Zardi et al., 2016).

Abiotic factors similarly shape elevational gradients and drive species differentiation in terrestrial systems as well. In mountainous regions, higher elevations are linked to lower temperatures, increased soil moisture, and shorter growing seasons (Anderson & Gezon, 2015;

Dunne et al., 2003), leading to microgeographic adaptations in various species. Examples include the perennial herb *Boechera stricta* (Anderson et al., 2015), the deciduous tree *Fagus sylvatica* (Gauzere et al., 2020), and insects such as *Dichroplus pratensis* and *D. vittatus* (Bidau et al., 2012). In both marine and terrestrial systems, strong environmental gradients generate selective pressures strong enough to override the neutralizing effects of gene flow leading to microgeographic adaptation. These extreme gradients contribute to genetic and phenotypic divergence in species, revealing how the intensity of environmental stressors on small spatial scales contributes to the evolution and adaptation of species who persist across heterogenous environments.

CONCLUSION

The complex relationship between genetic and environmental influences on phenotypic variation presents a major challenge to understanding the consequences of global change for species. In this study, we provided empirical evidence of spatially varying selection driving trait differentiation within the marine intertidal showing that adaptive trait evolution differs between functional traits, and that future evolutionary responses will be determined by the magnitude of environmental change and existing genetic adaptations (Burrows et al., 2011; Sunday et al., 2011). For foundation species, these responses will undoubtably reverberate through communities and alter ecosystem function (Des Roches et al., 2018; Smee et al., 2013; Whitham et al., 2020). Although there is evidence of the community and ecosystem implications of intrapopulation variation in foundational species (Hersch-Green et al., 2011), our understanding of the microevolutionary processes responsible for creating and sustaining within-species genetic diversity remains relatively limited. Our experiments revealed high intertidal mussels, who persist in an extreme environment, had significantly lower metabolic rates, greater age

variability, and increased frequencies of non-synonymous mutations in functionally relevant genes like HSP70 compared to their low intertidal counterparts, suggesting intrapopulation differentiation may play a key role in species persistence in stressful environments. As global change intensifies stress gradients across species ranges, understanding how these evolutionary responses feedback into phenotypic response and other ecological processes will be imperative for predicting future ecosystem function.

DATA AVAILABILITY

Genetic data deposited to the National Center for Biotechnology Information's (NCBI) Sequence Read Archive (BioProject ID: PRJNA1245383). Data and code used for analyses are made available on Dryad (https://datadryad.org/share/eJjTOSjG7Ile4_dRFjkLvpr8MDNqCwMmxTzwwTLUtwc).

APPENDIX A: SUPPLEMENTAL INFORMATION FOR CHAPTER 1

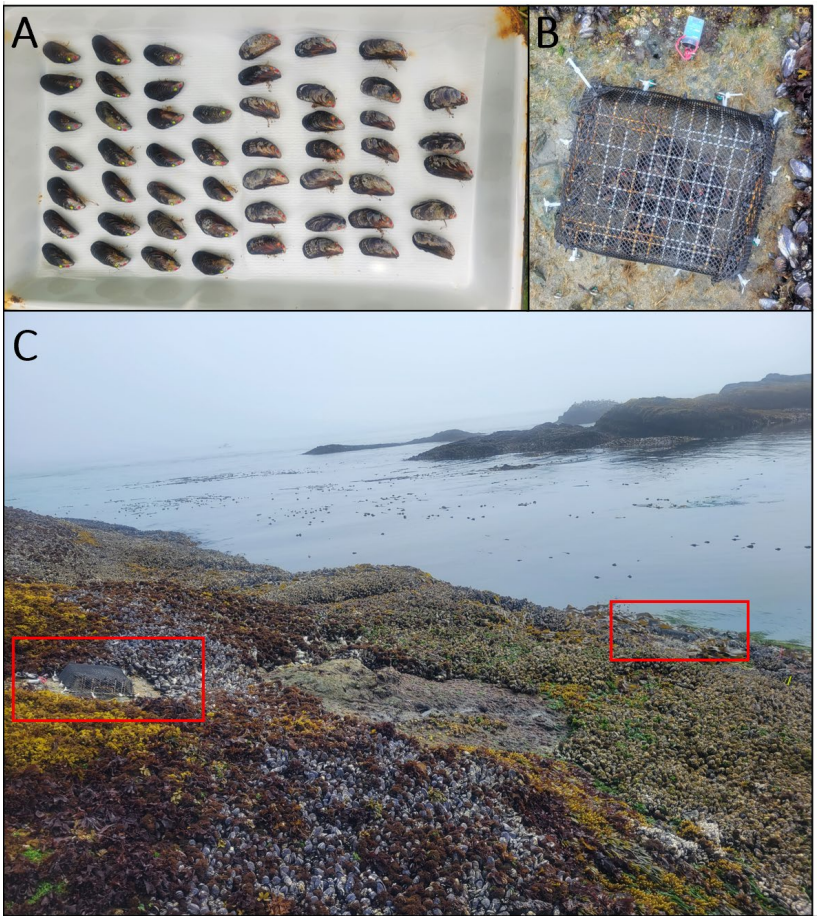

Figure A1: Site and design of reciprocal transplant experiment. (A) Individual mussels marked using glued bee tags and EZ Poxy paint on umbo of left and right shell valve (not all individuals depicted). (B) Cages with vexar mesh to house individual mussels in experimental plots. (C) Site of experimental intertidal plots for in-situ and transplanted mussels.

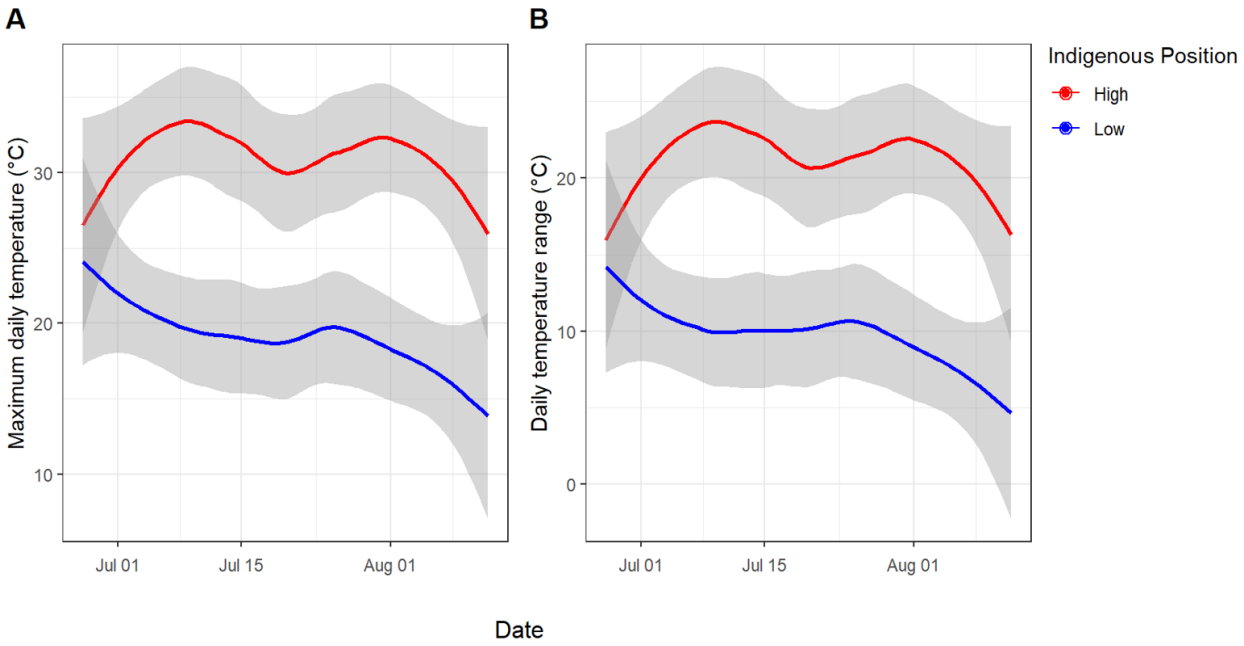

Figure A2: Regression lines of (A) maximum daily temperatures and (B) daily temperature ranges of low and high intertidal positions recorded in 5-minute intervals with Onset HOBO data loggers. Red and blue regression lines are from actual data using locally estimated scatterplot smoothing (LOESS) line where shaded grey areas represent the 95% CI.

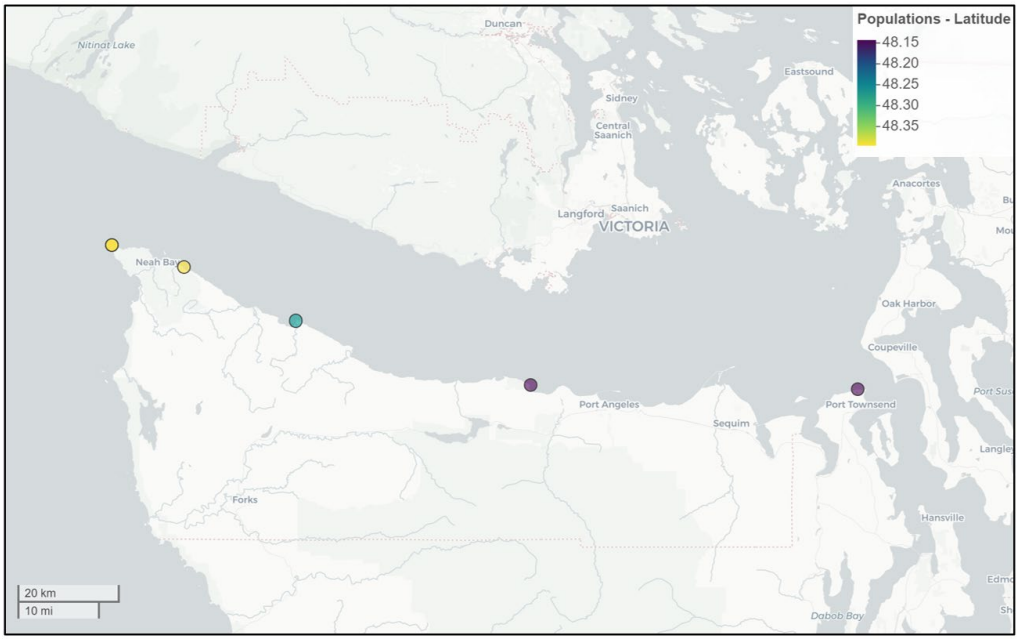

Figure A3: Locations of sampling sites 148km along the Strait of Juan de Fuca where 54 *Mytilus californianus* individuals were collected for Whole Genome Sequencing. Locations from left to right: Tatoosh Is., WA 48.394667, -124.736233; Snow Creek Boat Launch, WA: 48.355883, -124.547683; Slip Point, WA: 48.263817, -124.251717; Freshwater Bay, WA: 48.150733, -123.637883; Port Townsend, WA: 48.14415, -122.77735

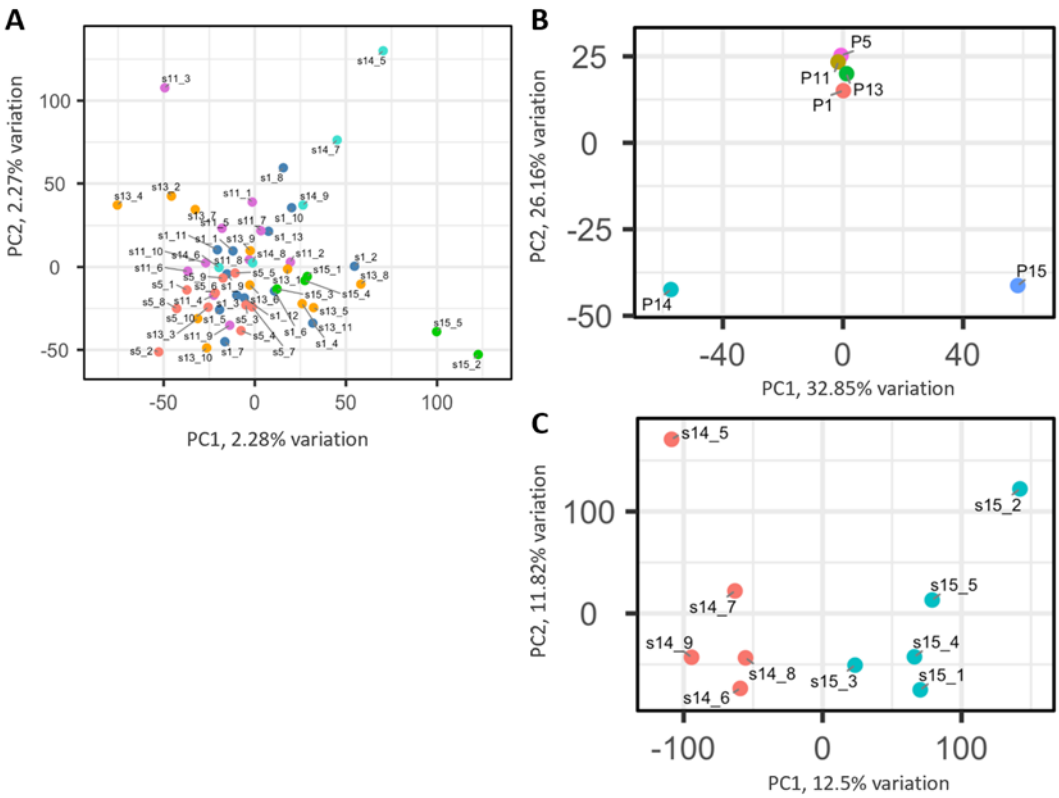

Figure A4: (A) Principal Component Analysis (PCA) of variant frequency for 54 *Mytilus californianus* individuals and (B) five populations using 133,617 Single Nucleotide Variants that had coverage in all samples and were present in at least 1 population at a frequency of 50% or higher. Numbers s14 (low intertidal) & s15 (high intertidal) in 4A correspond to Tatoosh Is. individuals. P14 (low intertidal) & P15 (high intertidal) in 4B correspond to the Tatoosh Is. population. (C) PCA using 19,000 Single Nucleotide Variants that had an absolute difference of proportion larger or equal to 0.0075 between 10 low (red dots) and high (blue dots) intertidal *M. californianus* individuals used in a reciprocal transplant experiment.

CHAPTER 2: GENETIC CONSEQUENCES OF ADAPTIVE TRAITS ACROSS HETEROGENOUS ENVIRONMENTS IN A BROADCAST SPAWNING SPECIES

ABSTRACT

In marine broadcast-spawning species, the interplay between selection and migration determines the genetic structure and adaptive potential of natural populations. Theory predicts that across spatially heterogeneous environments, strong selection can favor local adaptation over phenotypic plasticity, leading to the evolution of tightly linked genomic regions with large effects on organismal fitness. In contrast, spatially homogeneous environments are expected to favor phenotypic plasticity and lead to polygenic trait architectures where many alleles have a small effect on fitness. To test these hypotheses, we compared genetic and phenotypic responses across *Mytilus californianus* populations distributed along 181 km spanning from the western end of the Strait of Juan de Fuca, Washington, USA to Cattle Point, San Juan Island, a strong environmental gradient. We combined whole-genome sequencing with laboratory ocean manipulation experiments to assess metabolic responses of individuals exposed to decreased pH, elevated temperature, and decreased pH combined with increased temperature conditions. Populations on the outer coast and in the western Strait experience frequent low-pH conditions due to upwelling, while inner-coastal populations originating from the northern Salish Sea endure elevated sea surface and aerial exposure temperatures. Associated with these intense selective pressures, mussels from the inner coast of Washington exhibit increased linkage disequilibrium in heat shock proteins and decreased plasticity in increased temperature environments. Conversely, outer coastal populations, despite exhibiting reduced plasticity under low pH conditions, showed limited signatures of selection in fitness-related proteins, likely due to their larger effective population sizes limiting adaptive structural variation. Notably, centrally

located populations within the Strait of Juan de Fuca, which experience increased abiotic stress alongside higher migration rates, exhibited elevated plasticity across all treatments, tightly linked genomic regions, and higher genome-wide nucleotide diversity. This result suggest that gene flow between outer and inner coastal populations, coupled with increased selection, enhances the adaptive potential of these populations. Therefore, these findings support the hypothesis that strong selection across heterogenous environments favors local adaptation over plasticity in smaller populations which persist in stressful environments, even with high population connectivity. As ocean conditions continue to change, understanding the balance between local adaptation and phenotypic plasticity will be critical for predicting the resilience of marine species to environmental stressors.

INTRODUCTION

A fundamental theme of ecology and evolutionary biology is determining how genetic variation and the environment interact to shape phenotypic variation among populations. Understanding this relationship has become increasingly important as anthropogenic stressors continue to alter our planet, and standing genetic variation provides the raw material for adaptation to rapidly shifting environments (Barrett & Schluter, 2008; Bitter et al., 2019). For connected populations that persist throughout spatially heterogeneous environments, the balance between selection and migration will determine the genetic architecture of traits related to fitness and therefore, the rate of adaptation (Leimar et al., 2019; Yeaman & Whitlock, 2011). For example, in larger populations distributed across relatively homogenous environments, gene flow is often beneficial as it introduces novel genetic variation from surrounding populations, thereby maintaining intra-population diversity (Slatkin, 1985). Theoretical evidence suggests that this results in the evolution of loosely connected genetic architectures or polygenic traits that have

many small allelic effects on fitness leading to increased phenotypic plasticity (Yeaman, 2022). Alternatively, for smaller populations that persist in more extreme environments, the homogenizing effect of gene flow can be disadvantageous as the introduction of maladaptive alleles from foreign populations can lead to the loss of adaptive genetic variation in locally adapted populations due to a process known as "swamping" (Yeaman, 2015). A possible evolutionary response to this genetic conflict between connected populations is tightly linked clusters of Single Nucleotide Polymorphisms (SNPs) in locally adapted alleles (Nosil et al., 2009; Roda et al., 2017; Shi et al., 2023). However, these results have varied across taxonomic groups and systems (Schaal & Smith, 2023). Although simulations using two-allele model approaches have shown that strong selection associated with spatial environmental heterogeneity influences local adaptation by favoring tightly linked clusters of SNPs in isolated genomic regions (Bürger & Akerman, 2011; Yeaman & Otto, 2011), it has rarely been tested in natural systems (Yeaman, 2022). Sessile marine species that broadcast spawn such as mussels provide an excellent system to test these hypotheses as they are numerically abundant, highly panmictic, and adapted to a variety of environments (Gaitán-Espitia et al., 2016; Lourenço et al., 2017). They are also an ecologically important foundational species across ocean ecosytems (Gutiérrez et al., 2003; Paine & Levin, 1981).

Mytilus californianus is a bivalve species that dominates rocky intertidal shores throughout the northeastern Pacific Ocean (Gaitán-Espitia et al., 2016). Within its geographic range, a significant environmental gradient emerges within the Strait of Juan de Fuca as salinity fluctuations, sea surface temperature, and air temperature drastically increase moving eastward into the Strait of Juan de Fuca, while chlorophyll-*a* (food availability) decreases, creating conditions unfavorable for mussels (MacCready et al., 2021; Mackas & Harrison, 1997; Masson

& Peña, 2009). A study of the demographic history of *M. californianus* mussels within this region documented significant declines in mussel density and recruitment moving into the Strait of Juan de Fuca (Kandur, 2014). Declines in population density and recruitment have also been observed in other bivalve species persisting across a wide variety of environmental gradients, including salinity (Honig et al., 2015), aerial exposure (McGrorty & Goss-Custard, 1995), and wave exposure (Kotta et al., 2015). Strong environmental gradients in nature provide ideal conditions to experimentally test if strong selection associated with decreased migration favor the persistence of tightly linked clusters of SNPs in natural populations that reside in more extreme environments.

To test these hypotheses, we compared population structure in adaptive candidate loci and metabolic responses to experimentally induced environmental stress. We hypothesized that *M. californianus* mussels at open coast areas who live in larger populations, will exhibit polygenic trait architectures and therefore increased phenotypic plasticity. In contrast, mussels originating from the San Juan Islands in the Northern Salish Sea are geographically isolated, persist in smaller populations, and experience more intense abiotic pressures, so will exhibit locally adapted genomic architectures. Locally adapted genomic architectures are characterized by tightly linked clusters of SNPs that have a large effect on fitness, resulting in trait fixation (decreased plasticity) with traits optimized to the local environment to maximize fitness (Sultan & Spencer, 2002; Velotta & Cheviron, 2018; Yeaman, 2022). Using surveys across a 181km environmental gradient and an experimental manipulation of environmental stress, we compared population structure of divergent adaptive loci and the metabolic responses of mussels from different populations.

METHODS

Common garden experiments quantifying phenotypic plasticity across populations

In the summer of 2024, after shellfish transfer permits were obtained (WDFW Shellfish Transfer Permit # 24-1277) using preliminary results from Scientific Collection Permit: RICHARDS 23-290, we collected 72 individuals (approximately 40-55mm in length) from three of the 14 sampled populations analyzed genetically stratified across the environmental gradient (Tatoosh Island, Slip Point, Freshwater Bay; Figure 2.3A & 2.3B). All individuals werewere kept in a 19L aquarium filled with fresh seawater maintained at 12°C. The following morning, all 72 mussels (24 individuals per population) were transferred into a single 19L bucket filled with fresh seawater and transported to Friday Harbor Laboratories, WA in the San Juan Islands, and 24 additional individual mussels 40-55mm in length were collected on arrival at the furthest inner coastal site where mussels were previously sampled and genotyped at Cattle Point, San Juan Island Historical Park. To acclimate the mussels for the experimental treatments, all 96 mussels from the four populations were placed in a 113L quarantine aquarium maintained at 12°C for 96 hours that was emptied and filled with fresh seawater every morning. Mussels were fed with 5ml of Reef Phytoplankton (Seachem, Madison, Georgia, USA) added to the quarantine aquarium daily. After this acclimatization period, we assessed individual mussel response to pH and temperature changes to quantify phenotypic plasticity between populations. Mussels awaiting treatment remained in quarantine conditions until randomly selected.

Seawater pH and temperature for the treatment tanks were manipulated using tank heaters and equimolar additions of $NaHCO_3$ and HCl following the methods from Riebesell et al. (2010), allowing the responses of individual mussels across all populations to be assayed in a common garden experiment. The common garden experiment consisted of four 113L tanks (Igloo™

coolers) filled with the same fresh seawater: one control tank and three experimental treatment tanks. In the control tank, the ambient pH (7.95) and temperature (12 °C) of the inflowing seawater at Friday Harbor Laboratories was maintained using tank chillers. In the three treatment tanks, seawater conditions were experimentally manipulated as described above to create treatments of increased temperature (17 °C, pH: 7.95), decreased pH (12 °C, pH: 7.45), and increased temperature combined with decreased pH (17 °C, pH: 7.45).

The metabolic responses of mussels were assayed by placing four mussels from the same population in either the control tank or one of the experimental treatment tanks for approximately one hour. The four mussels were then removed from their treatment or control tank and immediately placed into individual closed 12-ounce glass containers that were filled with seawater from their respective tank for a 30-minute period where oxygen consumption over time (mg O_2 g^{-1} h^{-1}) was measured using a FireSting FSPRO-4 equipped with oxygen sensor spots and a temperature sensor (Pyroscience, Aachen, Germany). These steps were repeated for the other three populations on the same day. We replicated these experiments across multiple days (6X) until all 96 mussels had undergone an experimental treatment, alternating the order of the populations each day as a control. This experimental design yielded a dataset of metabolic responses from 96 individuals across four populations exposed to control conditions or environmentally induced stress (24 individuals per population; six individuals per control or treatment).

Metabolic responses were used to quantify phenotypic plasticity of respiration rates at the population level using the Plasticity Index (PI) from Valladares et al. (2006). The PI was used to estimate overall plasticity for each population as indices using maximum and minimum values are better estimators of overall plasticity when the degree of response across sampled

populations is not equal throughout heterogenous environments (e.g. lower/higher phenotypic values towards one end of the environmental gradient) (Valladares et al., 2006). Prior to analysis, respiration rates (mg O_2 g^{-1} h^{-1}) were log-transformed to reduce deviations from normality and heteroscedasticity. For each population, Plasticity Index (PI) scores were quantified by first calculating the mean respiration rate for each treatment (including control), where each treatment mean was calculated from 6 individuals per population. Let $\bar{R}_{T_i}$ denote the mean respiration rate of a given population under treatment T_i. The PI was then calculated as:

$$\text{PI} = \frac{\max \bar{R}_{T_i} - \min \bar{R}_{T_i}}{\max \bar{R}_{T_i}}, \quad \text{equation (1)}$$

where $\max(\bar{R}_{T_i})$ and $\min(\bar{R}_{T_i})$ represent the maximum and minimum treatment-specific mean respiration rates observed for that population across all experimental conditions. This formulation quantifies the proportional change in metabolic performance relative to the highest observed mean response. To estimate variability in PI while preserving the balanced experimental design, a systematic leave-one-replicate-out jackknife procedure was implemented (Efron, 1982). For each population, replicate i (where $i = 1, \ldots, 6$) was sequentially removed from every treatment group simultaneously, and PI was recalculated using the remaining replicates per treatment. This yielded six estimates of PI per population, where the mean and standard error of these estimates were used to characterize population-level variability in plasticity.

The Relative Distance Plasticity Index (RDPI) from Valladares et al. (2006) was also calculated as a complementary, scale-independent measure of phenotypic plasticity that incorporates within-population variation by performing pairwise comparisons. This is particularly advantageous when wanting to differentiate the effect each experimental treatment has on the plasticity of each population, as it compares phenotypic distances among individuals

exposed to different environments. Therefore, we calculated three separate RDPIs for each treatment using equation 2 and only respiration rates from the control and the focal treatment (increased temperature, decreased pH, and increased temperature combined with decreased pH).

$$\text{RDPI} = \sum(d_{ij} \rightarrow \text{i'j'}/(x_{\text{i'j'}} + d_{ij}))/n, \quad \text{equation (2)}$$

For a single population and trait, the data were structured as a matrix X_{ij}, where i(rows) represent environmental treatment and j(columns) represent an individual identity within each treatment. For all pairs of individuals in which $i \neq i'$(i.e., individuals exposed to different treatments), phenotypic distance $d_{ij \rightarrow i'j'}$ was calculated as the absolute difference between trait values ($| x_{i'j'} - x_{ij} |$). Relative distances were then obtained by dividing this difference by the sum of the paired trait values ($x_{i'j'} + x_{ij}$), yielding $rd_{ij \rightarrow i'j'} = d_{ij \rightarrow i'j'}/(x_{i'j'} + x_{ij})$. These calculations were performed for all valid inter-treatment pairs, where n represents the total number of pairwise comparisons. RDPI values range from 0 (no plasticity) to 1 (maximum plasticity). RDPI calculations and statistical summaries were implemented in R using the "rdpi" function from the "Plasticity" package (Ameztegui, 2017).

Statistical analysis of metabolic responses to environmental stress

All analyses were conducted in the R statistical platform version 4.4.1 (R Core Team, 2024). Respiration rates were first evaluated using a two-way ANOVA with population and treatment as the main fixed factors. We then performed stepwise model selection using Akaike Information Criterion (stepAIC), which indicated that respiration rate was best explained by treatment alone; the inclusion of population or the interaction term worsened model fit (increased AIC). Therefore, a one-way ANOVA was used to test the effect of treatment on respiration rate and to confirm that population did not have a significant effect. Tukey HSD (a posteriori comparison) was used to determine differences between groups. Differences in PI and RDPI

among populations were also evaluated using one-way ANOVA, followed by Tukey's HSD test for pairwise comparisons.

Whole Genome sequencing of DNA

To comprehensively profile population structure and signatures of local adaptation, we whole genome sequenced mussels across a naturally occurring environmental gradient in the Strait of Juan de Fuca (Pacific Northwest North America). At the population level, we collected *M. californianus* mussels along an 181km environmental gradient from Tatoosh Island, Makah Indian Reservation, Washington, at the western opening of the Strait of Juan de Fuca and to the furthest known inner coastal *M. californianus* population in the northern Salish Sea at Cattle Point, San Juan Island Historical Park, Washington (Figure 2.3A). In the summer of 2023, gill tissue from 75 *M. californianus* individuals 40-55mm in length were collected across 14 populations along this geographic extent, immediately placed in RNAlater (Introgen), and stored at −20°C until DNA extractions could be completed (WDFW Scientific Collection Permit # RICHARDS 23-290) (Figure 2.3A). Genomic DNA was extracted from gill tissue using the E.Z.N.A. DNA/RNA Isolation Kit (Omega Bio-Tek) according to the manufacturer's instructions. Whole genome DNA libraries were constructed using the NEB Ultra Express FS DNA library preparation kit (NEB Catalog #E3340L) following the manufacturers protocols. Analysis of the resulting DNA library size and quality of constructed DNA libraries was performed using a nanodrop spectrophotometer and Agilent Tape Station system. Whole Genome Sequence (WGS) libraries were pooled and sequenced on three NovaX-10B-300 lanes at the University of Chicago Functional Genomics Core Facility (RRID:SCR_019196), yielding an average coverage of 9.1× per sample (range: 3.28×–26.07×) across the 75 sequenced

individuals. The variation in sequencing coverage enabled haplotype-based analyses to detect candidate loci while retaining lower-coverage samples for population genomic analyses.

Read preprocessing and mapping

Raw sequencing reads from all samples were first quality-controlled and trimmed using fastp (version 1.3.3) to remove adapter sequences and low-quality bases (Chen et al., 2018). Trimmed reads were then screened for potential contamination using Kraken2 (version 2.17.0) (Wood et al., 2019) against a custom k-mer database, retaining only unambiguously assigned reads. Decontaminated reads were mapped to the *Mytilus californianus* reference genome (NCBI RefSeq assembly: GCA_021869535.1) (Paggeot et al., 2022), and individual alignment files were merged with samtools merge when multiple libraries existed per sample. Local realignment around indels was performed with GATK v4.6.2.0 to reduce alignment artifacts. The resulting BAM files provided the input for SNP calling and population genetic analyses.

Variant calling and filtering

Genotype likelihoods and single nucleotide polymorphisms (SNPs) were identified from aligned BAM files of sequenced *Mytilus californianus* individuals using ANGSD v0.940 (Korneliussen et al., 2014). The number of individuals sampled was used to set a minimum coverage threshold of 90% of individuals per site. Depth filters were applied using individual minimum and maximum coverage cutoffs derived from mean per-individual depth estimates as determined by mosdepth (Pedersen & Quinlan, 2018). To call SNPs, we employed the samtools genotype likelihood model (-GL 1) and applied multiple quality filters, including minimum mapping quality (-minMapQ 20), base quality (-minQ 20), and removal of poor-quality or ambiguous reads (-remove_bads 1, -uniqueOnly 1). Triallelic sites were skipped (-skipTriallelic 1), and only biallelic SNPs with minor allele frequency ≥ 0.05 were retained (-minMaf 0.05).

ANGSD also calculated per-site statistics, including allele counts, major/minor alleles (-doMajorMinor 1), Hardy–Weinberg equilibrium statistics (-doHWE 1), strand bias (-sb_pval 1e-6), and heterozygosity bias (-hetbias_pval 1e-6). The program produced multiple output files: a SNPs statistics file (.snpStat.gz), a minor allele frequency file (.mafs.gz), a Hardy–Weinberg statistics file (.hwe.gz), and genotype likelihoods in Beagle format (.beagle.gz). The total number of SNPs was determined from the SNPs statistics file, which includes one row per variant site. These ANGSD-derived outputs included genotype likelihoods, allele frequencies, and SNP statistics which provided the input data for subsequent population structure analysis.

Population structure and clustering analysis

Filtered SNPs from ANGSD were used as input for PCAngsd (Meisner & Albrechtsen, 2018) to estimate individual covariance and population structure without relying on hard genotype calls. From the covariance matrix generated by PCAngsd, principal components were computed and plotted to visualize genetic clustering among individuals, highlighting patterns of population differentiation and admixture (Figure 2.3B & 2.3C). The optimal number of ancestral populations (K) was determined using the ΔK method from Evanno et al. (2005). For each tested value of K, replicate NGSadmix (Meisner & Albrechtsen, 2018) runs were performed and the mean log-likelihood of the data, $L(K)$, and its standard deviation were calculated across runs. Because $L(K)$ often plateaus or increases monotonically with increasing K, ΔK was used to identify the value of K corresponding to the strongest change in likelihood. ΔK was calculated based on the second-order rate of change of the likelihood function with respect to K. Specifically, first-order differences were computed as $L'(K) = L(K) - L(K-1)$, and second-order differences as $L''(K) = L'(K+1) - L'(K)$. The absolute values of these second-order differences were scaled by the standard deviation of $L(K)$ across replicates to obtain ΔK. The

value of *K* corresponding to the maximum ΔK was interpreted as the most likely number of ancestral populations. For each *K*, the replicate run with the highest log-likelihood was retained to generate diagnostic summary tables and Evanno plots to evaluate model support across K values. Although likelihoods continued to increase with K, ancestry estimates stabilized at K = 3, with additional clusters at higher K primarily subdividing existing structure without revealing biologically distinct groups (Figure B1).

Using K = 3 as our best estimate, individual ancestry proportions were estimated with NGSadmix. The resulting Q-matrix was post-processed to summarize individual cluster membership and admixture status. Individual ancestry proportions (q_K1, q_K2, q_K3) were extracted from the NGSadmix output and summarized in real_clusters.tsv. For each individual, the ancestral cluster with the highest ancestry proportion was identified, and the difference between the largest and second-largest ancestry proportions was calculated as a measure of assignment confidence. Individuals were classified as belonging to a discrete cluster (K1, K2, or K3) when a single ancestry component predominated, whereas individuals lacking a strongly dominant ancestry component were classified as admixed. This file retains full quantitative ancestry estimates for all individuals, enabling visualization and interpretation of admixture patterns. To facilitate analyses requiring discrete population assignments, a simplified metadata table (meta_clusters.tsv) was generated from these results. This table retained only individual identifiers and final group designations (K1, K2, K3, or admixed), omitting quantitative ancestry values. Together, these outputs separate quantitative ancestry estimation from categorical population assignment, providing both detailed admixture information and standardized groupings for population genetic analyses. By restricting analyses to non-admixed individuals, these estimates provide robust measures of within- and among-population genetic variation while

minimizing the influence of recent admixture (Kidd et al., 2012; Long, 1991). For clarity, we renamed the ancestral clusters according to their predominant geographic distributions: K1 as the Central Strait ancestral cluster, K2 as the Northern Salish Sea ancestral cluster, and K3 as the Western Strait ancestral cluster.

Using the discrete population assignments described above, we estimated genetic diversity by calculating the fraction of heterozygous sites (H_o), nucleotide diversity (π), Watterson's θ (θ_W), and Tajima's D using the Site Frequency Spectrum (SFS) implemented in ANGSD v0.940 (Korneliussen et al., 2014). BAM lists were generated for each discrete cluster (Central Strait, Northern Salish Sea, Western Strait), excluding admixed individuals, to ensure that population-specific estimates were not confounded by recent gene flow. Genotype likelihoods were computed under the SAMtools model (-GL 1) with quality filters set at -minMapQ 20 and -minQ 20, duplicate and poorly mapped reads removed, and base alignment quality adjustments applied. For each population, one-dimensional SFS were estimated with -doSaf 1 and -doCounts 1 and subsequently processed with realSFS to produce maximum likelihood SFS. These SFS were converted to θ estimates with saf2theta, and summary statistics (π, θ_W, Tajima's D) were calculated genome-wide using thetaStat. Pairwise population comparisons were performed by generating two-dimensional SFS, which were used to compute F_{ST} with realSFS fst index/fst stats and absolute sequence divergence (d_{XY}) from allele frequency differences across all sites.

Estimates of spatial patterns of gene flow and population connectivity

Estimated Effective Migration Surfaces (EEMS) were calculated following the methods from Petkova et al. (2016) to visualize spatial population connectivity across the sampled *M. californianus* populations. To achieve this, we quantified pairwise F_{ST} between 11

geographically distributed populations with realSFS fst index/fst stats. These pairwise estimates were then reformatted into a symmetric population-by-population matrix, where diagonal elements were set to zero and off-diagonal elements correspond to pairwise F_{ST} values (Figure 2.4A). To generate a genetic dissimilarity matrix suitable for EEMS, the F_{ST} matrix was transformed using multidimensional scaling (MDS). Specifically, the matrix was decomposed using "cmdscale" in R, retaining $k = n - 1$ dimensions (where $n = 11$ populations), and Euclidean distances were calculated among populations in this reduced space, converting pairwise F_{ST} values into a distance matrix that satisfies the assumptions of EEMS. The resulting Euclidean distance matrix was exported as a numeric, header-free file for downstream analysis. EEMS analyses were conducted using a grid of 300 demes across the study region, with populations treated as diploid and a total of 10,858,565 sites included. Markov chain Monte Carlo (MCMC) simulations were run for 3,000,000 iterations, with a burn-in of 2,000,000 iterations and thinning every 9,999 steps. These results were summarized, examined for convergence, and plotted using the "rEEMSplots" R package (Petkova et al., 2016) (Figure 2.4B & 2.4C).

Detection of selection using haplotype-based statistics and linkage disequilibrium patterns

To complement SFS-based estimates with haplotype-level signatures of selection, we conducted population-specific phasing and haplotype-based scans using only individuals confidently assigned to a single ancestral cluster. SNPs corresponding to each cluster (Central Strait, Northern Salish Sea, Western Strait) were extracted from the filtered VCF and phased independently for each population using Beagle. Phased VCFs were indexed and converted to rehh-compatible formats. Within-population selection was assessed using the integrated haplotype score (iHS), while between-population contrasts were evaluated using cross-

population extended haplotype homozygosity (XP-EHH) for all pairwise population comparisons. XP-EHH analyses were conducted in R using the rehh package, with contig boundaries defined using a genome sizes file to accommodate a scaffolded reference genome. Selection statistics were calculated in non-overlapping 50kb windows along each contig, excluding contigs below the default minimum length threshold. Prior to calculation of haplotype-based statistics, SNPs were filtered for minor allele frequency (MAF ≥ 0.05) and genotype completeness. XP-EHH results were subsequently combined across contigs to generate genome-wide summaries and Manhattan-style plots, enabling identification of genomic regions exhibiting extreme haplotype differentiation (top 1%) consistent with recent or ongoing selection. This process identified 10,376 SNPs between the three identified genetic clusters which were used as our candidate loci in the downstream environmental association analysis described later.

To characterize patterns of linkage disequilibrium (LD) within populations and in genes of interest, we estimated LD decay separately for each ancestral cluster using ngsLD. Pairwise LD was calculated directly from genotype likelihoods for all SNP pairs within 50 kb of one another, using a minimum minor allele frequency threshold of 0.05. Genotype likelihoods, SNP positions, and sample sizes were provided to ngsLD to compute pairwise LD statistics (r^2) while accounting for genotype uncertainty. LD decay curves were then estimated by fitting r^2 as a function of physical distance using the fit_LDdecay.R script provided with ngsLD. LD decay was modeled using 250 bp distance bins up to a maximum distance of 50 kb, with uncertainty assessed via 100 bootstrap replicates. Decay curves were plotted on a scaled distance axis to facilitate comparison among populations, and the fitted LD decay profiles were used to evaluate the extent of linkage (Figure B2).

Environmental association analysis with candidate loci

To identify loci associated with environmental variation, we conducted environmental association analyses using Bayenv2 (Günther & Coop, 2013). Variant discovery was restricted to individuals classified as non-admixed individuals within each clustering group and sampled from their corresponding geographic locations of their corresponding genetic cluster to minimize confounding effects of admixture and the presence of individuals occurring outside their primary genetic cluster. The included individuals comprised three geographic locations: Cattle Point (Northern Salish Sea ancestral cluster), Port Townsend and Freshwater Bay (Central Strait ancestral cluster), and Tatoosh Island (Western Strait ancestral cluster) (Figure 2.3B). A multi-sample VCF was generated using bcftools mpileup and bcftools call against the *M. californianus* reference genome (GCF_021869535.1) (Paggeot et al., 2022). Variant filtering retained only high-quality, biallelic SNPs using the following criteria: minimum quality score (QUAL ≥ 30), minimum read depth (DP ≥ 5), and minimum mapping quality (MQ ≥ 30). Genotypes were extracted from the filtered VCF, and sites were further filtered to remove invariant loci and loci with missing data. Only polymorphic SNPs segregating within the dataset were retained. Additional filtering removed monomorphic comparisons across populations to ensure that all loci included in downstream analyses exhibited allele frequency variation. Filtered genotype data were converted to Bayenv2 input format using a custom Python script. Individuals were assigned to populations based on a population map file, and allele counts (reference and alternate) were summed within each population. For each SNP, two rows were generated corresponding to counts of the reference and alternate alleles across populations. To account for population structure, a covariance matrix was estimated using a random subset of 50,000 putatively neutral, unlinked SNPs from the ngsLD output. These loci were selected to minimize LD and the

influence of selection, ensuring an unbiased estimate of the underlying population covariance structure. The resulting covariance matrix was used in all subsequent Bayenv2 analyses.

Environmental data included sea surface temperature, air temperature, and pH (Table 2.1). Sea surface and air temperature values for each locale were derived from historical records from the nearest buoy (<10 km), calculated as the mean August temperature (the hottest month of the year) across all available years (https://www.ndbc.noaa.gov/). The average bottom pH for historical year 2000 from Khangaonkar et al. (2019) were used as inputs for pH. These variables were standardized (mean-centered and scaled by standard deviation) prior to analysis to ensure comparability across variables. Candidate SNPs were identified independently from genome-wide XP-EHH scans. Significant SNPs (top 1%) from all pairwise comparisons were combined, and duplicate genomic positions were removed. These candidate loci were then extracted from the filtered SNP dataset for environmental association testing. To facilitate computational efficiency, SNPs were split into batches of individual loci (two lines per SNP in Bayenv format). Bayenv2 was run on each SNP using the following parameters: 300,000 MCMC iterations, a fixed random seed (12345), four populations, and the precomputed covariance matrix. Bayes factors were calculated to assess the strength of association between allele frequencies and environmental variables. This analysis identified 275 SNPs with moderate associations to environmental covariates (Bayes factor >3 and <10) following the criteria of Kass and Raftery (1995), and an additional 26 SNPs with strong associations (Bayes factor >10) according to Jeffreys criteria (Jeffreys, 1998), which are available at Figshare: https://doi.org/10.6084/m9.figshare.32065689. The resulting environmentally associated SNP positions (Bayes factor >3 and Bayes factor >10, respectively) were converted to BED format using awk, and the longest isoform from each gene was derived from the reference genome

annotations (GCF_021869535.1) using agat_sp_keep_longest_isoform.pl from AGAT v1.5.1 (https://agat.readthedocs.io) (Dainat et al., 2024). The resulting annotations in GFF format were intersected with the environmentally associated SNP positions in BED format using bedtools v2.31.1 (Quinlan & Hall, 2010).

Table 2.1: Average air temperature, sea surface temperature, and pH values for each population used as environmental covariates in the environmental association analysis.

	Tatoosh Is.	Freshwater Bay	Port Townsend	Cattle Point
Air Temperature	12.5°C	14.8°C	14.8°C	15.1°C
Sea Surface Temperature	10.9°C	10.0°C	11.1°C	11.8°C
pH	7.70	7.80	7.85	7.85

RESULTS

Metabolic responses to induced environmental stress

Metabolic rates of *M. californianus* individuals were assessed across four populations using common garden experiments to determine how temperature and pH stress influence physiological performance and phenotypic plasticity. Metabolic responses did not differ between populations (one-way ANOVA: $F_{(3,92)} = 0.615$, $p = 0.607$), though respiration rate differed across treatments ($F_{(3,92)} = 6.403$, $p = 0.0005$), as *M. californianus* individuals exposed to elevated temperatures exhibited significantly higher respiration rates (mean = 0.340 ± SE = 0.017 mg O_2 g^{-1} h^{-1}) when compared to individuals in control (0.246 ± 0.017 mg O_2 g^{-1} h^{-1}) and decreased pH environments (0.257 ± 0.020 mg O_2 g^{-1} h^{-1}, Figure 2.1). Although mussels demonstrated minimal responses to more acidic environments (control versus decreased pH; Figure 2.1), the combined stressors treatment indicated that

decreased pH reduced the magnitude of response to elevated temperature conditions (0.312 ± 0.014 mg O_2 g^{-1} h^{-1}, Figure 2.1).

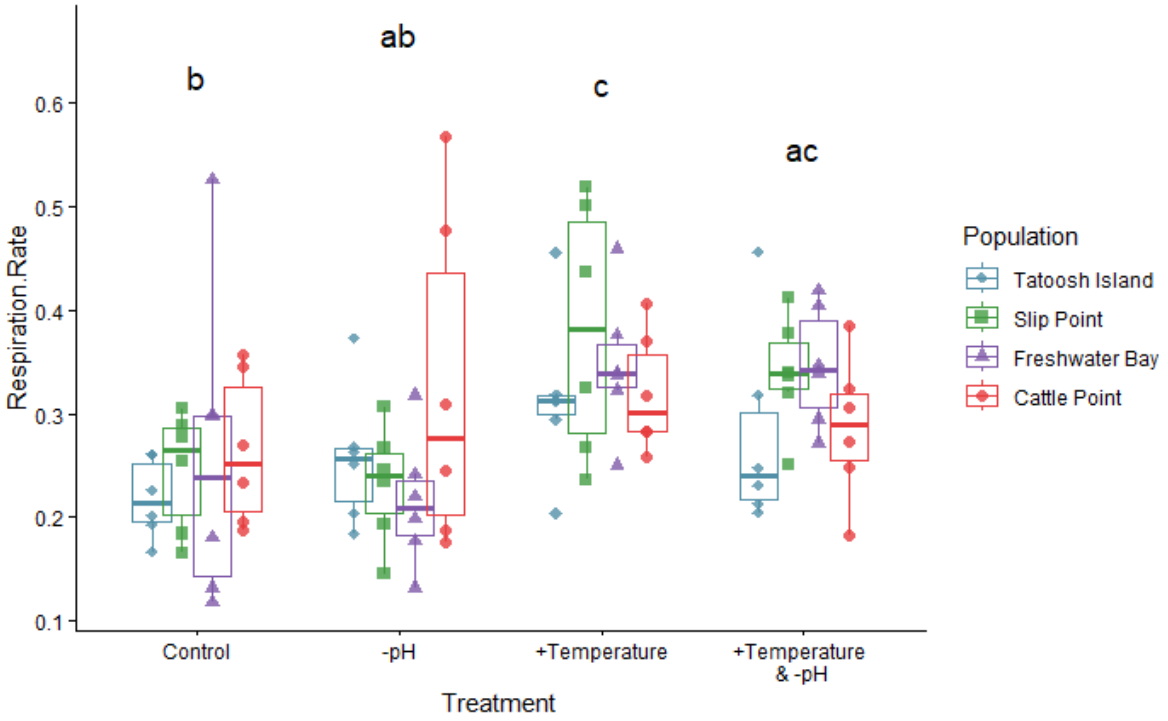

Figure 2.1: Respiration rates (mg O_2 g^{-1} h^{-1}) of *Mytilus californianus* individuals from populations exposed to control conditions and three treatment groups where seawater was experimentally manipulated: decreased pH, increased temperature, and combined stressors of decreased pH & increased temperature. Shapes and colors of points in boxplots represent individual respiration rates for each population exposed to various experimental conditions. Different letters above each treatment indicate significant differences between experimental treatments evaluated using the Tukey HSD test as a post hoc comparison.

Phenotypic plasticity differed across regions; mussels originating from the Western Strait and Northern Salish Sea exhibited decreased PI scores when compared to individuals from centrally located populations within the Strait of Juan de Fuca ($F_{(3,20)} = 199.5$, $p < 0.0001$, Table 2.2). RDPI showed that the source population had a significant effect on phenotypic plasticity across experimental treatments, with those from the Western Strait at Tatoosh Island exhibiting the lowest RDPI scores in decreased pH environments (Table 2.3 and Figure 2.2). In contrast, mussels originating from the Northern Salish Sea (i.e. Cattle Point) exhibited the lowest RDPI scores in increased temperature environments (Table 2.3 and Figure 2.2). Alternatively, mussels

from Freshwater Bay had the highest plasticity scores across all treatment groups, suggesting phenotypic plasticity to be an adaptive response to highly variable environments in centrally located populations (Table 2.3 and Figure 2.2).

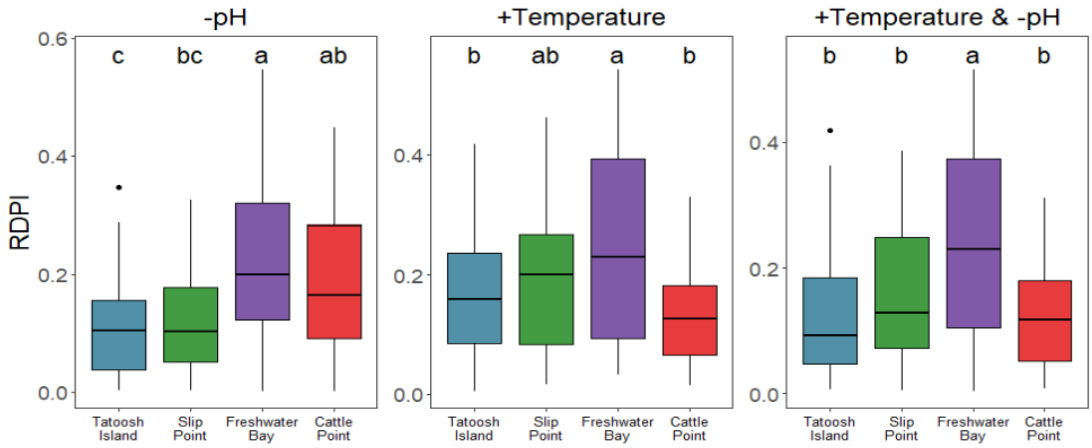

Figure 2.2: Relative Distance Plasticity Index (RDPI) scores calculated using the respiration rates (mg O_2 g^{-1} h^{-1}) of *Mytilus californianus* individuals from populations exposed to control conditions and three treatment groups where seawater was experimentally manipulated: decreased pH. increased temperature, and combined stressors of decreased pH & increased temperature. Colors of boxplots represent individual respiration rates for each population exposed to various experimental conditions.

Table 2.2: Average Plasticity Index (PI) scores calculated via jackknife using the respiration rates (mg O_2 g^{-1} h^{-1}) of *Mytilus californianus* individuals from populations exposed to control conditions and three treatment groups where seawater was experimentally manipulated: decreased pH, increased temperature, and combined stressors of decreased pH & increased temperature. Different letters correspond to significant differences ($P < 0.05$) between populations for each plasticity index separately using Tukey HSD test as a post hoc comparison.

Index	**Population**	**Mean**	**± SE**
Plasticity Index (PI)	Tatoosh Island	0.278^{b}	0.019
	Slip Point	0.348^{a}	0.013
	Freshwater Bay	0.353^{a}	0.015
	Cattle Point	0.174^{c}	0.006

Table 2.3: Average Relative Distance Plasticity Index (RDPI) scores per each treatment using the respiration rates (mg O_2 g^{-1} h^{-1}) of *Mytilus californianus* individuals from populations exposed to control conditions and three treatment groups where seawater was experimentally manipulated: decreased pH, increased temperature, and combined stressors of decreased pH & increased temperature. Different letters correspond to significant differences ($P < 0.05$) between populations for each treatment separately using Tukey HSD test as a post hoc comparison.

Treatment	Population	Mean	± SE
Decreased pH	Tatoosh Island	0.109^{c}	0.014
	Slip Point	0.121^{bc}	0.015
	Freshwater Bay	0.213^{a}	0.022
	Cattle Point	0.184^{ab}	0.020
Increased Temperature	Tatoosh Island	0.169^{b}	0.016
	Slip Point	0.199^{ab}	0.021
	Freshwater Bay	0.246^{a}	0.026
	Cattle Point	0.131^{b}	0.014
Decreased pH & Increased Temperature	Tatoosh Island	0.127^{b}	0.018
	Slip Point	0.157^{b}	0.017
	Freshwater Bay	0.242^{a}	0.026
	Cattle Point	0.128^{b}	0.014

Genetic diversity across the genome

Results from ANGSD and PCAangsd identified 3,769,416 SNPs among the 75 *Mytilus californianus* individuals, with very little genetic structure between populations (Figure 2.3A, 2.3B). NGSadmix supported these results as 35 out of the 75 sequenced individuals were admixed or had ancestry proportions distributed across multiple genetic clusters (Figure 2.3C, Figure B1), which is expected in a highly panmictic species. However, NGSadmix also identified three ancestral lineages that were separated by geography, with western strait populations predominately assigned to the Western Strait ancestral cluster, centrally located populations primarily associated with the Central Strait ancestral cluster, and the innermost coastal population at Cattle Point forming a distinct Northern Salish Sea ancestral cluster (Figure 2.3A & 2.3C). The distribution of these ancestral lineages across geographic regions is consistent with high dispersal-mediated gene flow in this broadcast-spawning species, as reflected by the relatively low genome-wide differentiation among lineages (pairwise F_{ST}: Central Strait vs

Northern Salish Sea = 0.031, Western Strait vs Northern Salish Sea = 0.022, Western Strait vs Central Strait = 0.077) and high nucleotide diversity within populations (π: Central Strait = 0.0086, Northern Salish Sea = 0.0074, Western Strait = 0.0065). Linkage disequilibrium (LD) decayed rapidly within all three lineages (Figure B2), further supporting high recombination and large effective population sizes, a characteristic of highly connected broadcast-spawning species. Because genetic drift is reduced in larger populations, recombination more effectively breaks down associations between alleles over time (Slatkin, 1994; Wright, 1969). Accordingly, differences in LD among clustering groups reflect variation in effective population size, with the Western Strait and Central Strait ancestral clusters exhibiting larger effective population sizes than the Northern Salish Sea ancestral cluster (Figure B2).

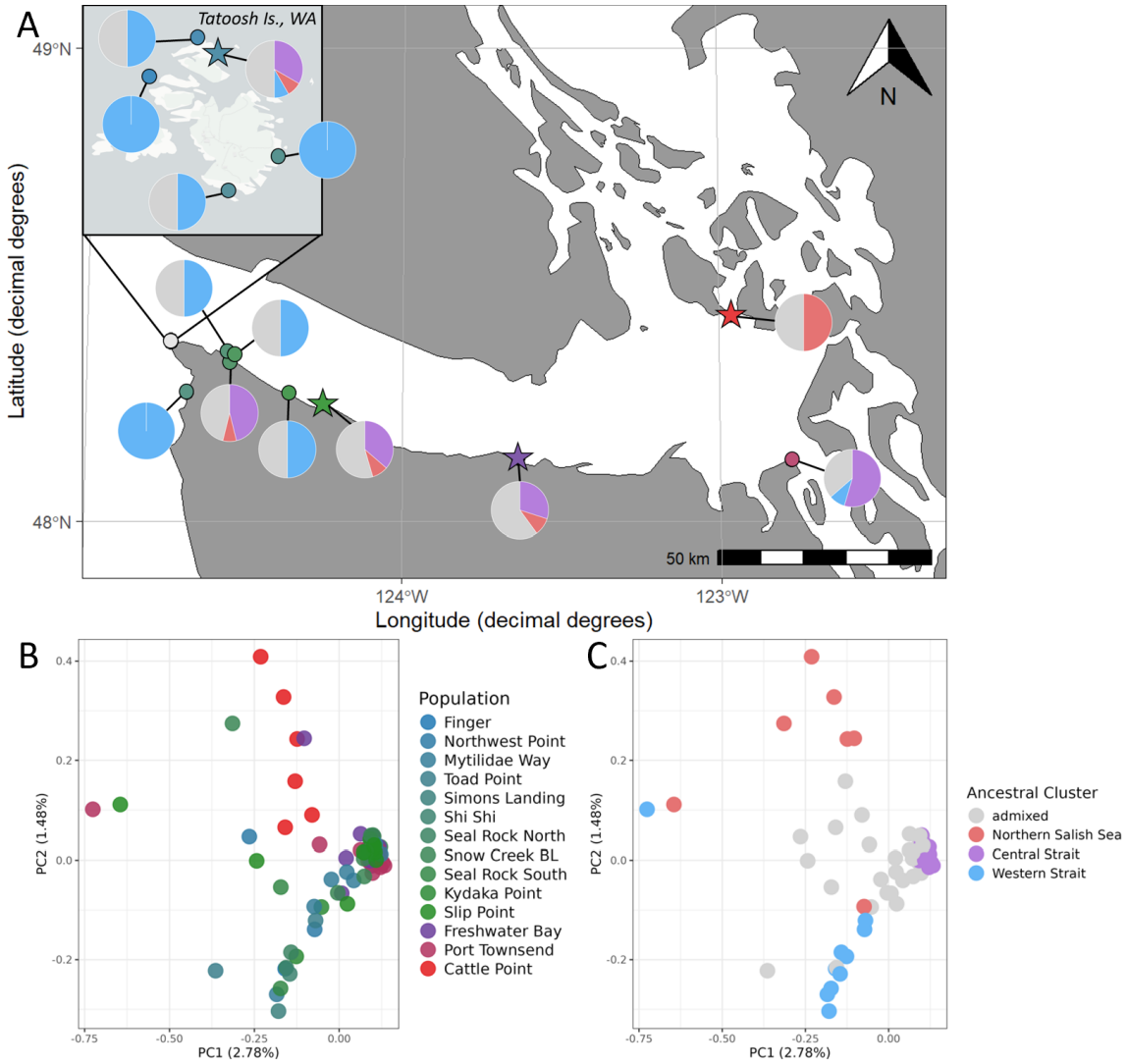

Figure 2.3: (A) Map of sampling sites of *Mytilus californianus* individuals used in temperature and pH manipulation experiments (stars) and for genetic analysis (dots & stars). Colors of dots and stars correspond to population colors in figure 2.3B; colors of proportions in pie charts next to each population correspond to genetic clustering groups of the sampled individuals in figure 2.3C. PCAs of 3,769,416 SNPs among 75 individuals using PCAngsd before (B) and after (C) clustering analysis using NGSadmix to estimate best K and identify admixed individuals (Meisner & Albrechtsen, 2018).

Gene flow patterns of *Mytilus californianus* in the Strait of Juan de Fuca

Migration calculations revealed distinct patterns in larval dispersal, as centrally located populations within the Strait of Juan de Fuca received higher rates of gene flow compared to Northern Salish Sea and Western Strait populations resulting in higher genetic similarity (lower F_{ST}) in these populations (Figure 2.4A & 2.4B). Additionally, the posterior probabilities of

effective migration rates highlighted Kydaka Point and Cattle Point as populations that receive lower than average migration compared to neighboring populations, implying reduced gene flow in these populations (Figure 2.4C).

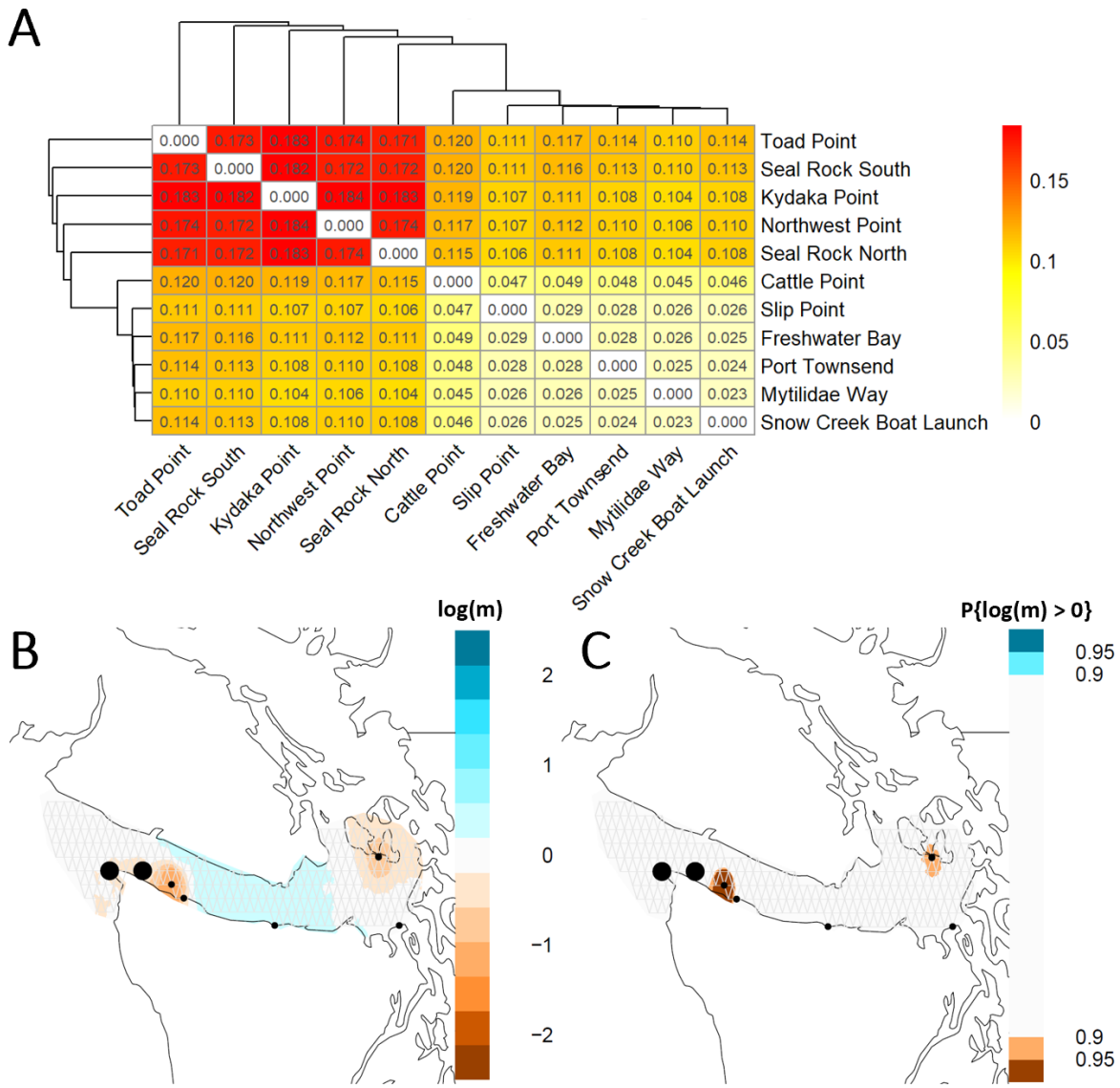

Figure 2.4: (A) Pairwise FST heatmap with associated dendrogram between 11 geographically separated *Mytilus californianus* populations distributed throughout the Strait of Juan de Fuca using 10,858,565 SNPs. Refer to figure 2.3 for population locations. (B) Posterior mean and (C) probabilities of effective migration rates (m) estimated with the EEMS software (Petkova et al., 2016). Log(m) denotes the effective migration rate on a log10 scale relative to the overall migration rate through space, and P{log(m)>0} denotes the posterior probabilities of migration between populations. Blue colors represent higher than average effective migration rates, while orange colors signify lower than average. Dot sizes correspond to the number of populations in each deme.

Population structure within candidate loci

XP-EHH analysis uncovered a combined total of 10,376 SNPs under selection between the three clustering groups (Figure 2.5). Environmental Association Analysis of these SNPs using Bayenv2 (Günther & Coop, 2013) revealed that 273 were associated with air temperature, 28 were associated with air temperature and pH, and none were associated with sea surface temperature (Figure 2.5). These 301 SNPs were subsequently used as candidate loci for investigating local adaptation. Annotation of these candidate loci revealed many of them to be within functionally relevant proteins that have been characterized to affect survival across many calcifying species including osmotic stress: von Willebrand factor D and EGF domains (VWDE) (Abo-Al-Ela & Faggio, 2021); embryonic development: mesenchyme-specific cell surface glycoprotein (MSP) (Kabakoff et al., 1992; Katow, 2020); DNA repair: F-box/LRR (Bai et al., 2025; Zhou et al., 2009); anatomical structure development: fibrillin-1 (Dou et al., 2018); hypoxia and immune response: NF-kappa-B (Koutsogiannaki & Kaloyianni, 2010; Nie, Wang, et al., 2020); heat stress: sacsin (Takahashi-Kariyazono & Terai, 2021); heat stress and immune response: E3 ubiquitin ligases (Guo et al., 2024); and ciliary beating: Kinesin heavy chain like protein (KHC) (Gurr et al., 2025; Venkataraman et al., 2022). With sacsin, MSP, F-box/LRR, and KHC having extremely strong associations (Bayes factor > 10) with environmental covariates of interest (Figure 2.5).

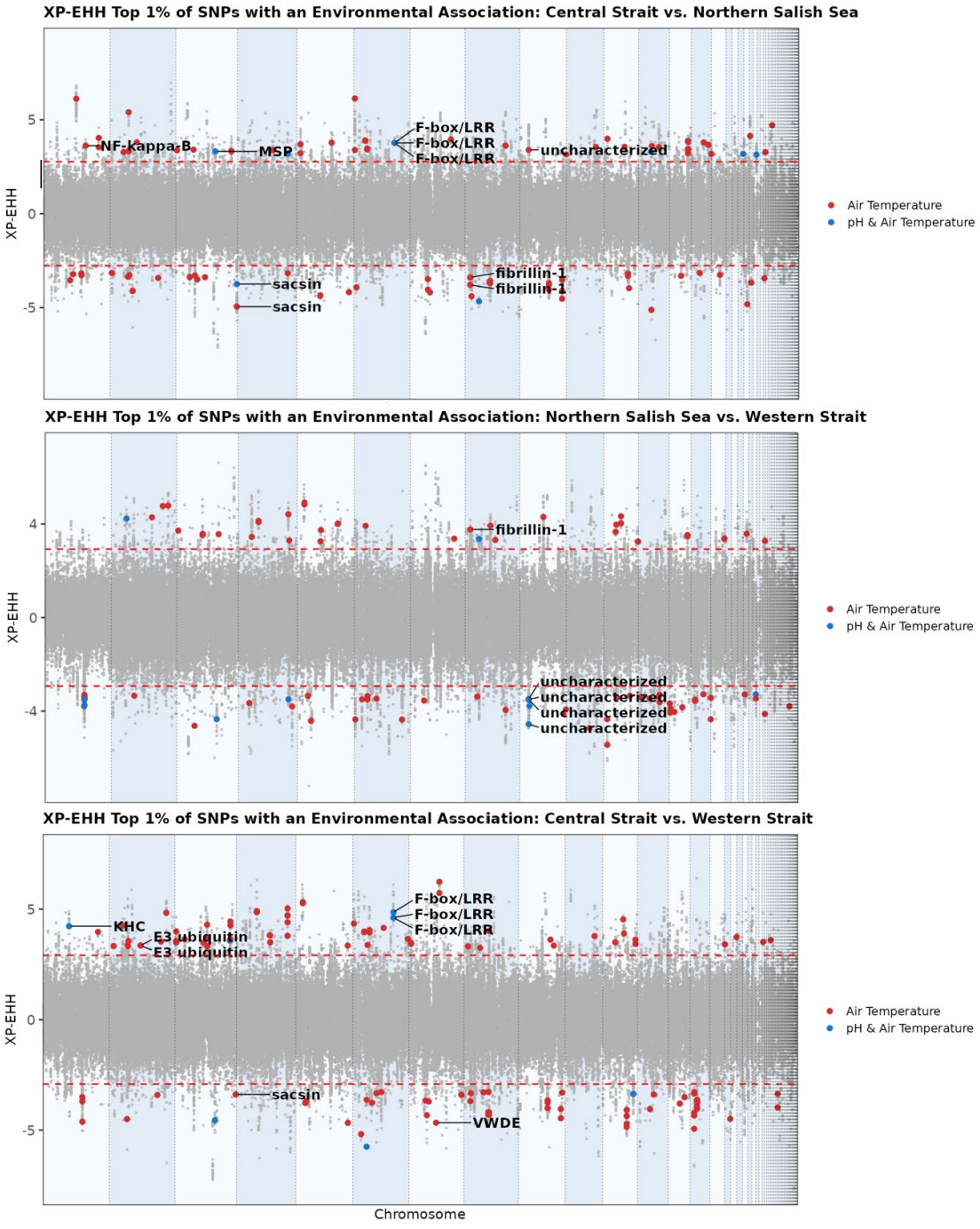

Figure 2.5: Genome-wide Cross-population Extended Haplotype Homozygosity (XP-EHH) scans of pairwise comparisons among three genetically clustered *Mytilus californianus* populations (Western Strait, Central Strait, Northern Salish Sea). Each point represents a SNP, with alternating light and dark shading for chromosomes. Red dashed lines denote the top 1% of XP-EHH values, highlighting putative regions under selection. Points above the top red dashed line represent selection in the first clustering group listed in the panel title, and points below the bottom red dashed line represent selection in the second clustering group listed in the panel title. Colored points indicate SNPs that show significant associations with environmental covariates, as identified using Bayenv2 (Günther & Coop, 2013). Gene names next to SNPs are functionally relevant proteins associated with fitness in this taxon.

Generating 50 kb LD blocks of these genes revealed increased LD in genomic regions associated with sacsin proteins in Northern Salish Sea and Central Strait populations relative to Western Strait populations, indicating stronger selection on these proteins in these populations (Figure 2.6). Similar patterns were observed in KHC, MSP, and F-box/LPR, suggesting that the genetic architecture of these traits is more strongly influenced by local adaptation opposed to phenotypic plasticity (Figure 2.6). In contrast, Western Strait populations) did not exhibit any proteins with strong associations to environmental covariates. However, many genes under selection showed moderate associations across the genome (Bayes factor > 3 and <10), including a tight cluster of four uncharacterized proteins linked to pH and air temperature, which did not show increased LD in the Western Strait populations (Figure 2.5 & 2.6). This region also contained substantially fewer SNPs compared to the Northern Salish Sea population (398 vs. 451), indicating fewer polymorphisms in this genomic region for Western Strait populations (Figure 2.6). These results suggest that phenotypic plasticity may play a stronger role in shaping the genetic architecture of fitness-related traits in Western Strait populations.

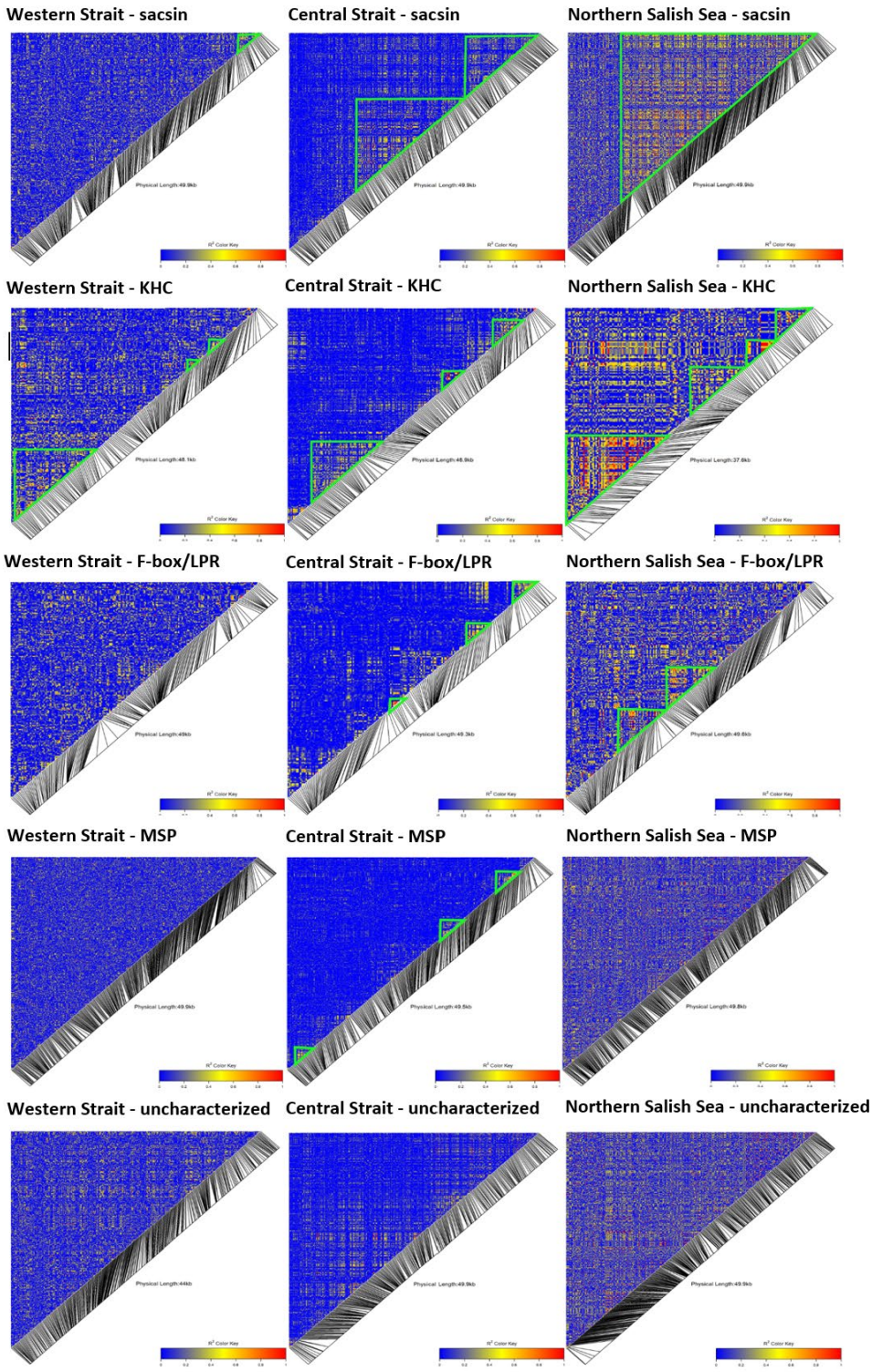

Figure 2.6: Linkage Disequilibrium (LD) blocks of five selected genes shown to be under selection and associated with environmental covariates of interest between three *Mytilus californianus* clusters (Western Strait, Central Strait, Northern Salish Sea). Cool colors represent pairwise SNPs in low LD while warm colors represent pairwise SNPs in high LD. Green triangles represent increased structural variation within each genomic region across each cluster. Black lines represent individual SNPs.

DISCUSSION

Our study provides empirical evidence that the interaction between migration and environmental heterogeneity shapes both the genomic architecture and phenotypic responses of natural populations. Despite the high dispersal potential and largely panmictic structure of *Mytilus californianus*, we detected fine-scale genetic structuring across populations distributed throughout the Strait of Juan de Fuca that aligns with environmental gradients and variation in migration rates. These findings support theoretical predictions from Oomen et al. (2020), that even in highly connected systems, reductions in gene flow combined with strong selection can favor tightly linked genomic architectures.

Genome-wide patterns indicated low genetic differentiation and linkage between alleles (Figure B2), consistent with high recombination and large effective population sizes typical of broadcast-spawning marine invertebrates. However, this overall genetic homogeneity masked pronounced divergence at candidate loci associated with environmental stressors, particularly air temperature. The identification of over 10,000 SNPs under selection, including a subset of 301 SNPs associated with key environmental stressors (Figure 2.5), demonstrates that selection can act on specific genomic regions despite the homogenizing effects from high population connectivity. Consistent with this pattern, our results support models predicting that local adaptation is maintained through the clustering of adaptive variants into tightly linked clusters of SNPs under strong selective pressure, particularly in functionally relevant proteins that influence fitness (Bürger & Akerman, 2011; Yeaman & Otto, 2011).

One such functionally relevant protein, sacsin, emerges as a strong candidate, exhibiting signatures of selection within central Strait and Northern Salish Sea populations, including extended haplotype homozygosity, increased LD within its genomic region, and significant

associations with increased air temperature, conditions under which these populations persist (Figure 2.5 & 2.6; Table 2.1). Sacsin is a heat shock protein co-chaperone involved in protein folding and cellular stress responses, particularly under conditions of thermal and oxidative stress (Parfitt et al., 2009). In marine systems, sacsin-like proteins have been linked to stress-induced expression, reactive oxygen species regulation, and long-term maintenance of adaptive variation, supporting its role in mediating fitness-related responses throughout heterogeneous environments (Hemond et al., 2014; Pespeni et al., 2013; Takahashi-Kariyazono & Terai, 2021). For Northern Strait populations, increased LD occurred alongside reduced migration and smaller population sizes, resulting in decreased plasticity under elevated thermal conditions supporting the hypotheses from Yeaman (2022) (Figures 2.4B, 2.4C, & 2.2; Table 2.1). In contrast, central populations, which experience higher migration rates, larger population sizes, and less intense thermal stressors (Figures 2.4B, 2.4C, & Figure B2; Table 2.1), also exhibited increased LD in sacsin-like proteins but maintained greater phenotypic plasticity under elevated temperatures supporting theoretical predictions from Sultan and Spencer (2002) (Figure 2.6 & 2.2). Together, these patterns suggest that reduced migration, smaller population sizes, and stronger thermal stress in Northern Strait populations favor fixed, locally adapted genetic architectures in sacsin proteins. Alternatively, in central populations, higher gene flow, larger population sizes, and less intense environmental stressors facilitate the coexistence of both tightly linked SNPs and phenotypic plasticity. These findings highlight how the interplay between environmental stress, population size, and effective migration shapes both the expression and functional diversity of adaptive proteins across populations.

The balance between migration and selection determines the adaptive potential of metapopulations

Understanding how organisms adapt to spatiotemporal environmental variation across their geographic ranges is a long standing question in ecology and evolutionary biology (Lewontin, 1957). In systems characterized by high population connectivity, the balance between gene flow, selection, and phenotypic plasticity is expected to play a critical role in shaping adaptive responses (Nicolaus & Edelaar, 2018). Our results demonstrate that phenotypic plasticity is not uniformly distributed across populations of *M. californianus* but instead varies predictably with both environmental stress and population connectivity. Centrally located populations exhibited the highest plasticity across all treatments, a result consistent with increased plasticity in variable environments (Bitter et al., 2021; Gratani, 2014; López et al., 2010), whereas inner and Western Strait populations showed reduced plasticity under their respective dominant stressors (Figure 2.2; Table 2.1). Northern Salish Sea populations, which experience elevated temperatures and reduced population sizes, exhibited higher LD in heat stress-associated loci (Figure 2.6), consistent with patterns of local adaptation observed in other marine species such as oysters (Wu et al., 2022), corals (Thomas et al., 2022), and salmon (Oomen et al., 2020). Alternatively, Western Strait populations, despite reduced plasticity under low pH conditions mimicking upwelling environments (Figure 2.2), did not exhibit corresponding increases in LD in fitness related proteins, likely because their larger effective population sizes constrain the formation of tightly linked genomic regions when the strength of selection is less intense (Wright, 1969) (Figure B2). Furthermore, pre-existing adaptations (e.g., thicker shells) and greater food availability, both of which can mitigate the effects of prolonged acidification on *M. californianus* individuals, suggest that pH may represent a comparatively

weaker selective pressure than elevated temperature in these populations (Fitzgerald-Dehoog et al., 2012; Man, 2018; Masson & Peña, 2009; Melzner et al., 2011; Thomsen et al., 2013). The presence of a sacsin protein under selection in the Western Strait population (top panel in Figure 2.5), and increased frequencies of heat shock proteins (HSP70) observed in high intertidal individuals on Tatoosh Island support this hypothesis (Richards et al., 2025). Freshwater Bay, which exhibited increased LD in proteins associated with local environmental conditions (Table 2.1), also experienced higher migration rates and larger population sizes, contributing to elevated phenotypic plasticity across a broader range of environments (Figures 2.4B, 2.6, & 2.2). In central populations such as Freshwater Bay, which experience highly dynamic and rapidly fluctuating environments (as the name implies), our results suggest that habitat choice and phenotypic plasticity may act in concert, thus increasing the adaptive capacity of these populations.

Habitat choice is the process by which mobile animals assess environmental conditions and select microhabitats that best match their phenotype, thereby maximizing fitness (Turko & Rossi, 2022). In mussels, this mechanism is especially relevant during the larval stage, when individuals are non-sessile and capable of actively dispersing to favorable habitats (Carl et al., 2012; Snelgrove et al., 1999). Plasticity allows individuals to adjust their physiology or behavior to local conditions, while habitat choice enables them to occupy microenvironments that best match their phenotype. Together, these mechanisms can create a positive feedback loop in highly variable environments such as the marine intertidal: individuals that actively choose more variable microhabitats benefit from deploying greater plasticity, which in turn reinforces both the adaptive value of habitat choice and the expression of plasticity (Nicolaus & Edelaar, 2018). This dynamic is consistent with theoretical and empirical work showing that, when plasticity and

habitat choice are heritable and predictable, their interaction can strengthen local specialization and promote adaptive variation while maintaining phenotypic plasticity (Bitter et al., 2021; Edelaar et al., 2017; Scheiner, 2016). In a metapopulation context, high gene flow and large effective population sizes, as observed in Freshwater Bay, may further amplify these positive feedbacks, allowing rapid, individual-level adaptation to temporal environmental heterogeneity while also maintaining genetic diversity across the network of populations. Collectively, these patterns support Nicolaus and Edelaar (2018) and illustrate that adaptive outcomes in natural populations are shaped by the combined effects of environmental stress, population size, and connectivity, which together maintain the balance between adaptive genetic variation and phenotypic plasticity. While central populations benefit from high connectivity and the reinforcing feedback between habitat choice and phenotypic plasticity, Northern Salish Sea populations, with smaller sizes, reduced connectivity, and stronger thermal stress, may be more vulnerable to environmental changes.

The physiological responses observed in *M. californianus* indicate that elevated temperature is a stronger stressor than reduced pH, with metabolic rates increasing significantly under thermal stress (Figure 2.1). However, when low pH is combined with elevated temperature, the metabolic response is slightly dampened, suggesting that acidification may constrain the adaptive responses to warming (Figure 2.1). Northern Salish Sea populations, which already exhibit reduced phenotypic plasticity and smaller effective population sizes, appear particularly vulnerable to these compounded stressors. This vulnerability is highlighted by follow-up surveys in 2023 conducted by C. Richards and L. Sims at the furthest inner coastal sites originally surveyed by Kandur (2014), which indicate apparent extirpations of mussels at Coffin Rocks and Deception Island, WA, both located near Cattle Point (reported to WDFW

under Scientific Research Permit 230505). These findings suggest that as oceans continue to warm and acidify, populations with fixed phenotypes to local environments and limited connectivity may be unable to cope with the increasing frequency and magnitude of environmental extremes, leading to local population declines or extirpations. From an evolutionary perspective, these populations likely depend on tightly linked clusters SNPs, which optimize traits for the local environment but limit their capacity to respond to novel or combined stressors (Sultan & Spencer, 2002; Velotta & Cheviron, 2018; Yeaman, 2022). Nevertheless, such coadapted gene complexes can facilitate rapid adaptation in less adapted populations by increasing phenotypic variability within the metapopulation, thereby enhancing the potential for evolutionary responses to environmental change. Alternatively, larger populations with polygenic trait architectures and low LD between alleles exhibit greater phenotypic stochasticity due to genetic drift, producing intermediate phenotypes that limit the variation upon which selection can act (Mérot et al., 2020; Oomen et al., 2020). In more central, highly connected populations, high plasticity, increased LD in functionally relevant proteins, and greater genetic diversity can buffer individuals against rapid environmental changes. However, this flexibility may also allow maladaptive alleles to persist or spread through the metapopulation, potentially reducing the overall adaptive efficiency (Ghalambor et al., 2007; Mérot et al., 2020). Here, gene flow and large effective population sizes facilitate polygenic traits to respond flexibly to fluctuating environmental conditions, while selection maintains adaptive genetic variation within the metapopulation.

CONCLUSION

Ultimately, the magnitude and rate of environmental change and the degree of connectivity among populations will determine the evolutionary trajectories of *Mytilus*

californianus populations and their capacity to respond to intensified stressors. Northern Salish Sea populations, with fixed phenotypes and tightly linked SNPs in isolated genomic regions, are optimized for extreme temperature conditions but have limited flexibility under novel or compounded stressors. Western Strait populations, despite reduced plasticity under low pH conditions, maintain polygenic trait architectures, allowing some phenotypic flexibility without forming tightly linked adaptive regions. Central, highly connected populations combine high phenotypic plasticity, structural variation, and genetic diversity to buffer against environmental fluctuations. Collectively, these different mechanisms across populations generate and maintain genetic diversity throughout the metapopulation, providing a broad evolutionary "toolkit" that enhances adaptive capacity and resilience (Hersch-Green et al., 2011). This genetic diversity is critical for the long-term persistence and conservation of a species facing increasingly unpredictable and extreme environmental conditions. Therefore, understanding the interplay between migration, selection, and phenotypic plasticity is key to predicting the adaptive capacity of broadcast-spawning marine organisms under future ocean conditions.

DATA AVAILABILITY

Data and code used for analyses are made available on Figshare: https://doi.org/10.6084/m9.figshare.32065689

APPENDIX B: SUPPLEMENTAL INFORMATION FOR CHAPTER 2

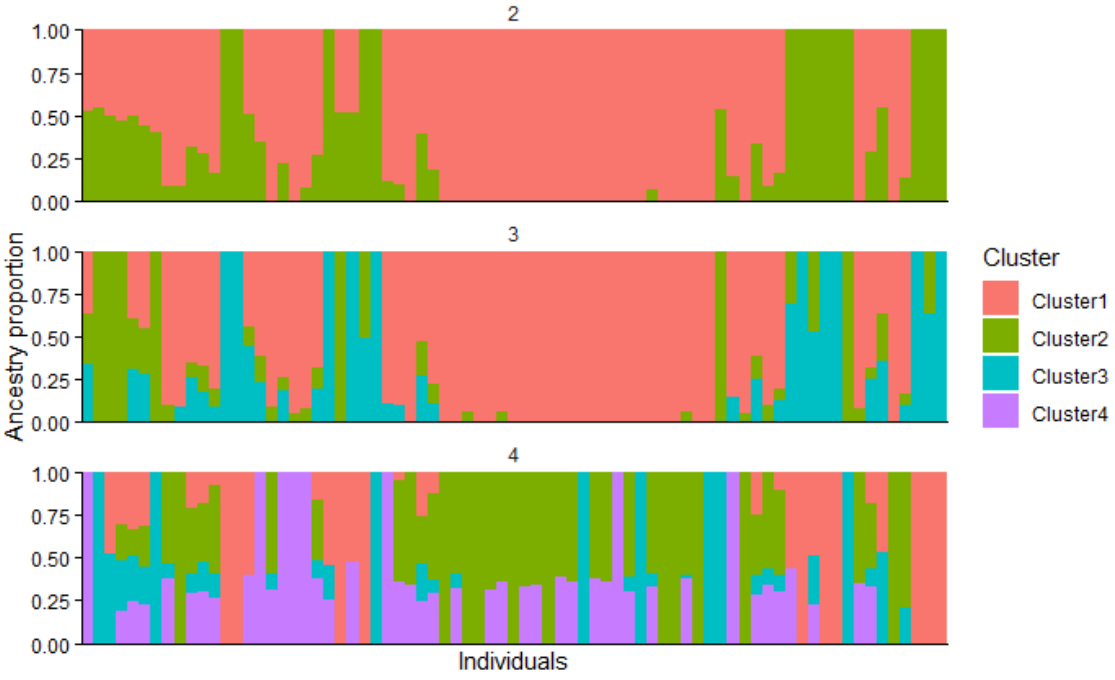

Figure B1: Admixture plots (K2, K3, K4) of 75 individuals across all sampling sites using 3,769,416 SNPs identified from ANGSD.

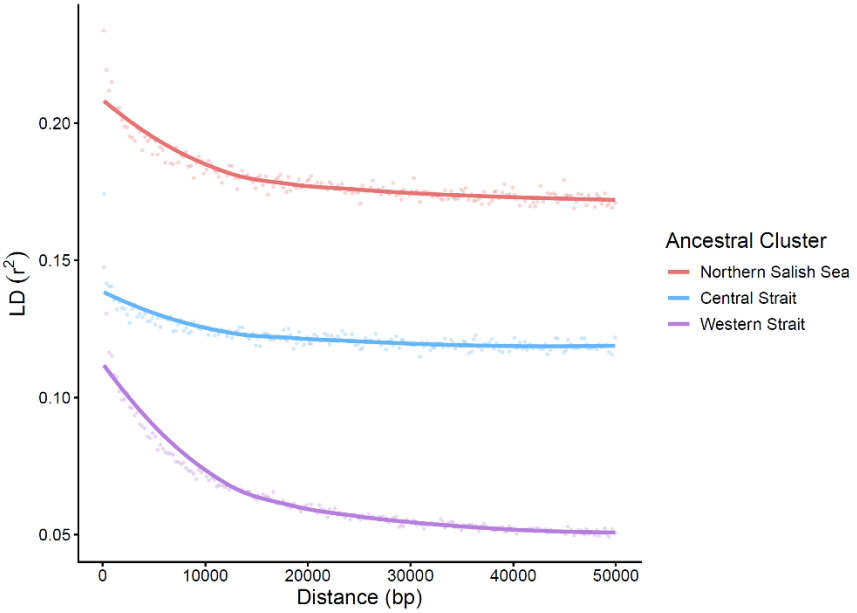

Figure B2: Linkage disequilibrium (LD) decay rates across three genetically clustered *Mytilus californianus* populations (Western Strait, Central Strait, Northern Salish Sea). Pairwise LD (r^2) between SNPs was calculated from sampled loci identified from ANGSD, and LD decay with physical distance (bp) is shown up to a maximum distance of 50 kb. Colored lines represent the smoothed decay curves for each population. The decay rate (rate at which LD decreases with distance) for each population is indicated above the corresponding line. Points represent binned average LD values across 250 bp intervals.

CHAPTER 3: DIVERSITY MAINTENANCE PROCESSES AND COMMUNITY RESPONSES TO ENVIRONMENTAL VARIATION ON AN INTERTIDAL SHORE

ABSTRACT

Quantifying how biodiversity influences community stability is a central theme in ecology, with a growing importance of understanding how climate change will alter these dynamics. While theory predicts that greater species diversity and evenness will promote temporal stability of community abundance through mechanisms like portfolio effects, empirical studies suggest that communities dominated by one or a few species may also achieve stability by buffering against environmental stress. Rocky intertidal ecosystems, dominated by the foundational mussel species *Mytilus californianus*, provide an ideal system to examine these contrasting mechanisms. Using a long-term experimental manipulation that spanned 31 years on Tatoosh Island, WA, we tested how community structure influences the temporal stability of community abundance and its responses to environmental change. Mussel removal treatments created low dominance plots with greater species richness, while unmanipulated control plots resulted in high dominance plots dominated by *M. californianus*. Our results show that low dominance communities generally exhibited greater evenness, diversity, and asynchrony, supporting the hypothesis that portfolio effects act as a stabilizing mechanism in these communities. However, under intensifying environmental stress, these low dominance communities exhibited eroded diversity and increased species colonization from across the metacommunity, or 'invasions'. In contrast, high dominance communities, though less stable overall, displayed an alternative stability pathway: resilience was maintained through dominant species buffering environmental stress and by invaders filling functional niches. Together, these findings suggest that community responses to climate change will depend strongly on the

balance between diversity- and dominance-driven processes. In relatively stable environments, ecosystem stability is maintained through diversity, whereas in stressful environments, stability increasingly depends on dominance by the foundational species. Ultimately, our results underscore the need to consider both local community composition and magnitude of environmental change when predicting ecosystem stability under future ocean conditions.

INTRODUCTION

A reoccurring theme in ecology is determining how biodiversity affects the stability of ecological communities (i.e. the variance of aggregate abundance over time), with the goal of better predicting the impacts of biodiversity loss and environmental change on ecosystem function (Loreau, 2000). Climate change and anthropogenic activities are accelerating biodiversity loss, with the resulting impacts on community stability and ecosystem function still largely unknown (Worm et al., 2006). One essential service biodiversity offers is the stabilization of the overall abundance of a functional group of organisms that provide a particular ecosystem service or function, thereby reducing the vulnerability of ecosystem functioning to fluctuations in abundances of individual populations (Thibaut & Connolly, 2013). This diversity–stability relationship between species diversity and temporal stability of total community abundance is commonly referred to as a 'portfolio effect', where stability increases with diversity (Tilman, 1999). Models suggest that portfolio effects strengthen as asynchrony in population fluctuations within a community increases (Doak et al., 1998; Loreau, 2010). The biotic interactions between these populations (e.g. inter- and intra-specific competition) leads to increased evenness or "low dominance communities" allowing for more rapid community responses to environmental changes, thereby increasing resistance (Chapin Iii et al., 2000; Hillebrand et al., 2008). However, studies have also shown less diverse communities dominated by a few well adapted organisms,

or “high dominance communities” can increase community stability by increasing resilience to environmental stress (Hillebrand et al., 2008; Pennekamp et al., 2018; Pfisterer & Schmid, 2002). The contrast between low dominance and high dominance communities highlights the importance of understanding the functional role that biodiversity has on ecosystem stability.

Species richness can be distributed differently among communities, with evenness or dominance describing the relative abundance of species within a community assemblage. High dominance communities are characterized by low evenness, whereas low dominance communities’ abundance is more evenly distributed across species. In low dominance communities portfolio effects may maintain community stability, while experimental studies in high dominance communities show stabilizing effects of community biomass and stability with dominant species (Lepš, 2004; Sasaki & Lauenroth, 2011; Wayne Polley et al., 2007). Theoretical evidence suggests the stabilizing effect of species diversity on community stability is most evident in low dominance communities (Doak et al., 1998). Because one or a few species contribute so disproportionately to total biomass in high dominance communities the averaging effect from a higher number of species (which typically reduces variability) is lost, thereby weakening the stabilizing role of diversity (Cottingham et al., 2001). This is analogous to Taylor`s power law which states that the log stationary variance in population fluctuations scale with the log mean population implying larger population sizes experience decreased variance (Taylor, 1961). Although high dominance communities are characterized by decreased diversity, they are more susceptible to species invasions, or species colonization from throughout the metacommunity compared to low dominance communities (Dunstan & Johnson, 2006). Overall, species invasions may play an important role in maintaining community stability in high

dominance communities, whereas in low dominance communities stability is driven by diversity (Dunstan & Johnson, 2006; Smith et al., 2004).

The ability for a community to resist invasions from neighboring populations defines its "invasibility". Empirical studies investigating the relationship between dominance and invasibility have found largely positive correlations, as high dominance communities often lack functional group diversity, resulting in unoccupied niches that are more vulnerable to invasion (Dunstan & Johnson, 2006). In contrast, low dominance communities with higher evenness experience increased resistance to invaders as they tend to occupy more local niches from available functional groups (Losure et al., 2007; Mwangi et al., 2007). This evenness–invasibility relationship can have a significant effect on ecosystem functioning (Sousa et al., 2011), with the strength and impact of evenness or invasibility on ecosystem function strongly dependent on the severity of environmental stress (Gallien & Carboni, 2017). For example, De Roy et al. (2013) found in microbial microcosm experiments that communities with higher evenness resisted invaders significantly greater than communities with lower evenness. However, when stress was induced, communities with lower evenness demonstrated increased ecosystem functioning and had a similar number of invaders when compared to communities with high evenness under the same conditions. This suggests that in stressful environments invaders will play a key role in the maintenance of ecosystem functioning in low evenness communities, but do not provide a benefit for ecosystem functioning in high evenness communities. Smith et al. (2004) show similar results in tallgrass prairies and argued invasion is facilitated by dominant species, as invaders increase environmental stress for non-dominant species. The ability of invaders to maintain ecosystem function in low evenness communities by filling critical functional roles (De Roy et al., 2013), and the capacity of dominant species to increase resilience to environmental

stress (Pennekamp et al., 2018; Pfisterer & Schmid, 2002), suggest that communities that are more resilient to environmental extremes will be characterized by high dominance.

Aggregations of mussels in the genus *Mytilus* form beds that dominate temperate rocky intertidal shores globally (Stephenson et al., 1972). Foundational species like *Mytilus californianus* drive intertidal community dynamics by contributing to most of the community aggregate biomass and enhancing structural complexity (Dayton, 1972). This structural complexity provides habitat for a multitude of species and ameliorates physical stressors by serving as a refuge during times of high environmental stress (Angelini et al., 2011; Dayton, 1975; Ellison et al., 2005). Rocky intertidal shores have historically provided valuable insights into community structuring processes (Dayton, 1972; Paine, 1974; Wootton, 2005), with a recent emphasis of the implications of climate change on these systems (Hawkins et al., 2009; Helmuth et al., 2011; Wootton & Pfister, 2012). Daily environmental fluctuations, steep sloping coastlines, and high biodiversity force sessile intertidal species into constrained niches as abiotic and biotic pressures narrow ecological ranges (Richards et al., 2025). Due to these intense selective pressures, sessile marine species along an intertidal gradient exhibit rapid responses to environmental shifts, often serving as early indicators of ecosystem change. These factors make rocky intertidal habitats ideal for studying community-associated responses to increasing environmental stress (Mieszkowska, 2025). The global distribution and current declines in abundance of *Mytilus spp.* (Baden et al., 2021; Petraitis & Dudgeon, 2020) provide a unique opportunity to quantify how strengthening environmental gradients effect community stability through mussel abundance.

In this study, we explored how the experimental generation of low and high dominance communities on an intertidal shore are related to temporal stability and responses to

environmental change. We used species abundance data from a long-term experimental manipulation of the mussel bed on Tatoosh Island, Makah Indian Reservation, WA, USA and associated environmental data (Wootton, 2004, 2005, 2010). The "low dominance" communities are experimental plots where individual *M. californianus* mussels, the dominant species in this community, were selectively and chronically removed by hand from 1993 to 2024. The "high dominance" communities are unmanipulated control plots where *M. californianus* mussels were left in situ. We hypothesized that low dominance communities would be associated with increased community asynchrony (decreased synchrony), evenness, diversity, resistance to invaders, and decreased productivity in response to environmental stress. Alternatively, in high dominance communities we hypothesized decreased community asynchrony (increased synchrony), evenness, diversity, resistance to invaders resulting in increased species turnover, and increased productivity in response to environmental stress (Chapin Iii et al., 2000; De Roy et al., 2013; Hillebrand et al., 2008; Smith et al., 2004; Tilman, 1999).

METHODS

The long-term experimental manipulation of the mussel bed on Tatoosh Island was initiated in 1993. The experimental design consists of 15 65 x 65 cm experimental plots (low dominance communities) and 10 unmanipulated 65 x 65 cm control plots (high dominance communities), both sets of which are permanently marked, located in the mussel-dominated middle intertidal zone of wave-swept rock benches on Tatoosh Island (Wootton, 2004, 2005, 2010). Both sets of plots were annually surveyed in early June by JTW for every organism that was visually identifiable *in situ*. Percent area of available surface area was also quantified for each plot. Data used in this paper were collected from 1993-2024, with the first three years of data removed to ensure plots returned to a stable state after initial experimental disturbance.

Because the plots served to document ecological dynamics over time, the plots could not be destructively sampled. Therefore, several groups of small-bodied and/or morphologically similar taxa (mites, amphipods, and filamentous red algae) which require careful inspection under the microscope to permit identification, are lumped together during these surveys. Additionally, microbial flora and fauna are not surveyed (Pfister et al., 2014). Nevertheless, the study offers a clear comparison of habitats with and without the dominant species *Mytilus californianus* using the same observer, sampling effort, and methodology. The dataset includes both sessile organisms dependent on primary or secondary attachment space, and mobile animals associated with the habitats in the two treatments. For the scope of this study and model fitting purposes, all non-sessile species were removed from the dataset for analysis. Sessile species used in this analysis include *Mytilus californianus, Mytilus trossulus, Pollicipes polymerus, Semibalanus cariosus, Balanus glandula, Halosaccion glandiforme, Corallina vancouveriensis, Endocladia muricatum, Ulva spp., Porphyra spp., the Petrocelis form of Mastocarpus pappilatus, Ralfsias spp., Acrosiphonia coalita, diatoms, Microcladia borealis, Halichondria spp., Haliclona spp., Hedophyllum sessile, Anthopleura spp., Polysiphonia spp., Iridrea cordata, and Callithamnion spp*. Due to low population abundances and functional trait similarities, the following species were grouped together: *Petrocelis* and *Ralfsia*; *Halichondria* and *Haliclona; Polysiphonia spp., Microcladia borealis, Endocladia muricata,* and *Callithamnion* (FILR-filamentous Rhodophytes); *Mastocarpus papillatus* and *Iridea cordata* (FLR-foliose Rhodophytes); *Porphyra* and *Ulva* (EA-ephemeral algae).

Community dynamics

To compare community dynamics through time between low (mussel removal) and high (control) dominance communities, we calculated the average annual abundance of each species

across all replicate plots. To compare community dynamics across space, we calculated the average annual abundance of each species for each replicate plot. Using these two matrices and the R software package 'codyn' we quantified Simpson`s evenness, species richness, Shannon diversity, species turnover, Loreau synchrony, rate of community change, and community stability resulting in community dynamic metrics for both treatments across time and space (Hallett et al., 2016). Species turnover for each year was used as a metric to measure the invasibility of each community and was calculated by taking the annual sum of species gained and species lost divided by the annual total number of species observed. Loreau synchrony measures the variance of aggregated species abundances with the summed variances of individual species for each replicate plot, where values of 0 represent perfect asynchrony and values of 1 represent perfect synchrony (Loreau & de Mazancourt, 2008). Rate of community change was determined by calculating the slope of a regression line of the Euclidean distances in species composition in each plot as a function of increasing time intervals. Community stability was quantified by calculating the temporal mean divided by the temporal standard deviation of aggregate species abundance:

$$\text{Stability} = \frac{\overline{A}}{\sigma_A},$$

where $\overline{A}$ is the temporal mean of aggregate species abundance within each replicate plot and time-period, and σ_A is the temporal standard deviation of aggregate species abundance in each plot across time. To further assess the spatial patterns of community variability as described by Taylor`s power law, slope (z) values were estimated for each replicate plot by linear regression of the log variance in species abundance against the log mean abundance using the formula from the "fit_taylor" function in the 'ecofolio' R software package, $\log(\sigma_i^2) = c + z * \log(\mu_i) + \varepsilon_i$, where c represents a constant, z represents the parameter of interest (Taylor's power law

exponent), i represents a species, and ε_i represents the residual error term for species i (Anderson et al., 2013; Taylor, 1961). Taylor`s power law predicts that in ecological systems, as community abundance increases, the standard deviation increases sub-linearly resulting in the slope (z) of a log-log plot of the variance and mean species abundance to be $1 < z < 2$ (Ghosh & Matthews, 2024; Taylor & Woiwod, 1982).

Environmental covariates

Following the methods from Wootton and Pfister (2012), measurements and seawater data were collected from 2000-2024 in April or May through August or September at half hour intervals using Hydrolab DataSonde 4a/5× (Hach®) data loggers that included probes for electrochemically-measured pH, water temperature, dissolved oxygen, and salinity. These data were input into the CO2SYS program for Microsoft Excel (Pierrot et al., 2011) to calculate carbonate chemistry parameters including total alkalinity, calcite saturation, aragonite saturation, and monthly estimates of nutrient concentrations. These variables were chosen because they are directly tied to core physiological and ecological processes structuring intertidal communities, particularly calcification, metabolism, and primary production in calcifiers and algae.

Community-associated responses to environmental stress

To analyze the relationship between community responses and environmental stress, generalized linear latent variables models (GLLVMs) were formulated with the R Software package 'gllvm' using the average annual species abundance matrix with all of the environmental covariates (Niku et al., 2019). We incorporated latent variables as unmeasured environmental factors, or as ordination scores, to represent the primary axes of abundance covariation (after accounting for the observed environmental predictors). Latent variable models have an advantage over other ordination approaches as community responses to environmental

stress can be directly predicted using model coefficients (Niku et al., 2020). Before incorporating abundance data and environmental covariates into the GLLVMs, all data were first log-transformed, and environmental data were also rescaled using z-standardization. We began model construction by specifying a response distribution and the number of latent variables to incorporate into the model, employing likelihood-based tools for inference of best model fit (AICc) and QQ plots of Dunn-Smyth residuals to ensure there was no evidence of heteroscedasticity. Once GLLVMs for communities with and without environmental covariates were constructed, the trace of the residual covariance matrix between the unconstrained GLLVMs without environmental covariates and the final GLLVMs with environmental covariates allowed us to quantify the amount of variation in the data explained by the environment (Niku et al., 2019). Lastly, to identify significant species responses to specific environmental stressors, the estimated coefficients and their 95% confidence intervals were plotted to visualize these interactions.

Statistical analyses

All analyses were conducted using the R statistical platform version 4.4.1 (R Core Team, 2024). Using the 'trend' software package in R, we ran a Mann-Kendall trend test to detect trend changes across environmental covariates and total community abundance of each treatment (Pohlert et al., 2016). A Student's t-test was used to determine if community indices differed between both treatments. A one-way ANOVA was used to test if experimental treatment had a significant effect on stability. Two-way ANOVA`s were used to assess if the dominance treatments had an interactive effect with Simpson`s evenness, species richness, Shannon diversity, species turnover, and Loreau synchrony.

RESULTS

Environmental time series analysis

The coastal waters surrounding Tatoosh Island have changed significantly over the last few decades with significant decreases in pH as previously documented by Wootton and Pfister (2012) (one-sided Mann-Kendall trend test: z = -4.225, n = 23, $p < 0.0001$, Figure C1), salinity (z = -1.810, n = 24, p = 0.0350, Figure C1), alkalinity (z = -2.108, n = 24, p-value = 0.0175, Figure C1), aragonite saturation (z = -3.695, n = 24, p = 0.0001, Figure C1), calcite saturation (z = -3.646, n = 24, p = 0.0001, Figure C1), chlorophyll-*a* (z = -3.299, n = 24, p = 0.0004, Figure C1), and a significant increase in sea surface temperature (z = 2.482, n = 23, p = 0.0065, Figure C1). Although there have been fluctuations in nitrate, there are no detectable trends over time (two-sided Mann-Kendall trend test: z = -0.669, n = 24, p = 0.503, Figure C1). Together, these long-term changes describe an environment increasingly unfavorable for intertidal species that calcify and are temperature sensitive through reduced carbonate availability and increasing thermal stress.

Temporal community dynamics

The low- and high-dominance communities exhibited different dynamics of community structure and turnover through time. High dominance communities (with *M. californianus* individuals) had a 15.8% greater total community abundance (Student's t-test: $t_{(464.89)} = 10.631$, $p < 0.0001$, Figure 3.1) and covered 13% more area of available surface area per plot compared to low dominance communities (without *M. californianus* individuals) ($t_{(408.78)} = 11.534$, $p < 0.0001$). High dominance communities also exhibited a 114% greater species turnover rate compared to low dominance communities ($t_{(42.27)} = 5.639$, $p < 0.0001$, Figure 3.2a). In contrast, low dominance communities had 5.94% greater species richness ($t_{(32.337)} = -3.341$, p = 0.0021,

Figure 3.2b), 7.46% greater species evenness ($t_{(40.39)} = -3.272$, $p = 0.0021$, Figure 3.2c), and 15.71% greater species diversity (t-test: $t_{(50.14)} = -7.211$, $p < 0.0001$, Figure 3.2d). The rate of community change indicated that rank shifts, or the change in the relative rank of species within a community based on their abundance, became increasingly dissimilar over time in low dominance communities, signifying increased community divergence. In contrast, high dominance communities rank shifts occurred with very little directional change (Figure 3.2e).

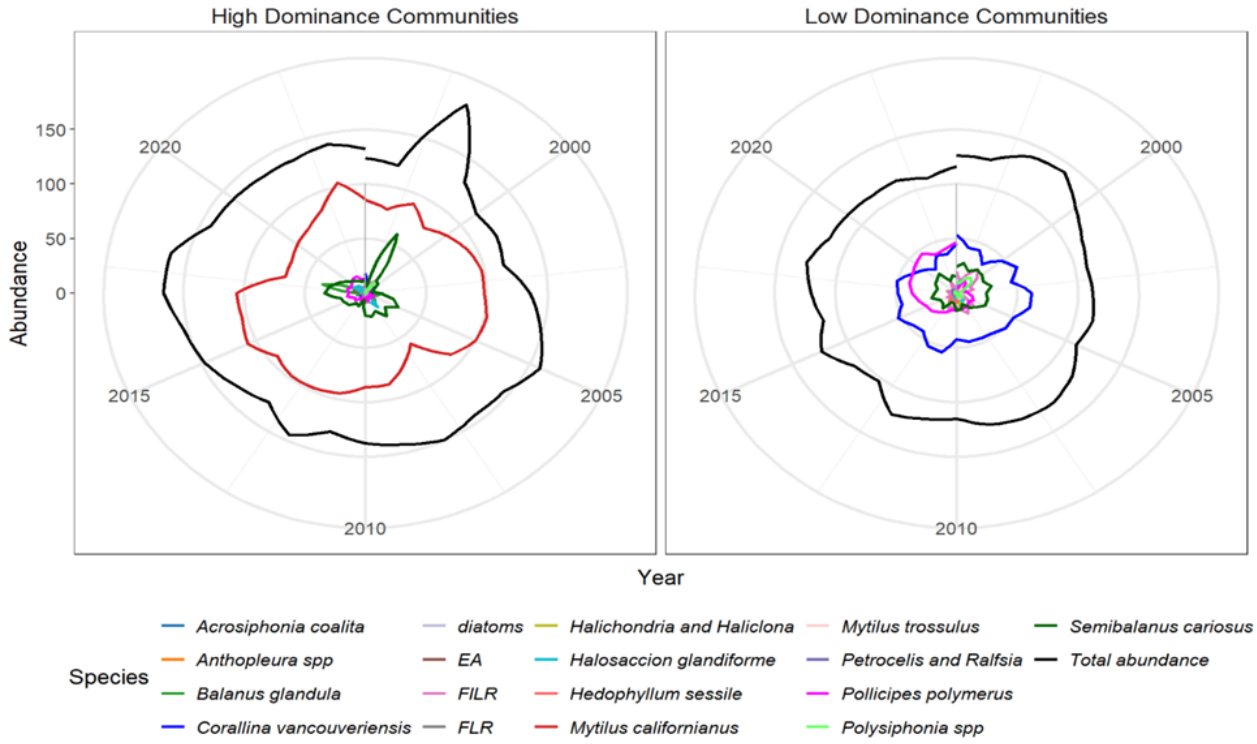

Figure 3.1: Rank clock plots of average sessile species abundance (colored lines) and total abundance (black line) over time in experimental plots where mussels (*M. californianus)* were present and resulted in high dominance communities versus consistently removed resulting in low dominance communities at Tatoosh Island, Makah Indian Reservation, WA. Vertical grey bars show the starting '12 o'clock' position on the rank clock corresponding to the year 1996 and the ending '12 o'clock' position corresponding to the year 2024. FILR-filamentous Rhodophytes; FLR-foliose Rhodophytes; EA-ephemeral algae.

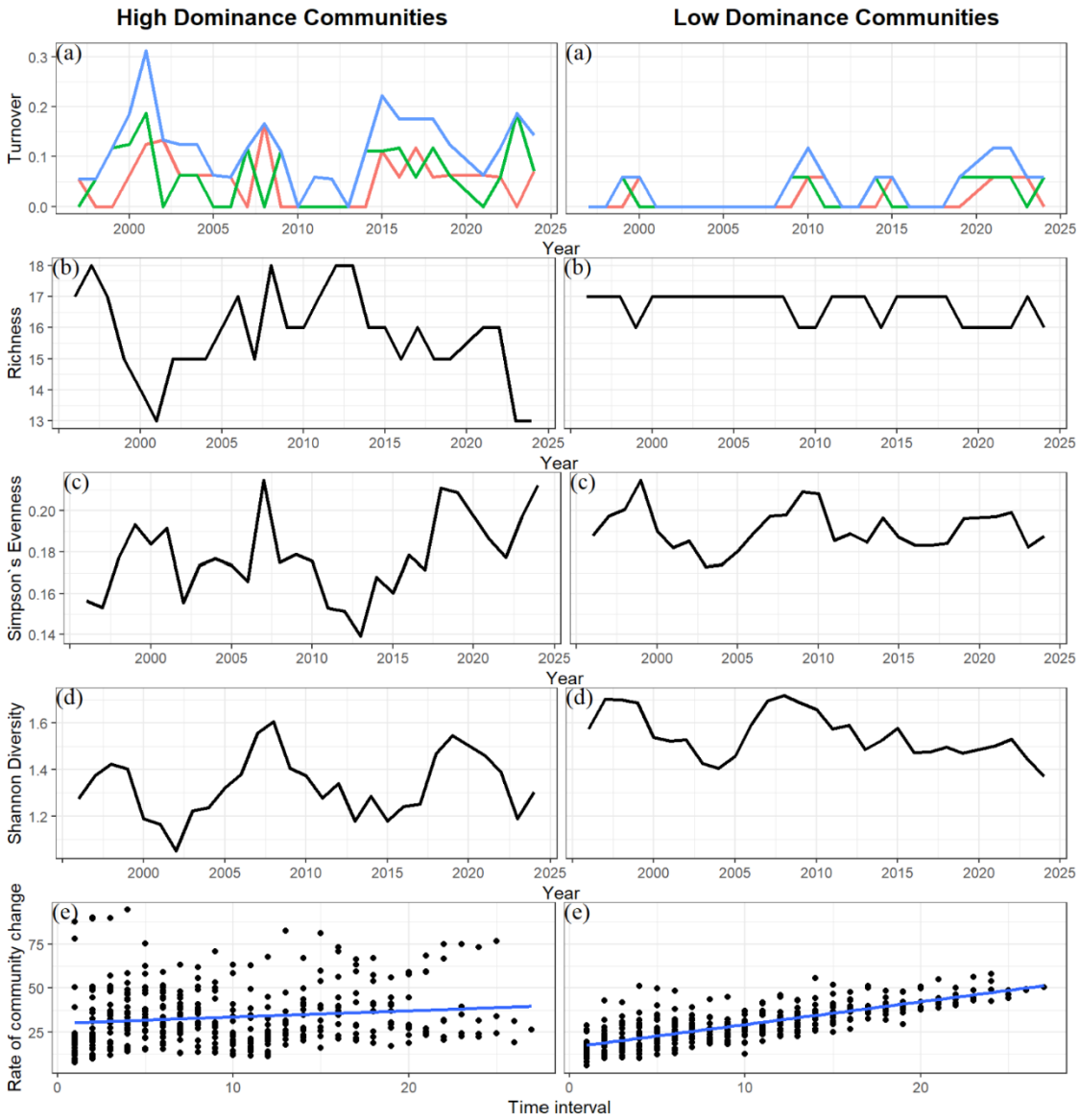

Figure 3.2: (a) Species turnover (total = light blue, appearances = green, disappearances = red), (b) richness (avg. annual number of species per 65 x 65cm plot, (c) Simpson`s evenness, (d) Shannon diversity, and (e) Rate of community change over time (Euclidean distances) in experimental plots where mussels (*M. californianus)* were present and resulted in high dominance communities versus consistently removed resulting in low dominance communities at Tatoosh Island, Makah Indian Reservation, WA.

Spatial community dynamics

Community dynamics across space for both low and high dominance communities satisfied Taylor`s Power Law with slopes $1 < z < 2$ (z mean: low = 1.49, high = 1.50) showing a decrease in variance at the community level with increasing aggregations of total species abundance ($t_{(22.161)} = 0.392$, $p = 0.6985$, Figure 3a). Furthermore, dominance was significantly related to community stability (one-way ANOVA: $F_{(1,23)} = 8.979$, $p = 0.0064$), with low dominance communities exhibiting significantly higher stabilities than high dominance communities ($t_{(22.707)} = 3.322$, $p = 0.0029$, Figure 3.3b). Synchrony within each community was also related to stability with increased synchrony associated with a decrease in overall stability (Figure 3.4a & Table 3.1). Low dominance communities were restricted to substantially lower levels of synchrony compared to high dominance communities, highlighting the interactive effect between synchrony and dominance treatment on community stability (Figure 3.4a & Table 3.1). Evenness was negatively correlated with community stability for both community types (Figure 3.4b & Table 3.1). When analyzing the results of species richness and diversity on community stability, diversity had a significant effect on stability (Table 3.1); low dominance communities had higher species richness (9.96 versus 7.52; $t_{(17.695)} = 9.844$, $p < 0.0001$, Figure 3.4c), therefore greater community diversity when compared to high dominance communities (1.31 versus 0.98; $t_{(20.431)} = 4.943$, $p < 0.0001$, Figure 3.4d). Alternatively, high dominance communities exhibited higher average species turnover rates compared to low dominance communities due to the rapid turnover of rare species (0.36 versus 0.31; $t_{(18.486)} = -2.869$, $p = 0.0100$, Table 3.1).

Table 3.1: Two-way ANOVA results of Loreau synchrony, Simpson`s evenness, richness, Shannon diversity, and species turnover in relation to community stability for experimental low (*Mytilus californianus* mussels removed) and high (*M. californianus* mussels present) dominance plots at Tatoosh Island, Makah Indian Reservation, WA.

Community Stability ANOVA Results				
Source	**df**	**MS**	***F***	***p***
Dominance Treatment (T)	1	39.82	22.04	**0.0001**
Synchrony (S)	1	29.51	16.33	**0.0005**
T x S	1	34.55	19.12	**0.0002**
Residuals	21	1.81		
Total	24			
Dominance Treatment (T)	1	39.82	10.926	**0.0033**
Evenness (E)	1	22.47	6.166	**0.0215**
T x E	1	3.00	0.822	0.3748
Residuals	21	3.64		
Total	24			
Dominance Treatment (T)	1	39.82	9.258	**0.0061**
Richness (R)	1	2.42	0.562	0.4617
T x R	1	9.26	2.153	0.1571
Residuals	21	4.3		
Total	24			
Dominance Treatment (T)	1	39.82	11.349	**0.0029**
Diversity (D)	1	17.07	4.864	**0.0387**
T x D	1	11.25	3.205	0.0878
Residuals	21	3.51		
Total	24			
Dominance Treatment (T)	1	39.82	9.001	**0.0068**
Turnover (To)	1	5.7	1.288	0.2692
T x To	1	3.4	0.769	0.3903
Residuals	21	4.42		
Total	24			

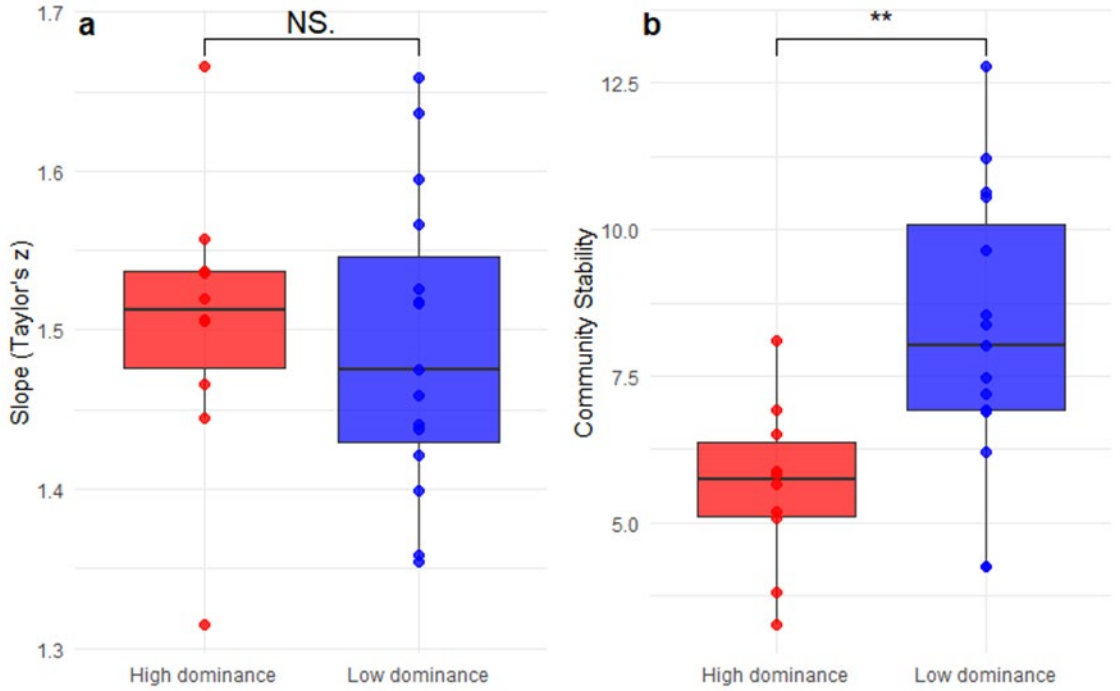

Figure 3.3: (a) Slopes of Taylor`s Power Law and (b) community stability in experimental plots where mussels (*M. californianus)* were present and resulted in high dominance communities versus consistently removed resulting in low dominance communities at Tatoosh Island, Makah Indian Reservation, WA.

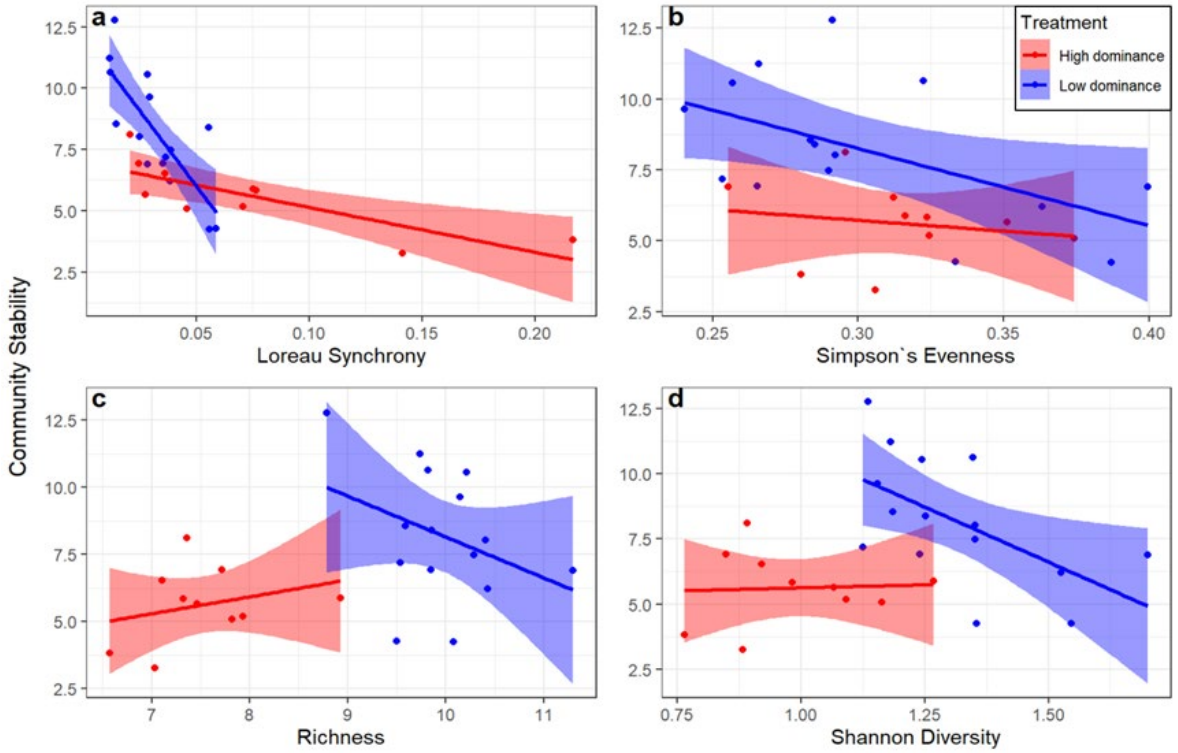

Figure 3.4: (a) Loreau synchrony, (b) Simpson`s evenness, (c) richness, (d) and Shannon diversity in relation to community stability in experimental plots where mussels (*M. californianus)* were present and resulted in high dominance communities versus consistently removed resulting in low dominance communities at Tatoosh Island, Makah Indian Reservation, WA.

Community responses to environmental stress

The Generalized Linear Latent Variable Models (GLLVMs) revealed a greater number of species associations in low compared to high dominance communities as the environment changed (Figure 3.5). For low dominance communities, the ratio of traces of the residual covariance matrices with and without environmental covariates suggests that environmental variables explain approximately 70% of the covariation in sessile species abundances (Figure 3.5), whereas the ratio of traces for high dominance communities suggests that environmental variables explain approximately 44% of the covariation in sessile species abundances (Figure 3.5). Species-specific responses to temperature further differed between dominance states. The presence of *Mytilus californianus* significantly reduces the effects of temperature stress for *Mytilus trossulus*, *Halosaccion glandiforme*, filamentous Rhodophytes (FILR), and foliose Rhodophytes (FLR) but exacerbates the effects of temperature stress on *Corallina vancouveriensis*, the most abundant species in low dominance communities (Figure 3.1, Figure C2, & C3). Lastly, total abundances of low dominance communities decreased by 7.92% ($z = -1.995$, $n = 28$, $p = 0.046$, Figure 3.1) from 1996-2024, whereas high dominance communities increased by 7% ($z = 1.086$, $n = 28$, $p = 0.2772$, Figure 3.1).

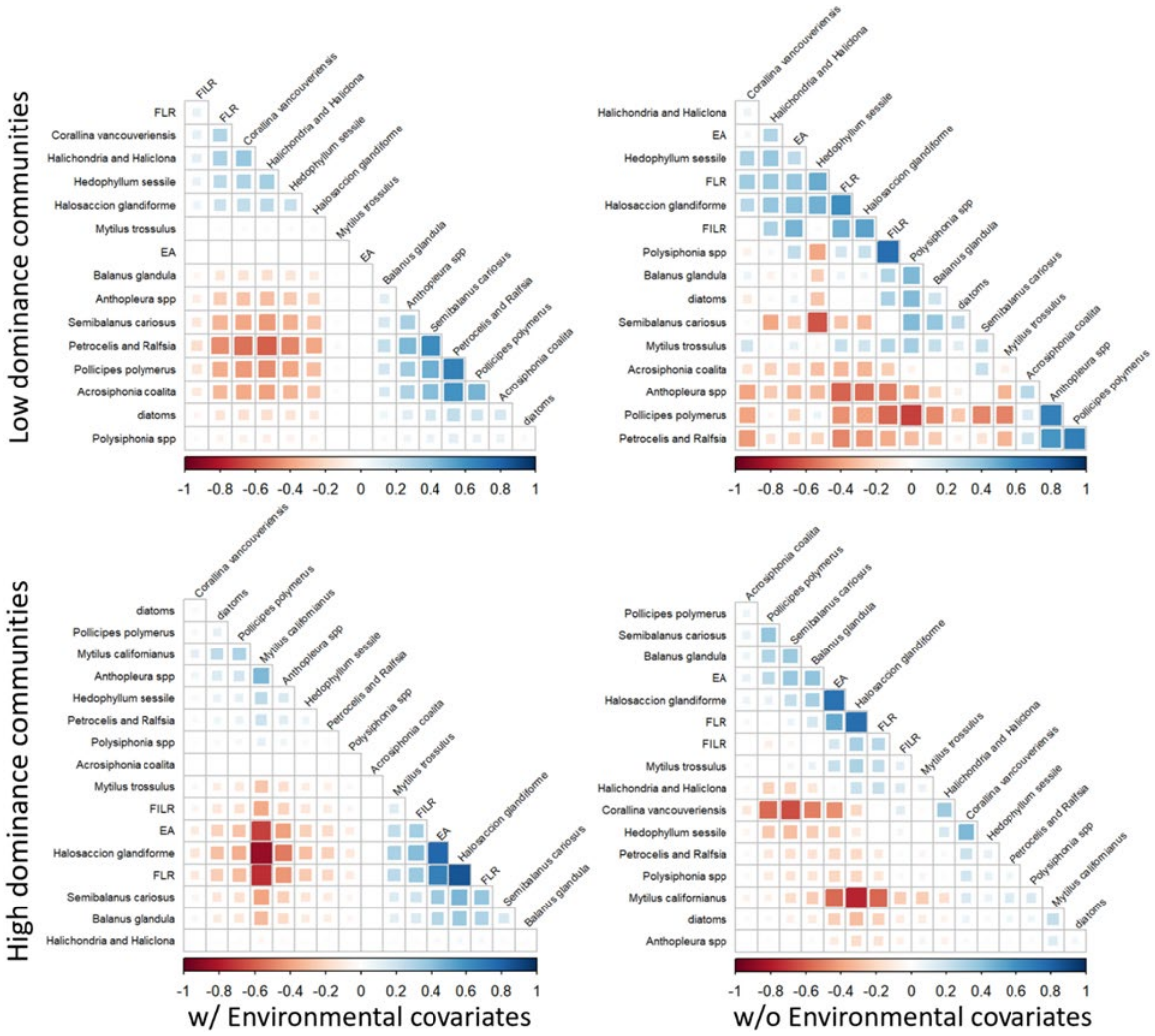

Figure 3.5: Correlation matrix of the residual annual species abundances with (left) or without (right) environmental covariates included in a Generalized Linear Latent Variable Model in experimental plots where *M. californianus* mussels were consistently removed resulting in low dominance communities (top) or in experimental plots where mussels (*M. californianus)* were present and resulted in high dominance communities (bottom) at Tatoosh Island, Makah Indian Reservation, WA. FILR-filamentous Rhodophytes; FLR-foliose Rhodophytes; EA-ephemeral algae. Colors correspond to positive (blue) and negative (red) correlations between species.

DISCUSSION

We measured community associated responses to increasing environmental stress, focusing on the dynamics between two features of communities in nature (i.e. diversity and dominance) on a rocky-intertidal shore. Low dominance communities exhibited greater species richness, evenness, diversity, and asynchrony resulting in increased stability (Figures 3.2, 3.3b,

& 3.4). These data support hypotheses from Doak et al. (1998) and Loreau (2010) that the stabilizing effect of species diversity is strongest in low dominance communities as a result of greater portfolio effects; a community with more asynchronously-responding species maintains higher average stability, much like diverse financial portfolios yield more stable returns (Markowitz, 1952). However, in contrast to Tilman (1999), increased evenness and diversity in low dominance communities decreased their stability (Figure 3.4b & 3.4d). Although high dominance communities maintained lower stability levels compared to low dominance communities (Figure 3.3b), evidence of each replicate plot satisfying Taylor`s power law (Figure 3.3a), and increasing total community abundances (Figure 3.1), suggest an alternative maintenance process: increases in ecosystem functioning in response to environmental stress. Empirical evidence demonstrates that the stabilizing effect of richness becomes negligible as synchrony among species increases, and high species turnover within synchronous communities results in decreased temporal variability (Ghosh & Matthews, 2024). Because environmental forcing decreases niche differentiation that results in increased synchrony among populations (Loreau & de Mazancourt, 2008), and communities exposed to extreme environmental duress are often characterized by unevenness, increased turnover, and low species richness (Shurin, 2007; Ulrich et al., 2016), suggest facilitative interactions between dominant and rare species may increase productivity in stressful environments for high dominance communities.

Diversity concedes to dominance in stressful environments

For communities vulnerable to environmental change, biological invasions or colonization by rare species can strengthen the resilience of these communities as introduced species fill functional niches responsible for maintaining function in novel environments (Chaffin et al., 2016). Callaway and Walker (1997) proposed the stress-gradient hypothesis as a

possible explanation of this phenomenon, where they argued environmental filtering amplifies facilitative interactions among species, which in turn increases the likelihood of invasion leading to shifts in local community composition. Von Holle (2013) demonstrated this in coastal heathlands where environmental stress facilitated the invasion of new species into communities due to increasing environmental gradients (i.e. increased wind and salt deposition) reducing the importance of species competition. Our results support these findings, as environmental covariates strengthened facilitative associations in high dominance communities but weakened facilitative associations in low dominance communities, where species turnover increased with intensifying environmental gradients (Figures 3.5, 3.6 & Figure C1).

In the 1990s, Weiher and Keddy (1995) proposed the stress-dominance hypothesis (SDH), suggesting that increasing environmental stress associated with climate change will lead to stronger habitat filtering on community assemblages, reducing the importance of species interactions as dominant species synchronize to changing environments. Our GLLVM results support the SDH as abiotic stress in low dominance communities led to decreased strength and number of pairwise associations suggesting increased habitat filtering in these communities (Figure 3.5). In contrast, our GLLVM results indicated that environmental stress in high dominance communities increased the strength and number of pairwise associations (Figure 3.5). Under stressful conditions, increased habitat filtering should reduce the effect of species interactions and lead to reductions in diversity as lower diversity systems show greater resilience to environmental perturbations (Jackson et al., 2001; Pfisterer & Schmid, 2002). Our analyses support these findings, as low dominance communities experienced decreased diversity after 2009 (Figure 3.2d) that was coincident with increased community divergence (Figure 3.2e) and decreasing total community abundance (Figure 3.1). In contrast, high dominance communities

exhibited lower diversity (Figure 3.2d), increasing total community abundance (Figure 3.1), and relatively little community divergence (Figure 3.2e). The decreased diversity after 2009 in low dominance communities coincided with increased sea surface temperature (Figure C1), species turnover (Figure 3.2a), and a rapid increase in population abundance of *Pollicipes polymerus* (Figure 3.1). Most of the taxonomic diversity of sessile species within the rocky intertidal consists of algae that are relatively susceptible to abiotic stress (Kaur et al., 2022). Throughout the experimental period, abiotic stressors drastically increased (Figure C1), with the algae *Hedophyllum sessile, Halosaccion glandiforme,* filamentous Rhodophytes, and foliose Rhodophytes in low dominance communities showing vulnerability to increasing sea surface temperatures (Figure C2), resulting in decreased community diversity as temperatures increased (Figure 3.1, 3.2d, & Figure C1). However, the introduction and subsequent population increase of *Pollicipes polymerus* and *Semibalanus cariosus* throughout all low dominance communities (Figure 3.1) combined with increased resistance to temperature stress (Figure C2) suggest the invasion of *Pollicipes polymerus* and *Semibalanus cariosus* in low dominance communities indirectly increased ecosystem functioning as the environment changed.

The role of biotic interactions in a changing ocean

A central theme in ecology is understanding how individual species dynamics and interactions yield direct and indirect effects on ecosystem functioning. One of the most well-known studies in ecology is the sea star removal experiment on the Pacific coast of Washington state done a half-century ago by Paine (1966). A central conclusion was that the sea star *Pisaster ochraceus* promoted species diversity by consuming the dominant competitor for space in the system, the mussel *Mytilus californianus*, thereby reducing competitive exclusion among prey species, a situation that led Paine (1969) to subsequently term species like *P. ochraceus* with

such wide-ranging effects as keystone species. Our results conform with Paine (1966), in that the absence of *M. californianus* increased the diversity of sessile species within the marine intertidal that resulted in increased community stability in low dominance communities (Figure 3.2d). However, as environmental gradients strengthen because of climate change, the ability of mussels to provide structural complexity and ameliorate physical stressors for other species within the community highlight the importance of dominant species. Currently, increasing environmental stressors have already had a significant effect on trophic interactions within rocky intertidal ecosystems, as sea star wasting disease has driven *P. ochraceus* population sizes across the northeast Pacific to low densities (Pfister et al., 2016). Experimental studies demonstrated that the removal of *P. ochraceus* from rocky intertidal communities indirectly reduced species coexistence resulting in shifts to alternative community states dominated by mussels (Paine, 1974; Paine & Trimble, 2004). Additionally, *Corallina vancouveriensis*, the ubiquitous sessile species in low-dominance communities, has shown sensitivity to rising sea surface temperature and decreasing pH (McCoy & Kamenos, 2015), a vulnerability that could further accelerate community shifts to favor mussels within rocky intertidal ecosystems. However, these responses may not be identical across all populations. For example, in *C. vancouveriensis,* temperate populations have broader thermal windows (Krieger et al., 2023), while leading edge populations experience skeletal composition plasticity in response to more acidic environments (Kolzenburg et al., 2023). *Mytilus spp.* have also demonstrated the capacity to respond to warming and acidifying conditions through adaptive genetic variation (Araneda et al., 2016; Bitter et al., 2019). Indeed, intraspecific diversity may play a critical role in determining responses to changing environments, with intraspecific differentiation within the metapopulation promoting niche variation within populations (Svanbäck & Bolnick, 2007), enhancing population responses

across heterogenous environments (Richards et al., 2025), and positively influencing community and ecosystem processes (Hersch-Green et al., 2011).

CONCLUSION

Overall, our experiments reveal ecosystem-associated responses to biodiversity shifts will depend upon existing community composition and the magnitude of environmental change. For metacommunities experiencing minimal environmental change, low dominance communities may result. For metacommunities undergoing extensive environmental change, high dominance communities may result as larger populations of dominant species increase resilience to environmental fluctuations by facilitating invaders to occupy critical functional niches that indirectly increase temporal community stability (De Roy et al., 2013). However, we would also expect an adaptive community-associated response in low dominance communities, as increased habitat filtering reduces the role of competition, leading to greater dominance and reduced species diversity. Ultimately, climate change will affect ecosystems disproportionately across time and space, highlighting the importance of competing maintenance processes among local communities in strengthening ecosystem responses to varying conditions. Therefore, more in-depth analyses of local community compositions and intraspecific diversity across heterogeneous environments are essential for understanding how well-equipped regional systems are to climate change.

DATA AVAILABILITY

Data and code used for analyses are made available on Figshare: https://doi.org/10.6084/m9.figshare.32095033

APPENDIX C: SUPPLEMENTAL INFORMATION FOR CHAPTER 3

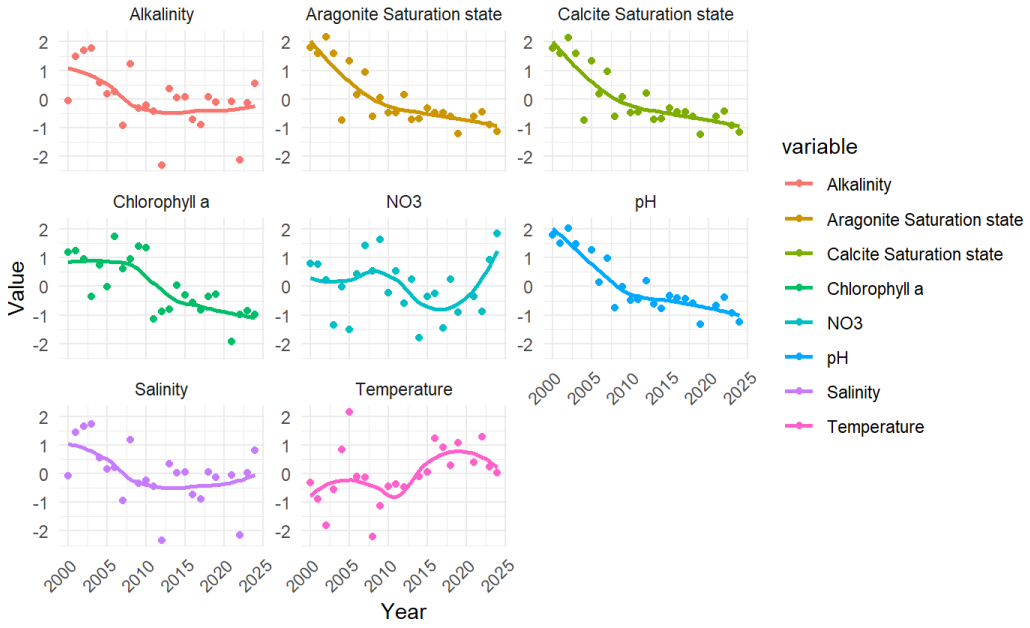

Figure C1: Annual averages of measured environmental variables from 2000-2024 at Tatoosh Island, Makah Indian Reservation, WA. All data has been log transformed and scaled using Z-standardization for comparison between ocean variables.

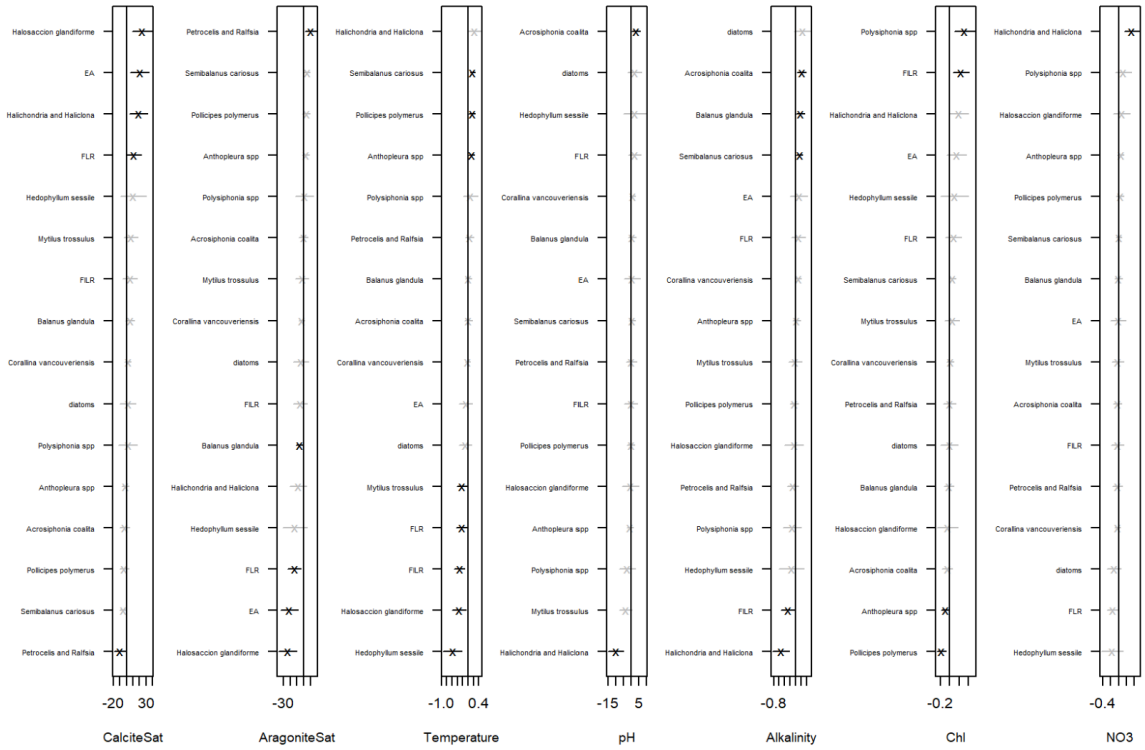

Figure C2: Covariate coefficients of environmental variables on species abundance in low dominance communities (*Mytilus californianus* mussels removed) from 2000-2024 at Tatoosh Island, Makah Indian Reservation, WA. Error bars represent 95% confidence intervals. Species with confidence intervals that do not cross zero are highlighted in bold, indicating significant changes in abundance relative to the respective environmental driver. FILR-filamentous Rhodophytes; FLR-foliose Rhodophytes; EA-ephemeral algae.

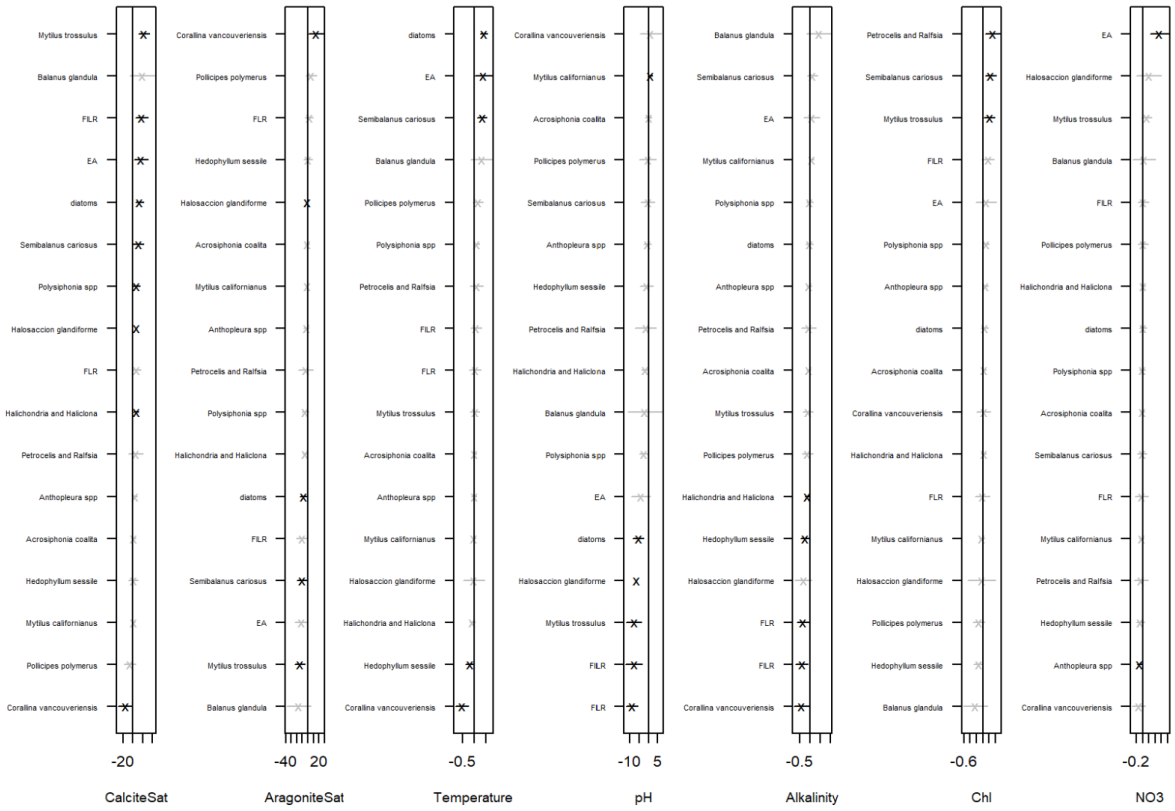

Figure C3: Covariate coefficients of environmental variables on species abundance in high dominance communities (*Mytilus californianus* mussels present) from 2000-2024 at Tatoosh Island, Makah Indian Reservation, WA. Error bars represent 95% confidence intervals. Species with confidence intervals that do not cross zero are highlighted in bold, indicating significant changes in abundance relative to the respective environmental driver. FILR-filamentous Rhodophytes; FLR-foliose Rhodophytes; EA-ephemeral algae.

CONCLUDING REMARKS

In this dissertation, I test species' plasticity and resilience in changing environments, thereby providing insight into adaptive responses to environmental stressors, the potential for adaptation, and the ability to occupy future oceans. In conjunction, the three chapters address this central objective by linking organismal, evolutionary, and ecological responses across scales of biological organization. Chapter 1 demonstrates that spatially varying selection within the intertidal zone leads to differences in functional trait evolution within *Mytilus californianus*, with morphological traits exhibiting phenotypic plasticity while physiological traits are constrained due to local adaptation. These results highlight how different components of organismal function respond uniquely to environmental stress, revealing trait-specific trade-offs that enhance the adaptive potential within populations (Hays et al., 2021). Chapter 2 extends this framework across broader spatial gradients, showing that in connected populations across heterogeneous environments, the degree of gene flow and selection between populations shapes the genetic structure and phenotypic plasticity of adaptive traits, directly influencing rates of adaptation across species ranges (Leimar et al., 2019; Yeaman & Whitlock, 2011). Despite high population connectivity, strong selection across heterogeneous environments generates fixed, co-adapted gene complexes within populations, while gene flow increases genetic diversity and enhances plasticity among populations. Together, these processes expand the evolutionary "toolkit" of metapopulations for responding to novel environmental stressors (Hersch-Green et al., 2011). Chapter 3 scales these organismal and evolutionary processes to the community level, demonstrating that foundation species maintain ecosystem stability by buffering environmental stress and structuring community responses through facilitative interactions. Collectively, these findings support the central hypothesis that environmental gradients in the intertidal drive trait-

specific evolutionary responses, which scale up through population genetic structure and community dynamics to determine ecosystem function. Rather than acting independently, phenotypic plasticity, local adaptation, gene flow, and community composition are tightly integrated processes, jointly shaping the fitness of a foundational marine species in a variable environment, and contributing to its persistence under ongoing climate-driven changes.

REFERENCES

Abo-Al-Ela, H. G., & Faggio, C. (2021). MicroRNA-mediated stress response in bivalve species. *Ecotoxicology and environmental safety*, *208*, 111442.

Ameztegui, A. (2017). Plasticity: An R package to determine several plasticity indices. *GitHub repository*.

Anderson, J. T., & Gezon, Z. J. (2015). Plasticity in functional traits in the context of climate change: a case study of the subalpine forb Boechera stricta (Brassicaceae). *Global Change Biology*, *21*(4), 1689-1703.

Anderson, J. T., Perera, N., Chowdhury, B., & Mitchell-Olds, T. (2015). Microgeographic patterns of genetic divergence and adaptation across environmental gradients in Boechera stricta (Brassicaceae). *The American Naturalist*, *186*(S1), S60-S73.

Anderson, S. C., Cooper, A. B., & Dulvy, N. K. (2013). Ecological prophets: quantifying metapopulation portfolio effects. *Methods in Ecology and Evolution*, *4*(10), 971-981. https://doi.org/10.1111/2041-210X.12093

Angelini, C., Altieri, A. H., Silliman, B. R., & Bertness, M. D. (2011). Interactions among foundation species and their consequences for community organization, biodiversity, and conservation. *Bioscience*, *61*(10), 782-789. https://doi.org/https://doi.org/10.1525/bio.2011.61.10.8

Antonovics, J. (2006). Evolution in closely adjacent plant populations X: long-term persistence of prereproductive isolation at a mine boundary. *Heredity*, *97*(1), 33-37.

Araneda, C., Larraín, M. A., Hecht, B., & Narum, S. (2016). Adaptive genetic variation distinguishes Chilean blue mussels (Mytilus chilensis) from different marine environments. *Ecology and evolution*, *6*(11), 3632-3644. https://doi.org/10.1002/ece3.2110

Atkinson, C. L., Vaughn, C. C., Forshay, K. J., & Cooper, J. T. (2013). Aggregated filter-feeding consumers alter nutrient limitation: consequences for ecosystem and community dynamics. *Ecology*, *94*(6), 1359-1369. https://doi.org/10.1890/12-1531.1

Bachmann, J. C., Jansen van Rensburg, A., Cortazar-Chinarro, M., Laurila, A., & Van Buskirk, J. (2020). Gene flow limits adaptation along steep environmental gradients. *The American Naturalist*, *195*(3), E67-E86.

Baden, S., Hernroth, B., & Lindahl, O. (2021). Declining populations of Mytilus spp. in North Atlantic coastal waters—a Swedish perspective. *Journal of Shellfish Research*, *40*(2), 269-296. https://doi.org/10.2983/035.040.0207

Bai, X., Zhou, Y., Bi, W., Hu, H., Xu, C., & Li, Q. (2025). Transcriptome Analysis of the Susceptibility to High Temperature of the Tetraploid Pacific Oyster Crassostrea gigas. *Journal of Ocean University of China*, *24*(3), 721-734. https://doi.org/10.1007/s11802-025-5990-0

Baldwin, J. M. (1896). A new factor in evolution. *The American Naturalist*, *30*, 441-451.

Barrett, R. D., & Schluter, D. (2008). Adaptation from standing genetic variation. *Trends in ecology & evolution*, *23*(1), 38-44. https://doi.org/10.1016/j.tree.2007.09.008

Bidau, C. J., Mino, C. I., Castillo, E. R., & Martí, D. A. (2012). Effects of abiotic factors on the geographic distribution of body size variation and chromosomal polymorphisms in two neotropical grasshopper species (Dichroplus: Melanoplinae: Acrididae). *Psyche: A Journal of Entomology*, *2012*(1), 863947.

Bitter, M., Kapsenberg, L., Gattuso, J.-P., & Pfister, C. (2019). Standing genetic variation fuels rapid adaptation to ocean acidification. *Nature communications*, *10*(1), 1-10. https://doi.org/10.1038/s41467-019-13767-1

Bitter, M. C., Kapsenberg, L., Silliman, K., Gattuso, J.-P., & Pfister, C. A. (2021). Magnitude and predictability of pH fluctuations shape plastic responses to ocean acidification. *The American Naturalist*, *197*(4), 486-501. https://doi.org/10.1086/712930

Bulmer, M. (1971). The effect of selection on genetic variability. *The American Naturalist*, *105*(943), 201-211.

Bürger, R., & Akerman, A. (2011). The effects of linkage and gene flow on local adaptation: a two-locus continent–island model. *Theoretical population biology*, *80*(4), 272-288. https://doi.org/10.1016/j.tpb.2011.07.002

Burrows, M. T., Schoeman, D. S., Buckley, L. B., Moore, P., Poloczanska, E. S., Brander, K. M., Brown, C., Bruno, J. F., Duarte, C. M., & Halpern, B. S. (2011). The pace of shifting climate in marine and terrestrial ecosystems. *Science*, *334*(6056), 652-655.

Callaway, R. M., & Walker, L. R. (1997). Competition and facilitation: a synthetic approach to interactions in plant communities. *Ecology*, *78*(7), 1958-1965. https://doi.org/10.1890/0012-9658(1997)078[1958:CAFASA]2.0.CO;2

Carl, C., Poole, A. J., Williams, M. R., & de Nys, R. (2012). Where to settle—settlement preferences of Mytilus galloprovincialis and choice of habitat at a micro spatial scale. *PloS one*, *7*(12), e52358. https://doi.org/10.1371/journal.pone.0052358

Chaffin, B. C., Garmestani, A. S., Angeler, D. G., Herrmann, D. L., Stow, C. A., Nyström, M., Sendzimir, J., Hopton, M. E., Kolasa, J., & Allen, C. R. (2016). Biological invasions, ecological resilience and adaptive governance. *Journal of Environmental Management*, *183*, 399-407. https://doi.org/10.1016/j.jenvman.2016.04.040

Chapin Iii, F. S., Zavaleta, E. S., Eviner, V. T., Naylor, R. L., Vitousek, P. M., Reynolds, H. L., Hooper, D. U., Lavorel, S., Sala, O. E., & Hobbie, S. E. (2000). Consequences of changing biodiversity. *Nature*, *405*(6783), 234-242. https://doi.org/10.1038/35012241

Chen, S., Zhou, Y., Chen, Y., & Gu, J. (2018). fastp: an ultra-fast all-in-one FASTQ preprocessor. *Bioinformatics*, *34*(17), i884-i890. https://doi.org/10.1093/bioinformatics/bty560

Cingolani, P., Platts, A., Wang, L. L., Coon, M., Nguyen, T., Wang, L., Land, S. J., Lu, X., & Ruden, D. M. (2012). A program for annotating and predicting the effects of single nucleotide polymorphisms, SnpEff: SNPs in the genome of Drosophila melanogaster strain w1118; iso-2; iso-3. *fly*, *6*(2), 80-92.

Connell, J. H. (1972). Community interactions on marine rocky intertidal shores. *Annual review of ecology and systematics*, *3*(1), 169-192.

Connor, K., & Gracey, A. Y. (2020). Cycles of heat and aerial-exposure induce changes in the transcriptome related to cell regulation and metabolism in Mytilus californianus. *Marine Biology*, *167*(9), 132.

Conover, D. O., Duffy, T. A., & Hice, L. A. (2009). The covariance between genetic and environmental influences across ecological gradients: reassessing the evolutionary significance of countergradient and cogradient variation. *Annals of the new York Academy of Sciences*, *1168*(1), 100-129.

Cottingham, K., Brown, B., & Lennon, J. (2001). Biodiversity may regulate the temporal variability of ecological systems. *Ecology Letters*, *4*(1), 72-85. https://doi.org/10.1046/j.1461-0248.2001.00189.x

Dainat, J., Hereñú, D., Murray, D. K., Davis, E., Ugrin, I., Crouch, K., Agostinho, N., & Zollman, Z. (2024). NBISweden/AGAT: AGAT-v1. 4.1. *Zenodo*.

Dayton, P. K. (1971). Competition, disturbance, and community organization: the provision and subsequent utilization of space in a rocky intertidal community. *Ecological Monographs*, *41*(4), 351-389.

Dayton, P. K. (1972). Toward an understanding of community resilience and the potential effects of enrichments to the benthos at McMurdo Sound, Antarctica. *Proceedings of the colloquium on conservation problems in Antarctica.*, *Parker BC , ed.*, 81-95, Allen Press.

Dayton, P. K. (1975). Experimental evaluation of ecological dominance in a rocky intertidal algal community. *Ecological Monographs*, *45*(2), 137-159. https://doi.org/https://doi.org/10.2307/1942404

De Roy, K., Marzorati, M., Negroni, A., Thas, O., Balloi, A., Fava, F., Verstraete, W., Daffonchio, D., & Boon, N. (2013). Environmental conditions and community evenness

determine the outcome of biological invasion. *Nature communications*, *4*(1), 1383. https://doi.org/10.1038/ncomms2392

Denny, M. W., Dowd, W. W., Bilir, L., & Mach, K. J. (2011). Spreading the risk: small-scale body temperature variation among intertidal organisms and its implications for species persistence. *Journal of Experimental Marine Biology and Ecology*, *400*(1-2), 175-190.

Des Roches, S., Post, D. M., Turley, N. E., Bailey, J. K., Hendry, A. P., Kinnison, M. T., Schweitzer, J. A., & Palkovacs, E. P. (2018). The ecological importance of intraspecific variation. *Nature Ecology & Evolution*, *2*(1), 57-64.

Doak, D. F., Bigger, D., Harding, E., Marvier, M., O'malley, R., & Thomson, D. (1998). The statistical inevitability of stability-diversity relationships in community ecology. *The American Naturalist*, *151*(3), 264-276. https://doi.org/10.1086/286117

Dou, H., Miao, Y., Li, Y., Li, Y., Dai, X., Zhang, X., Liang, P., Liu, W., Wang, S., & Bao, Z. (2018). Characterization of chiton Ischnochiton hakodadensis foot based on transcriptome sequencing. *Journal of Ocean University of China*, *17*(3), 632-640. https://doi.org/10.1007/s11802-018-3525-7

Duarte, C., Navarro, J. M., Acuña, K., Torres, R., Manríquez, P. H., Lardies, M. A., Vargas, C. A., Lagos, N. A., & Aguilera, V. (2015). Intraspecific variability in the response of the edible mussel Mytilus chilensis (Hupe) to ocean acidification. *Estuaries and Coasts*, *38*, 590-598.

Dunne, J. A., Harte, J., & Taylor, K. J. (2003). Subalpine meadow flowering phenology responses to climate change: integrating experimental and gradient methods. *Ecological Monographs*, *73*(1), 69-86.

Dunstan, P. K., & Johnson, C. R. (2006). Linking richness, community variability, and invasion resistance with patch size. *Ecology*, *87*(11), 2842-2850. https://doi.org/10.1890/0012-9658(2006)87[2842:LRCVAI]2.0.CO;2

Edelaar, P., Jovani, R., & Gomez-Mestre, I. (2017). Should I change or should I go? Phenotypic plasticity and matching habitat choice in the adaptation to environmental heterogeneity. *The American Naturalist*, *190*(4), 506-520. https://doi.org/10.1086/693345

Efron, B. (1982). *The jackknife, the bootstrap and other resampling plans*. SIAM.

Ellison, A. M. (2019). Foundation species, non-trophic interactions, and the value of being common. *Iscience*, *13*, 254-268.

Ellison, A. M., Bank, M. S., Clinton, B. D., Colburn, E. A., Elliott, K., Ford, C. R., Foster, D. R., Kloeppel, B. D., Knoepp, J. D., & Lovett, G. M. (2005). Loss of foundation species: consequences for the structure and dynamics of forested ecosystems. *Frontiers in*

Ecology and the Environment, *3*(9), 479-486. https://doi.org/10.1890/1540-9295(2005)003[0479:LOFSCF]2.0.CO;2

Elser, J. J., Dobberfuhl, D. R., MacKay, N. A., & Schampel, J. H. (1996). Organism size, life history, and N: P stoichiometry: toward a unified view of cellular and ecosystem processes. *Bioscience*, *46*(9), 674-684. https://doi.org/10.2307/1312897

Endler, J. A. (1986). *Natural selection in the wild*. Princeton University Press.

Evanno, G., Regnaut, S., & Goudet, J. (2005). Detecting the number of clusters of individuals using the software STRUCTURE: a simulation study. *Molecular ecology*, *14*(8), 2611-2620. https://doi.org/10.1111/j.1365-294X.2005.02553.x

Fitzgerald-Dehoog, L., Browning, J., & Allen, B. J. (2012). Food and heat stress in the California mussel: evidence for an energetic trade-off between survival and growth. *The Biological Bulletin*, *223*(2), 205-216. https://doi.org/10.1086/BBLv223n2p205

Gaitán-Espitia, J. D., Quintero-Galvis, J. F., Mesas, A., & D'Elía, G. (2016). Mitogenomics of southern hemisphere blue mussels (Bivalvia: Pteriomorphia): Insights into the evolutionary characteristics of the Mytilus edulis complex. *Scientific reports*, *6*(1), 26853. https://doi.org/10.1038/srep26853

Gallien, L., & Carboni, M. (2017). The community ecology of invasive species: where are we and what's next? *Ecography*, *40*(2), 335-352. https://doi.org/10.1111/ecog.02446

Gauzere, J., Klein, E. K., Brendel, O., Davi, H., & Oddou-Muratorio, S. (2020). Microgeographic adaptation and the effect of pollen flow on the adaptive potential of a temperate tree species. *New Phytologist*, *227*(2), 641-653.

Gehman, A. L. M., & Harley, C. D. (2019). Symbiotic endolithic microbes alter host morphology and reduce host vulnerability to high environmental temperatures. *Ecosphere*, *10*(4), e02683.

Ghalambor, C. K., McKay, J. K., Carroll, S. P., & Reznick, D. N. (2007). Adaptive versus non-adaptive phenotypic plasticity and the potential for contemporary adaptation in new environments. *Functional ecology*, *21*(3), 394-407. https://doi.org/10.1111/j.1365-2435.2007.01283.x

Ghosh, S., & Matthews, B. (2024). Temporal turnover in species' ranks can explain variation in Taylor's slope for ecological timeseries. *Ecology*, *105*(9), e4381. https://doi.org/10.1002/ecy.4381

Gibbs, S. J., Bown, P. R., Ridgwell, A., Young, J. R., Poulton, A. J., & O'Dea, S. A. (2016). Ocean warming, not acidification, controlled coccolithophore response during past greenhouse climate change. *Geology*, *44*(1), 59-62. https://doi.org/10.1130/G37273.1

Gratani, L. (2014). Plant phenotypic plasticity in response to environmental factors. *Advances in botany*, *2014*(1), 208747. https://doi.org/10.1155/2014/208747

Günther, T., & Coop, G. (2013). Robust Identification of Local Adaptation from Allele Frequencies. *Genetics*, *195*(1), 205-220. https://doi.org/10.1534/genetics.113.152462

Guo, F., Xin, Z., Dong, Z., & Ye, Y. (2024). Genome-Wide Identification, Characterization, and Transcriptional Profile of the HECT E3 Ubiquitin Ligase Gene Family in the Hard-Shelled Mussel Mytilus coruscus Gould. *Genes*, *15*(8), 1085. https://doi.org/10.3390/genes15081085

Gurr, S. J., Meseck, S. L., Bernatchez, G., Redman, D., Dixon, M. S., Guy, L., MacDonald, A., Stiles, S., & McFarland, K. (2025). Transcriptome-To-Phenome Response of Larval Eastern Oysters Under Multiple Drivers of Aragonite Undersaturation. *Ecology and evolution*, *15*(2), e70953. https://doi.org/10.1002/ece3.70953

Gurski, L. M. (2016). *Microgeographic adaptation in a broadcast-spawning marine invertebrate* Texas A&M University-Corpus Christi].

Gutiérrez, J. L., Jones, C. G., Strayer, D. L., & Iribarne, O. O. (2003). Mollusks as ecosystem engineers: the role of shell production in aquatic habitats. *Oikos*, *101*(1), 79-90.

Hallett, L. M., Jones, S. K., MacDonald, A. A. M., Jones, M. B., Flynn, D. F., Ripplinger, J., Slaughter, P., Gries, C., & Collins, S. L. (2016). codyn: An r package of community dynamics metrics. *Methods in Ecology and Evolution*, *7*(10), 1146-1151. https://doi.org/10.1111/2041-210X.12569

Hawkins, S., Sugden, H., Mieszkowska, N., Moore, P., Poloczanska, E., Leaper, R., Herbert, R. J., Genner, M., Moschella, P., & Thompson, R. (2009). Consequences of climate-driven biodiversity changes for ecosystem functioning of North European rocky shores. *Marine Ecology Progress Series*, *396*, 245-259. https://doi.org/10.3354/meps08378

Hays, C., Hanley, T., Hughes, A., Truskey, S., Zerebecki, R., & Sotka, E. (2021). Local adaptation in marine foundation species at microgeographic scales. *The Biological Bulletin*, *241*(1), 16-29.

Helmuth, B., Broitman, B. R., Blanchette, C. A., Gilman, S., Halpin, P., Harley, C. D., O'Donnell, M. J., Hofmann, G. E., Menge, B., & Strickland, D. (2006). Mosaic patterns of thermal stress in the rocky intertidal zone: implications for climate change. *Ecological Monographs*, *76*(4), 461-479.

Helmuth, B., Yamane, L., Lalwani, S., Matzelle, A., Tockstein, A., & Gao, N. (2011). Hidden signals of climate change in intertidal ecosystems: what (not) to expect when you are expecting. *Journal of Experimental Marine Biology and Ecology*, *400*(1-2), 191-199. https://doi.org/10.1016/j.jembe.2011.02.004

Hemond, E. M., Kaluziak, S. T., & Vollmer, S. V. (2014). The genetics of colony form and function in Caribbean Acropora corals. *BMC Genomics*, *15*(1), 1133. https://doi.org/10.1186/1471-2164-15-1133

Hersch-Green, E. I., Turley, N. E., & Johnson, M. T. (2011). Community genetics: what have we accomplished and where should we be going? *Philosophical Transactions of the Royal Society B: Biological Sciences*, *366*(1569), 1453-1460.

Hillebrand, H., Bennett, D. M., & Cadotte, M. W. (2008). Consequences of dominance: a review of evenness effects on local and regional ecosystem processes. *Ecology*, *89*(6), 1510-1520. https://doi.org/10.1890/07-1053.1

Hlaing, S. M. M., Lou, J., Cheng, J., Xun, X., Li, M., Lu, W., Hu, X., & Bao, Z. (2020). Tissue-biased and species-specific regulation of glutathione peroxidase (GPx) genes in scallops exposed to toxic dinoflagellates. *Toxins*, *13*(1), 21.

Hofmann, G. E., & Somero, G. N. (1995). Evidence for protein damage at environmental temperatures: seasonal changes in levels of ubiquitin conjugates and hsp70 in the intertidal mussel Mytilus trossulus. *Journal of Experimental Biology*, *198*(7), 1509-1518.

Hollander, J. (2008). Testing the grain-size model for the evolution of phenotypic plasticity. *Evolution*, *62*(6), 1381-1389.

Honig, A., Supan, J., & Peyre, M. L. (2015). Population ecology of the gulf ribbed mussel across a salinity gradient: recruitment, growth and density. *Ecosphere*, *6*(11), 1-13. https://doi.org/10.1890/ES14-00499.1

Hönisch, B., Ridgwell, A., Schmidt, D. N., Thomas, E., Gibbs, S. J., Sluijs, A., Zeebe, R., Kump, L., Martindale, R. C., & Greene, S. E. (2012). The geological record of ocean acidification. *Science*, *335*(6072), 1058-1063.

Horne, B. D., & Camp, N. J. (2004). Principal component analysis for selection of optimal SNP-sets that capture intragenic genetic variation. *Genetic Epidemiology: The Official Publication of the International Genetic Epidemiology Society*, *26*(1), 11-21.

Jackson, D. A., Peres-Neto, P. R., & Olden, J. D. (2001). What controls who is where in freshwater fish communities the roles of biotic, abiotic, and spatial factors. *Canadian journal of fisheries and aquatic sciences*, *58*(1), 157-170. https://doi.org/10.1139/f00-239

Jeffreys, H. (1998). *The theory of probability*. OuP Oxford.

Jump, A. S., Hunt, J. M., MARTÍNEZ-IZQUIERDO, J. A., & Peñuelas, J. (2006). Natural selection and climate change: temperature-linked spatial and temporal trends in gene frequency in Fagus sylvatica. *Molecular ecology*, *15*(11), 3469-3480.

Kabakoff, B., Hwang, S.-P. L., & Lennarz, W. J. (1992). Characterization of post-translational modifications common to three primary mesenchyme cell-specific glycoproteins involved in sea urchin embryonic skeleton formation. *Developmental biology*, *150*(2), 294-305. https://doi.org/10.1016/0012-1606(92)90243-A

Kandur, A. S. (2014). *The distribution of Mytilus californianus in the Strait of Juan de Fuca*. The University of Chicago.

Kass, R. E., & Raftery, A. E. (1995). Bayes factors. *Journal of the american statistical association*, *90*(430), 773-795.

Katow, H. (2020). Role of a primary mesenchyme cell surface specific antigen during early morphogenesis in sea urchin embryos. In *Biology of Echinodermata* (pp. 453-459). CRC Press. https://doi.org/10.1201/9781003077565-108

Kaur, M., Saini, K. C., Ojah, H., Sahoo, R., Gupta, K., Kumar, A., & Bast, F. (2022). Abiotic stress in algae: response, signaling and transgenic approaches. *Journal of Applied Phycology*, *34*(4), 1843-1869. https://doi.org/10.1007/s10811-022-02746-7

Kelly, M. (2019). Adaptation to climate change through genetic accommodation and assimilation of plastic phenotypes. *Philosophical Transactions of the Royal Society B*, *374*(1768), 20180176.

Khangaonkar, T., Nugraha, A., Xu, W., & Balaguru, K. (2019). Salish Sea response to global climate change, sea level rise, and future nutrient loads. *Journal of Geophysical Research: Oceans*, *124*(6), 3876-3904. https://doi.org/10.1029/2018JC014670

Kidd, Jeffrey M., Gravel, S., Byrnes, J., Moreno-Estrada, A., Musharoff, S., Bryc, K., Degenhardt, Jeremiah D., Brisbin, A., Sheth, V., Chen, R., McLaughlin, Stephen F., Peckham, Heather E., Omberg, L., Bormann Chung, Christina A., Stanley, S., Pearlstein, K., Levandowsky, E., Acevedo-Acevedo, S., Auton, A., . . . Bustamante, Carlos D. (2012). Population Genetic Inference from Personal Genome Data: Impact of Ancestry and Admixture on Human Genomic Variation. *The American Journal of Human Genetics*, *91*(4), 660-671. https://doi.org/10.1016/j.ajhg.2012.08.025

Kolzenburg, R., Moreira, H., Storey, C., & Ragazzola, F. (2023). Structural integrity and skeletal trace elements in intertidal coralline algae across the Northeast Atlantic reveal a distinct separation of the leading and the trailing edge populations. *Marine Environmental Research*, *190*, 106086. https://doi.org/10.1016/j.marenvres.2023.106086

Korneliussen, T. S., Albrechtsen, A., & Nielsen, R. (2014). ANGSD: analysis of next generation sequencing data. *BMC bioinformatics*, *15*(1), 356. https://doi.org/10.1186/s12859-014-0356-4

Kotta, J., Oganjan, K., Lauringson, V., Pärnoja, M., Kaasik, A., Rohtla, L., Kotta, I., & Orav-Kotta, H. (2015). Establishing functional relationships between abiotic environment,

macrophyte coverage, resource gradients and the distribution of Mytilus trossulus in a brackish non-tidal environment. *PloS one*, *10*(8), e0136949. https://doi.org/10.1371/journal.pone.0136949

Kourtidis, A., Drosopoulou, E., Nikolaidis, N., Hatzi, V. I., Chintiroglou, C. C., & Scouras, Z. G. (2006). Identification of several cytoplasmic HSP70 genes from the Mediterranean mussel (Mytilus galloprovincialis) and their long-term evolution in Mollusca and Metazoa. *Journal of molecular evolution*, *62*, 446-459.

Koutsogiannaki, S., & Kaloyianni, M. (2010). Signaling molecules involved in immune responses in mussels. *Invertebrate survival journal*, *7*(1).

Krieger, E. C., Taise, A., Nelson, W. A., Grand, J., Le Ru, E., Davy, S. K., & Cornwall, C. E. (2023). Tolerance of coralline algae to ocean warming and marine heatwaves. *PloS Climate*, *2*(1), e0000092. https://doi.org/10.1371/journal.pclm.0000092

Kroeker, K. J., Kordas, R. L., Crim, R. N., & Singh, G. G. (2010). Meta-analysis reveals negative yet variable effects of ocean acidification on marine organisms. *Ecology Letters*, *13*(11), 1419-1434. https://doi.org/10.1111/j.1461-0248.2010.01518.x

Lalejini, A., Ferguson, A. J., Grant, N. A., & Ofria, C. (2021). Adaptive phenotypic plasticity stabilizes evolution in fluctuating environments. *Frontiers in Ecology and Evolution*, *9*, 715381.

Lande, R. (2009). Adaptation to an extraordinary environment by evolution of phenotypic plasticity and genetic assimilation. *Journal of evolutionary biology*, *22*(7), 1435-1446.

Lang, G. I., Murray, A. W., & Botstein, D. (2009). The cost of gene expression underlies a fitness trade-off in yeast. *Proceedings of the National Academy of Sciences*, *106*(14), 5755-5760.

Leimar, O., Dall, S. R., McNamara, J. M., Kuijper, B., & Hammerstein, P. (2019). Ecological genetic conflict: genetic architecture can shift the balance between local adaptation and plasticity. *The American Naturalist*, *193*(1), 70-80.

Lenormand, T. (2002). Gene flow and the limits to natural selection. *Trends in ecology & evolution*, *17*(4), 183-189.

Lepš, J. (2004). Variability in population and community biomass in a grassland community affected by environmental productivity and diversity. *Oikos*, *107*(1), 64-71. https://doi.org/10.1111/j.0030-1299.2004.13023.x

Levins, R. (1968). *Evolution in changing environments: some theoretical explorations*. Princeton University Press.

Lewontin, R. C. (1957). The adaptations of populations to varying environments. Cold Spring Harbor Symposia on Quantitative Biology,

Liggins, L., Treml, E. A., & Riginos, C. (2020). Seascape genomics: contextualizing adaptive and neutral genomic variation in the ocean environment. *Population genomics: Marine organisms*, 171-218.

Liu, H.-h., He, J.-y., Chi, C.-f., & Shao, J. (2014). Differential HSP70 expression in Mytilus coruscus under various stressors. *Gene*, *543*(1), 166-173.

Long, J. C. (1991). The genetic structure of admixed populations. *Genetics*, *127*(2), 417-428. https://doi.org/10.1093/genetics/127.2.417

López, B. A., Ramírez, R. P., Guaitro, S. Y., & López, D. A. (2010). Interspecific differences in the phenotypic plasticity of intertidal barnacles in response to habitat changes. *Journal of Crustacean Biology*, *30*(3), 357-365. https://doi.org/10.1651/09-3211.1

Loreau, M. (2000). Biodiversity and ecosystem functioning: recent theoretical advances. *Oikos*, *91*(1), 3-17. https://doi.org/10.1034/j.1600-0706.2000.910101.x

Loreau, M. (2010). *From populations to ecosystems: Theoretical foundations for a new ecological synthesis (MPB-46)*. Princeton University Press. https://doi.org/10.1515/9781400834167

Loreau, M., & de Mazancourt, C. (2008). Species synchrony and its drivers: neutral and nonneutral community dynamics in fluctuating environments. *The American Naturalist*, *172*(2), E48-E66. https://doi.org/10.1086/589746

Losure, D. A., Wilsey, B. J., & Moloney, K. A. (2007). Evenness–invasibility relationships differ between two extinction scenarios in tallgrass prairie. *Oikos*, *116*(1), 87-98. https://doi.org/10.1111/j.2006.0030-1299.15341.x

Lourenço, C. R., Nicastro, K. R., McQuaid, C. D., Chefaoui, R. M., Assis, J., Taleb, M. Z., & Zardi, G. I. (2017). Evidence for rangewide panmixia despite multiple barriers to dispersal in a marine mussel. *Scientific reports*, *7*(1), 10279.

Luttikhuizen, P., Drent, J., Van Delden, W., & Piersma, T. (2003). Spatially structured genetic variation in a broadcast spawning bivalve: quantitative vs. molecular traits. *Journal of evolutionary biology*, *16*(2), 260-272.

MacCready, P., McCabe, R., Siedlecki, S., Lorenz, M., Giddings, S., Bos, J., Albertson, S., Banas, N., & Garnier, S. (2021). Estuarine circulation, mixing, and residence times in the Salish Sea. *Journal of Geophysical Research: Oceans*, *126*(2), e2020JC016738. https://doi.org/10.1029/2020JC016738

Mackas, D. L., & Harrison, P. J. (1997). Nitrogenous nutrient sources and sinks in the Juan de Fuca Strait/Strait of Georgia/Puget Sound estuarine system: assessing the potential for eutrophication. *Estuarine, Coastal and Shelf Science*, *44*(1), 1-21. https://doi.org/10.1006/ecss.1996.0110

Malachowicz, M., & Wenne, R. (2019). Mantle transcriptome sequencing of Mytilus spp. and identification of putative biomineralization genes. *PeerJ*, *6*, e6245.

Man, T. D. (2018). The interactive effects of ocean acidification, food availability, and source location on the growth and physiology of the California mussel.

Marcil, J., Swain, D. P., & Hutchings, J. A. (2006). Countergradient variation in body shape between two populations of Atlantic cod (Gadus morhua). *Proceedings of the Royal Society B: Biological Sciences*, *273*(1583), 217-223.

Markowitz, H. (1952). Portofolio selection. *Journal of finance*, *7*, 77-91.

Marquet, N., Nicastro, K. R., Gektidis, M., McQuaid, C. D., Pearson, G. A., Serrao, E. A., & Zardi, G. I. (2013). Comparison of phototrophic shell-degrading endoliths in invasive and native populations of the intertidal mussel Mytilus galloprovincialis. *Biological Invasions*, *15*, 1253-1272.

Masson, D., & Peña, A. (2009). Chlorophyll distribution in a temperate estuary: The Strait of Georgia and Juan de Fuca Strait. *Estuarine, Coastal and Shelf Science*, *82*(1), 19-28. https://doi.org/10.1016/j.ecss.2008.12.022

McCoy, S. J., & Kamenos, N. A. (2015). Coralline algae (Rhodophyta) in a changing world: integrating ecological, physiological, and geochemical responses to global change. *Journal of phycology*, *51*(1), 6-24. https://doi.org/10.1111/jpy.12262

McCoy, S. J., Kamenos, N. A., Chung, P., Wootton, T. J., & Pfister, C. A. (2018). A mineralogical record of ocean change: decadal and centennial patterns in the California mussel. *Global Change Biology*, *24*(6), 2554-2562.

McDonald, J. H., & Kreitman, M. (1991). Adaptive protein evolution at the Adh locus in Drosophila. *Nature*, *351*(6328), 652-654.

McGrorty, S., & Goss-Custard, J. (1995). Population dynamics of Mytilus edulis along environmental gradients: density-dependent changes in adult mussel numbers. *Marine Ecology Progress Series*, *129*, 197-213. https://doi.org/10.3354/meps129197

Meisner, J., & Albrechtsen, A. (2018). Inferring population structure and admixture proportions in low-depth NGS data. *Genetics*, *210*(2), 719-731. https://doi.org/10.1534/genetics.118.301336

Melzner, F., Stange, P., Trübenbach, K., Thomsen, J., Casties, I., Panknin, U., Gorb, S. N., & Gutowska, M. A. (2011). Food supply and seawater p CO2 impact calcification and internal shell dissolution in the blue mussel Mytilus edulis. *PloS one*, *6*(9), e24223. https://doi.org/10.1371/journal.pone.0024223

Mérot, C., Oomen, R. A., Tigano, A., & Wellenreuther, M. (2020). A roadmap for understanding the evolutionary significance of structural genomic variation. *Trends in ecology & evolution*, *35*(7), 561-572.

Messer, P. W., & Petrov, D. A. (2013). Population genomics of rapid adaptation by soft selective sweeps. *Trends in ecology & evolution*, *28*(11), 659-669.

Mieszkowska, N. (2025). Evidence of climate change (intertidal indicators). In *Energy and Climate Change* (pp. 43-66). Elsevier. https://doi.org/10.1016/B978-0-443-21927-6.00024-6

Mwangi, P. N., Schmitz, M., Scherber, C., Roscher, C., Schumacher, J., SCHERER-LORENZEN, M., Weisser, W. W., & Schmid, B. (2007). Niche pre-emption increases with species richness in experimental plant communities. *Journal of Ecology*, *95*(1), 65-78. https://doi.org/10.1111/j.1365-2745.2006.01189.x

Nicolaus, M., & Edelaar, P. (2018). Comparing the consequences of natural selection, adaptive phenotypic plasticity, and matching habitat choice for phenotype–environment matching, population genetic structure, and reproductive isolation in meta-populations. *Ecology and evolution*, *8*(8), 3815-3827. https://doi.org/10.1002/ece3.3816

Nie, H., Jiang, K., Li, N., Li, D., & Yan, X. (2020). Transcriptomic analysis of Ruditapes philippinarum under aerial exposure and reimmersion reveals genes involved in stress response and recovery capacity of the Manila clam. *Aquaculture*, *524*, 735271.

Nie, H., Wang, H., Jiang, K., & Yan, X. (2020). Transcriptome analysis reveals differential immune related genes expression in Ruditapes philippinarum under hypoxia stress: potential HIF and NF-κB crosstalk in immune responses in clam. *BMC Genomics*, *21*(1), 318. https://doi.org/10.1186/s12864-020-6734-6

Nielsen, M. B., Vogensen, T. K., Thyrring, J., Sørensen, J. G., & Sejr, M. K. (2021). Freshening increases the susceptibility to heat stress in intertidal mussels (Mytilus edulis) from the Arctic. *Journal of Animal Ecology*, *90*(6), 1515-1524.

Niku, J., Brooks, W., Herliansyah, R., Hui, F., Taskinen, S., Warton, D., & van der Veen, B. (2020). Gllvm: Generalized linear latent variable models. *R package version*, *1*(3), 10.1371.

Niku, J., Hui, F. K., Taskinen, S., & Warton, D. I. (2019). gllvm: Fast analysis of multivariate abundance data with generalized linear latent variable models in r. *Methods in Ecology and Evolution*, *10*(12), 2173-2182. https://doi.org/10.1111/2041-210X.13303

NOAA National Centers for Environmental Information. *Monthly National Climate Report for July 2022*. https://www.ncei.noaa.gov/access/monitoring/monthly-report/national/202207

Nosil, P., Funk, D. J., & Ortiz-Barrientos, D. (2009). Divergent selection and heterogeneous genomic divergence. *Molecular ecology*, *18*(3), 375-402. https://doi.org/10.1111/j.1365-294X.2008.03946.x

Oksanen, J., Blanchet, F. G., Friendly, M., Kindt, R., Legendre, P., McGlinn, D., Minchin, P., O'hara, R., Simpson, G., & Solymos, P. (2018). Community ecology package, version 2.5-2. In: Package 'Vegan.

Oomen, R. A., Kuparinen, A., & Hutchings, J. A. (2020). Consequences of single-locus and tightly linked genomic architectures for evolutionary responses to environmental change. *Journal of Heredity*, *111*(4), 319-332. https://doi.org/10.1093/jhered/esaa020

Osores, S. J., Lagos, N. A., San Martin, V., Manriquez, P. H., Vargas, C. A., Torres, R., Navarro, J. M., Poupin, M. J., Saldias, G. S., & Lardies, M. A. (2017). Plasticity and inter-population variability in physiological and life-history traits of the mussel Mytilus chilensis: a reciprocal transplant experiment. *Journal of Experimental Marine Biology and Ecology*, *490*, 1-12.

Paggeot, L. X., DeBiasse, M. B., Escalona, M., Fairbairn, C., Marimuthu, M. P., Nguyen, O., Sahasrabudhe, R., & Dawson, M. N. (2022). Reference genome for the California ribbed mussel, Mytilus californianus, an ecosystem engineer. *Journal of Heredity*, *113*(6), 681-688.

Paine, R. T. (1966). Food web complexity and species diversity. *The American Naturalist*, *100*(910), 65-75. https://doi.org/10.1086/282400

Paine, R. T. (1969). A note on trophic complexity and community stability. *The American Naturalist*, *103*(929), 91-93. https://doi.org/10.1086/282586

Paine, R. T. (1974). Intertidal community structure. *Oecologia*, *15*(2), 93-120.

Paine, R. T., & Levin, S. A. (1981). Intertidal landscapes: disturbance and the dynamics of pattern. *Ecological Monographs*, *51*(2), 145-178.

Paine, R. T., & Trimble, A. C. (2004). Abrupt community change on a rocky shore–biological mechanisms contributing to the potential formation of an alternative state. *Ecology Letters*, *7*(6), 441-445. https://doi.org/10.1111/j.1461-0248.2004.00601.x

Palmer, A. R. (1982). Growth in marine gastropods. A non-destructive technique for independently measuring shell and body weight. *Malacologia*, *23*(1), 63-74.

Palumbi, S. R. (1994). Genetic divergence, reproductive isolation, and marine speciation. *Annual review of ecology and systematics*, *25*(1), 547-572.

Parfitt, D. A., Michael, G. J., Vermeulen, E. G., Prodromou, N. V., Webb, T. R., Gallo, J.-M., Cheetham, M. E., Nicoll, W. S., Blatch, G. L., & Chapple, J. P. (2009). The ataxia protein

sacsin is a functional co-chaperone that protects against polyglutamine-expanded ataxin-1. *Human molecular genetics*, *18*(9), 1556-1565. https://doi.org/ 10.1093/hmg/ddp067

Pedersen, B. S., & Quinlan, A. R. (2018). Mosdepth: quick coverage calculation for genomes and exomes. *Bioinformatics*, *34*(5), 867-868. https://doi.org/10.1093/bioinformatics/btx699

Pennekamp, F., Pontarp, M., Tabi, A., Altermatt, F., Alther, R., Choffat, Y., Fronhofer, E. A., Ganesanandamoorthy, P., Garnier, A., & Griffiths, J. I. (2018). Biodiversity increases and decreases ecosystem stability. *Nature*, *563*(7729), 109-112. https://doi.org/10.1038/s41586-018-0627-8

Pespeni, M. H., Barney, B. T., & Palumbi, S. R. (2013). Differences in the regulation of growth and biomineralization genes revealed through long-term common-garden acclimation and experimental genomics in the purple sea urchin. *Evolution*, *67*(7), 1901-1914. https://doi.org/10.1111/evo.12036

Petkova, D., Novembre, J., & Stephens, M. (2016). Visualizing spatial population structure with estimated effective migration surfaces. *Nature genetics*, *48*(1), 94-100. https://doi.org/10.1038/ng.3464

Petraitis, P. S., & Dudgeon, S. (2020). Declines over the last two decades of five intertidal invertebrate species in the western North Atlantic. *Communications biology*, *3*(1), 1-7. https://doi.org/10.1038/s42003-020-01326-0

Pfister, C. A., Gilbert, J. A., & Gibbons, S. M. (2014). The role of macrobiota in structuring microbial communities along rocky shores. *PeerJ*, *2*, e631. https://doi.org/10.7717/peerj.631

Pfister, C. A., Paine, R. T., & Timothy Wootton, J. (2016). The iconic keystone predator has a pathogen. *Frontiers in Ecology & the Environment*, *14*(5). https://doi.org/10.1002/fee.1292

Pfisterer, A. B., & Schmid, B. (2002). Diversity-dependent production can decrease the stability of ecosystem functioning. *Nature*, *416*(6876), 84-86. https://doi.org/10.1038/416084a

Pierrot, D., Wallace, D., & Lewis, E. (2011). MS Excel program developed for CO2 system calculations. *Carbon dioxide information analysis center*. https://doi.org/10.3334/CDIAC/otg.CO2SYS_XLS_CDIAC105a

Piersma, T., & Drent, J. (2003). Phenotypic flexibility and the evolution of organismal design. *Trends in ecology & evolution*, *18*(5), 228-233. https://doi.org/10.1016/S0169-5347(03)00036-3

Place, S. P., Menge, B. A., & Hofmann, G. E. (2012). Transcriptome profiles link environmental variation and physiological response of Mytilus californianus between Pacific tides. *Functional ecology*, *26*(1), 144-155.

Pohlert, T., Pohlert, M. T., & Kendall, S. (2016). Package 'trend'. *Title non-parametric trend tests and change-point detection*.

Quinlan, A. R., & Hall, I. M. (2010). BEDTools: a flexible suite of utilities for comparing genomic features. *Bioinformatics*, *26*(6), 841-842.

R Core Team. (2024). *R: A Language and Environment for Statistical Computing. R Foundation for Statistical Computing. Retrieved from https://www.R-project.org/*. In https://www.R-project.org/

Redfield, A. C. (1934). *On the proportions of organic derivatives in sea water and their relation to the composition of plankton* (Vol. 1). University Press of Liverpool Liverpool.

Richards, C. S., Vera Cruz, D., Shapiro, J. W., Wootton, J. T., & Pfister, C. A. (2025). Spatially Varying Selection Amplifies Intrapopulation Differentiation Among Phenotypic Traits in the Rocky-Shore Mussel, Mytilus californianus. *Ecology and evolution*, *15*(7), e71641. https://doi.org/10.1002/ece3.71641

Ridgway, T., Hoegh-Guldberg, O., & Ayre, D. (2001). Panmixia in Pocillopora verrucosa from South Africa. *Marine Biology*, *139*, 175-181.

Riebesell, U., Fabry, V., Hansson, L., & Gattuso, J. (2010). Guide to Best Practices for Ocean Acidification Research and Data Reporting. Publications Office of the European Union, Luxembourg, 260 pp. *doi. org/10.2777/58454*.

Roberts, D. A., Hofmann, G. E., & Somero, G. N. (1997). Heat-shock protein expression in Mytilus californianus: acclimatization (seasonal and tidal-height comparisons) and acclimation effects. *The Biological Bulletin*, *192*(2), 309-320.

Roda, F., Walter, G. M., Nipper, R., & Ortiz-Barrientos, D. (2017). Genomic clustering of adaptive loci during parallel evolution of an Australian wildflower. *Molecular ecology*, *26*(14), 3687-3699. https://doi.org/10.1111/mec.14150

Sabine, C. L., Feely, R. A., Gruber, N., Key, R. M., Lee, K., Bullister, J. L., Wanninkhof, R., Wong, C., Wallace, D. W., & Tilbrook, B. (2004). The oceanic sink for anthropogenic CO2. *Science*, *305*(5682), 367-371.

Sanford, E., & Kelly, M. W. (2011). Local adaptation in marine invertebrates. *Annual review of marine science*, *3*, 509-535.

Sasaki, T., & Lauenroth, W. K. (2011). Dominant species, rather than diversity, regulates temporal stability of plant communities. *Oecologia*, *166*(3), 761-768. https://doi.org/10.1007/s00442-011-1916-1

Savolainen, O., Lascoux, M., & Merilä, J. (2013). Ecological genomics of local adaptation. *Nature Reviews Genetics*, *14*(11), 807-820.

Schaal, S. M., & Smith, S. J. (2023). Comparative study highlights how gene flow shapes adaptive genomic architecture. *Molecular ecology*, *32*(7), 1545-1548. https://doi.org/10.1111/mec.16882

Scheiner, S. M. (1998). The genetics of phenotypic plasticity. VII. Evolution in a spatially-structured environment. *Journal of evolutionary biology*, *11*(3), 303-320.

Scheiner, S. M. (2016). Habitat choice and temporal variation alter the balance between adaptation by genetic differentiation, a jack-of-all-trades strategy, and phenotypic plasticity. *The American Naturalist*, *187*(5), 633-646. https://doi.org/10.1086/685812

Scheiner, S. M., Barfield, M., & Holt, R. D. (2017). The genetics of phenotypic plasticity. XV. Genetic assimilation, the Baldwin effect, and evolutionary rescue. *Ecology and evolution*, *7*(21), 8788-8803.

Shi, Y., Bouska, K. L., McKinney, G. J., Dokai, W., Bartels, A., McPhee, M. V., & Larson, W. A. (2023). Gene flow influences the genomic architecture of local adaptation in six riverine fish species. *Molecular ecology*, *32*(7), 1549-1566. https://doi.org/10.1111/mec.16317

Shurin, J. B. (2007). How is diversity related to species turnover through time? *Oikos*, *116*(6), 957-965. https://doi.org/10.1111/j.0030-1299.2007.15751.x

Slatkin, M. (1985). Gene flow in natural populations. *Annual review of ecology and systematics*, 393-430.

Slatkin, M. (1994). Linkage disequilibrium in growing and stable populations. *Genetics*, *137*(1), 331-336. https://doi.org/10.1093/genetics/137.1.331

Smee, D. L., Overath, R. D., Johnson, K. D., & Sanchez, J. A. (2013). Intraspecific variation influences natural settlement of eastern oysters. *Oecologia*, *173*, 947-953.

Smith, M. D., Wilcox, J. C., Kelly, T., & Knapp, A. K. (2004). Dominance not richness determines invasibility of tallgrass prairie. *Oikos*, *106*(2), 253-262. https://doi.org/10.1111/j.0030-1299.2004.13057.x

Snelgrove, P., Grant, J., & Pilditch, C. (1999). Habitat selection and adult-larvae interactions in settling larvae of soft-shell clam Mya arenaria. *Marine Ecology Progress Series*, *182*, 149-159. https://doi.org/10.3354/meps182149

Sousa, R., Morais, P., Dias, E., & Antunes, C. (2011). Biological invasions and ecosystem functioning: time to merge. *Biological Invasions*, *13*(5), 1055-1058. https://doi.org/10.1007/s10530-011-9947-4

Stachowicz, J. J. (2001). Mutualism, facilitation, and the structure of ecological communities: positive interactions play a critical, but underappreciated, role in ecological communities by reducing physical or biotic stresses in existing habitats and by creating new habitats on which many species depend. *Bioscience*, *51*(3), 235-246. https://doi.org/10.1641/0006-3568(2001)051[0235:MFATSO]2.0.CO;2

Stamp, M. A., & Hadfield, J. D. (2020). The relative importance of plasticity versus genetic differentiation in explaining between population differences; a meta-analysis. *Ecology Letters*, *23*(10), 1432-1441.

Stephenson, T. A., Stephenson, A., & Stephenson, A. (1972). Life between tidemarks on rocky shores.

Suchanek, T. H. (1978). The ecology of Mytilus edulis L. in exposed rocky intertidal communities. *Journal of Experimental Marine Biology and Ecology*, *31*(1), 105-120.

Sultan, S. E., & Spencer, H. G. (2002). Metapopulation structure favors plasticity over local adaptation. *The American Naturalist*, *160*(2), 271-283.

Sunday, J. M., Crim, R. N., Harley, C. D., & Hart, M. W. (2011). Quantifying rates of evolutionary adaptation in response to ocean acidification. *PloS one*, *6*(8), e22881.

Svanbäck, R., & Bolnick, D. I. (2007). Intraspecific competition drives increased resource use diversity within a natural population. *Proceedings of the Royal Society B: Biological Sciences*, *274*(1611), 839-844. https://doi.org/10.1098/rspb.2006.0198

Takahashi-Kariyazono, S., & Terai, Y. (2021). Two divergent haplogroups of a sacsin-like gene in Acropora corals. *Scientific reports*, *11*(1), 23018. https://doi.org/10.1038/s41598-021-02386-w

Tay, Y., Chng, M., Sew, W., Rheindt, F., Tun, K., & Meier, R. (2016). Beyond the coral triangle: high genetic diversity and near panmixia in Singapore's populations of the broadcast spawning sea star Protoreaster nodosus. *Royal Society Open Science*, *3*(8), 160253.

Taylor, L., & Woiwod, I. (1982). Comparative synoptic dynamics. I. Relationships between inter- and intra-specific spatial and temporal variance/mean population parameters. *The Journal of Animal Ecology*, 879-906. https://doi.org/10.2307/4012

Taylor, L. R. (1961). Aggregation, variance and the mean. *Nature*, *189*(4766), 732-735. https://doi.org/10.1038/189732a0

Teixidó, N., Caroselli, E., Alliouane, S., Ceccarelli, C., Comeau, S., Gattuso, J. P., Fici, P., Micheli, F., Mirasole, A., & Monismith, S. G. (2020). Ocean acidification causes variable trait-shifts in a coral species. *Global Change Biology*, *26*(12), 6813-6830. https://doi.org/10.1111/gcb.15372

Thibaut, L. M., & Connolly, S. R. (2013). Understanding diversity–stability relationships: towards a unified model of portfolio effects. *Ecology Letters*, *16*(2), 140-150. https://doi.org/10.1111/ele.12019

Thomas, L., Underwood, J. N., Rose, N. H., Fuller, Z. L., Richards, Z. T., Dugal, L., Grimaldi, C. M., Cooke, I. R., Palumbi, S. R., & Gilmour, J. P. (2022). Spatially varying selection between habitats drives physiological shifts and local adaptation in a broadcast spawning coral on a remote atoll in Western Australia. *Science advances*, *8*(17), eabl9185. https://doi.org/10.1126/sciadv.abl9185

Thomsen, J., Casties, I., Pansch, C., Körtzinger, A., & Melzner, F. (2013). Food availability outweighs ocean acidification effects in juvenile Mytilus edulis: laboratory and field experiments. *Global Change Biology*, *19*(4), 1017-1027. https://doi.org/10.1111/gcb.12109

Tienderen, P. H. v. (1997). Generalists, specialists, and the evolution of phenotypic plasticity in sympatric populations of distinct species. *Evolution*, *51*(5), 1372-1380.

Tilman, D. (1999). The ecological consequences of changes in biodiversity: a search for general principles. *Ecology*, *80*(5), 1455-1474. https://doi.org/10.1890/0012-9658(1999)080[1455:TECOCI]2.0.CO;2

Trainer, V. L., Moore, S. K., Hallegraeff, G., Kudela, R. M., Clement, A., Mardones, J. I., & Cochlan, W. P. (2020). Pelagic harmful algal blooms and climate change: Lessons from nature's experiments with extremes. *Harmful Algae*, *91*, 101591. https://doi.org/10.1016/j.hal.2019.03.009

Trevelyan, G. A., & Chang, E. S. (1983). Experiments on larval rearing of the California mussel (Mytilus californianus). *Journal of the World Mariculture Society*, *14*(1-4), 137-148. https://doi.org/10.1111/j.1749-7345.1983.tb00068.x

Trussell, G. C. (2000). Phenotypic clines, plasticity, and morphological trade-offs in an intertidal snail. *Evolution*, *54*(1), 151-166.

Turko, A. J., & Rossi, G. S. (2022). Habitat choice promotes and constrains phenotypic plasticity. *Biology letters*, *18*(1). https://doi.org/10.1098/rsbl.2021.0468

Ulrich, W., Soliveres, S., Thomas, A. D., Dougill, A. J., & Maestre, F. T. (2016). Environmental correlates of species rank− abundance distributions in global drylands. *Perspectives in plant ecology, evolution and systematics*, *20*, 56-64. https://doi.org/10.1016/j.ppees.2016.04.004

Valladares, F., Sanchez-Gomez, D., & Zavala, M. A. (2006). Quantitative estimation of phenotypic plasticity: bridging the gap between the evolutionary concept and its ecological applications. *Journal of Ecology*, *94*(6), 1103-1116.

Velotta, J. P., & Cheviron, Z. A. (2018). Remodeling ancestral phenotypic plasticity in local adaptation: A new framework to explore the role of genetic compensation in the evolution of homeostasis. *Integrative and comparative biology*, *58*(6), 1098-1110.

Venkataraman, Y. R., White, S. J., & Roberts, S. B. (2022). Differential DNA methylation in Pacific oyster reproductive tissue in response to ocean acidification. *BMC Genomics*, *23*(1), 556. https://doi.org/10.1186/s12864-022-08781-5

Von Holle, B. (2013). Environmental stress alters native-nonnative relationships at the community scale. *Biological Invasions*, *15*(2), 417-427. https://doi.org/10.1007/s10530-012-0297-7

Wadgymar, S. M., DeMarche, M. L., Josephs, E. B., Sheth, S. N., & Anderson, J. T. (2022). Local adaptation: causal agents of selection and adaptive trait divergence. *Annual review of ecology, evolution, and systematics*, *53*(1), 87-111.

Wang, Q., Ning, X., Pei, D., Zhao, J., You, L., Wang, C., & Wu, H. (2013). Molecular cloning, characterization and expression profiles of thioredoxin 1 and thioredoxin 2 genes in Mytilus galloprovincialis. *Chinese Journal of Oceanology and Limnology*, *31*(3), 493-503.

Wayne Polley, H., Wilsey, B. J., & Derner, J. D. (2007). Dominant species constrain effects of species diversity on temporal variability in biomass production of tallgrass prairie. *Oikos*, *116*(12), 2044-2052. https://doi.org/10.1111/j.2007.0030-1299.16080.x

Weiher, E., & Keddy, P. A. (1995). Assembly rules, null models, and trait dispersion: new questions from old patterns. *Oikos*, 159-164. https://doi.org/10.2307/3545686

Whitham, T. G., Allan, G. J., Cooper, H. F., & Shuster, S. M. (2020). Intraspecific genetic variation and species interactions contribute to community evolution. *Annual review of ecology, evolution, and systematics*, *51*, 587-612.

Wood, D. E., Lu, J., & Langmead, B. (2019). Improved metagenomic analysis with Kraken 2. *Genome biology*, *20*(1), 257. https://doi.org/10.1186/s13059-019-1891-0

Wootton, J. T. (2004). Markov chain models predict the consequences of experimental extinctions. *Ecology Letters*, *7*(8), 653-660. https://doi.org/10.1111/j.1461-0248.2004.00621.x

Wootton, J. T. (2005). Field parameterization and experimental test of the neutral theory of biodiversity. *Nature*, *433*(7023), 309-312. https://doi.org/10.1038/nature03211

Wootton, J. T. (2010). Experimental species removal alters ecological dynamics in a natural ecosystem. *Ecology*, *91*(1), 42-48. https://doi.org/10.1890/08-1868.1

Wootton, J. T., & Pfister, C. A. (2012). Carbon system measurements and potential climatic drivers at a site of rapidly declining ocean pH. *PloS one*, *7*(12), e53396. https://doi.org/10.1371/journal.pone.0053396

Wootton, J. T., Pfister, C. A., & Forester, J. D. (2008). Dynamic patterns and ecological impacts of declining ocean pH in a high-resolution multi-year dataset. *Proceedings of the National Academy of Sciences*, *105*(48), 18848-18853. https://doi.org/10.1073/pnas.0810079105

Worm, B., Barbier, E. B., Beaumont, N., Duffy, J. E., Folke, C., Halpern, B. S., Jackson, J. B., Lotze, H. K., Micheli, F., & Palumbi, S. R. (2006). Impacts of biodiversity loss on ocean ecosystem services. *Science*, *314*(5800), 787-790. https://doi.org/10.1126/science.1132294

Wright, S. (1969). Evolution and the genetics of populations. Vol. 2. The theory of gene frequencies.

Wu, B., Chen, X., Yu, M., Ren, J., Hu, J., Shao, C., Zhou, L., Sun, X., Yu, T., & Zheng, Y. (2022). Chromosome-level genome and population genomic analysis provide insights into the evolution and environmental adaptation of Jinjiang oyster Crassostrea ariakensis. *Molecular Ecology Resources*, *22*(4), 1529-1544. https://doi.org/10.1111/1755-0998.13556

Yadav, S., J Stow, A., & Dudaniec, R. Y. (2021). Microgeographical adaptation corresponds to elevational distributions of congeneric montane grasshoppers. *Molecular ecology*, *30*(2), 481-498.

Yeaman, S. (2015). Local adaptation by alleles of small effect. *The American Naturalist*, *186*(S1), S74-S89. https://doi.org/10.1086/682405

Yeaman, S. (2022). Evolution of polygenic traits under global vs local adaptation. *Genetics*, *220*(1), iyab134. https://doi.org/10.1093/genetics/iyab134

Yeaman, S., & Otto, S. P. (2011). Establishment and maintenance of adaptive genetic divergence under migration, selection, and drift. *Evolution*, *65*(7), 2123-2129.

Yeaman, S., & Whitlock, M. C. (2011). The genetic architecture of adaptation under migration–selection balance. *Evolution*, *65*(7), 1897-1911.

Zardi, G. I., Nicastro, K. R., McQuaid, C., Ng, T., Lathlean, J., & Seuront, L. (2016). Enemies with benefits: parasitic endoliths protect mussels against heat stress. *Scientific reports*, *6*(1), 1-8.

Zhou, Y., Carpenter, Z. W., Brennan, G., & Nambu, J. R. (2009). The Unique Morgue Ubiquitination Protein Is Conserved in a Diverse but Restricted Set of Invertebrates.

Molecular biology and evolution, *26*(10), 2245-2259.
https://doi.org/10.1093/molbev/msp147